SYNTHESIS, CHARACTERIZATION, AND TOXICITY STUDIES OF DIRHODIUM AND DIIRIDIUM METAL-METAL BONDED ANTICANCER COMPOUNDS

A Thesis

by

SARAH MARGARET LANE

Submitted to the Office of Graduate Studies of
Texas A&M University
in partial fulfillment of the requirements for the degree of

MASTER OF SCIENCE

August 2012

Major Subject: Chemistry

SYNTHESIS, CHARACTERIZATION, AND TOXICITY STUDIES OF DIRHODIUM AND DIIRIDIUM METAL-METAL BONDED ANTICANCER COMPOUNDS

A Thesis

by

SARAH MARGARET LANE

Submitted to the Office of Graduate Studies of
Texas A&M University
in partial fulfillment of the requirements for the degree of

MASTER OF SCIENCE

Approved By:

Chair of Committee,	Kim R. Dunbar
Committee Members,	Francois P. Gabbai
	Wenshe Liu
	Robert Burghardt
Head of Department,	David H. Russell

August 2012

Major Subject: Chemistry

ABSTRACT

Synthesis, Characterization, and Toxicity Studies of Dirhodium and Diiridium Metal-Metal Bonded Anticancer Compounds. (August 2012)

Sarah Margaret Lane, B.S., Bridgewater State University

Chair of Advisory Committee: Dr. Kim R. Dunbar

The anticancer properties of dirhodium tetraacetate were discovered in the 1970's, and subsequently motivated the research of several dirhodium paddlewheel derivatives. The promising results of this research led the Dunbar group to investigate the biological properties of dirhodium partial paddlewheel compounds. Previous work in our group has focused on dirhodium carboxylate derivatives with a series of diimine ligands, namely 1,10-phenanthroline (phen), dipyrido[3,2-f:2',3'-h]quinoxaline (dpq), dipyrido[3,2a:2´,3´c] phenazine (dppz), and benzo[i]dipyrido[3,2-a:2',3'-c]phenazine) (dppn). Current research has expanded this diimine series by substituting the carobxylate bridging group with p-methoxyphenylphosphine (PMP). This new series of compounds was characterized by several techniques, including: X-Ray crystallography, ^{1}H NMR spectroscopy, and electronic absorption spectroscopy.

The cytotoxicity of these compounds towards HeLa cells was investigated in presence and absence of light in an effort to investigate the ability to use these compounds as photodynamic therapy (PDT) agents. Cytotoxicity

measurements were carried out using the 3-(4,5-dimethylthiazol-2-yl)-2,5 diphenyltetrazolium bromide (MTT) assay. It was found that in the dark $[Rh_2(PMP)_2(dppz)_2][BF_4]_2$ (the dppz derivative of the dirhodium PMP compound) had no cytotoxicity towards HeLa cells, but experienced a 7 fold increase in cytotoxicity upon irradiation (with λi_{rr} equal to 350 nm). This dramatic increase in cytotoxicity upon irradiation makes this compound a potential PDT agent.

Diiridium (II,II) compounds were prepared in a dual attempt to determine how the properties of the dirhodium core effect the biological activities of these compounds, as well as investigate the biological activity of a set of compounds that has yet to be explored. The compound $[Ir_2(DTolF)_2(CH_3CN)_6][BF_4]_2$ was chosen because it has a well understood dirhodium analogue, and it is a known compound. However, it was discovered that there was a potential silver contamination in the final product, stemming from the silver trifluoroacetate oxidant used during synthesis. Consequently, a new method of preparing this compound was required. The new synthetic pathway for the diiridium compound $[Ir_2(DTolF)_2(CH_3CN)_6][BF_4]_2$ was devised, and the cytotoxicity and photocytotoxicity studies were performed for the first time (to our knowledge) on a diiridium (II,II) compound. Despite the stability of the compound, it was determined to be highly toxic, both in the dark and upon irradiation.

To my friends and family;

I don’t know what I would do without you.

TABLE OF CONTENTS

LIST OF FIGURES

FIGURE Page

LIST OF TABLES

CHAPTER I

INTRODUCTION:

CANCER AND CHEMOTHERAPY

Cancer

A Definition

Cancer is one of the most common causes of death in the United States; second only to heart disease[1]. The statistics of this disease are daunting – analysis from 2010 reported statistics of 1 in 2 men, and 1 in 3 women will have, or die, from cancer. This same report states that 1 in 8 women will be diagnosed with breast cancer. In the year 2010 there were 1,529,560 million cases of cancer diagnosed in the US, and 569,490 deaths predicted for the year 2010[2]. It is tantamount to first understand what cancer is in order to develop a rational strategy to combat this threat.

Cancer is a disease where abnormal cells divide uncontrollably and can invade other tissue. It is classified based on the type of tissue affected: adenocarcinoma (glandular tissue), blastoma (embryonic tissue), carcinoma (epithelial tissue), leukemia (tissues that form blood), lymphoma (lymphatic tissue), myeloma (bone marrow), and sarcoma (connective or supportive tissue – bone, cartilage, muscle). The extent to which the disease has spread is

---

This thesis follows the style of the Journal of the American Chemical Society.

indicated in stages that range from I to IV, with IV being the most severe. When staging cancer, the size of the tumor, the number of lymph nodes to which it has spread to, and how many organs to which it has metastasized are considered (known as the TNM classification system)[2].

While cancer is a current focus in modern scientific research, it is a problem that has existed for centuries. There have been several breakthroughs in methods of treatment since the first recorded cases of cancer. And while medicine has made drastic leaps since the time of ancient Egypt, there is much progress to be made. In order to put the course of treatments into perspective one must go back to the beginning and retrace the course of cancer treatments.

Ancient Egypt to Modern Day

Cancer first got its name from Hippocrates – the father of western medicine[3]. While Hippocrates may have been the first to name this disease, cancer had been known to exist for much longer. The first evidence of the disease includes the abnormal bone growths seen on some ancient Egyptian mummies. The first known text on cancer also dates back to ancient Egypt. The Edwin Smith Papyrus describes the ancient Egyptians attempt to cauterize breast cancer tumors, and the text concludes that there is no cure for this ailment.[4]

It was almost unheard of for a person to survive breast cancer until the introduction of mastectomies. In the early 1600's mastectomies became the primary treatment of breast cancer in Germany, and within the next few centuries this treatment method spread to other western cultures; including the United States. At this time the twenty year odds of surviving breast cancer were still 1 in 10. It wasn't until William Stewart Halstead from Johns Hopkins University developed the radical mastectomy that the twenty year odds of surviving breast cancer rose to fifty percent (a radical mastectomy involves removing the breast tissue, lymph nodes under the armpits, and the chest muscles). Even with the advent of chemotherapies, super-radical mastectomies, and lumpectomies, this was the last great improvement to the 20 year survival rate of breast cancer patients in the 20th century.

In the late 1990's it was found that the survival rate of people diagnosed with cancer had increased from 50% to 68% since the late nineteen seventies. This is attributed to the increased ability to diagnose cancer at an early stage, as well as improved treatments. Current treatments include surgery, radiation, hormone therapy, biological therapy, targeted therapy, and chemotherapy (above reference). It was also around this time that people with early stage breast cancer were treated with both surgery *and* chemotherapy. This new approach came after the repeated confirmation from researchers that chemotherapy helped patients stay cancer free for longer periods of time.

Chemotherapy

A Brief History

In 1909 the first modern chemotherapy agent was discovered by physicist Paul Ehrlich – the man who coined the term chemotherapy.[5] Ehrlich's objective was to find drugs that killed the disease without harming the person, and, in that pursuit, he discovered that arsphenamine – a drug which killed the bacteria that caused syphilis. Arsphenamine expanded to the use of sulfonamides and penicillin.[5]

It wasn't until the 1940's that chemotherapy – nitrogen mustards and folic acid – was used to treat cancer.[6,7] This line of research started as a result of Dr. Stewart Francis Alexander's findings during the autopsies of people exposed to mustard gas bombs during World War II.[6] He found that mustard gas reduced the reproduction of cells that normally rapidly divided. Nitrogen mustards were then studied in rats, and subsequently patients with non-Hodgkin's lymphoma. It was discovered that the drug reduced tumor size for a brief period, and therefore chemotherapy was shown to be a possible treatment for cancer. [6] After this time the word 'chemotherapy' became best known as a term for cancer treatment.

In 1965 combination chemotherapy's revolutionized cancer treatment.[6] Taking a cue from the treatment of tuberculosis, scientists came up with the idea of using several drugs that have different mechanisms of action in one treatment. This would make it more difficult for cancer cells to become resistant

to chemotherapies, as well as treat cancer cells in different stages of development. The first combination therapy (POMP regimen) resulted in long term remission in children with acute lymphoblastic leukemia.[6] Combination therapy is used in almost all chemotherapy treatment today.

Around this time the idea of adjuvant therapy took hold. It was shown that chemotherapy was more effective in smaller tumors; adjuvant therapy is the use of chemotherapy after the surgical removal of cancer.[8] Several studies showed that adjuvant therapy improved the odds of survival in people with cancer. An increase in survival rate was especially noticed in people with late stage cancer.[8]

Classes of Anticancer Drugs

There are several different mechanisms and sites of action for chemotherapies (Figure I.1).[9] The more commonly studied (or traditional) classes include: alkylating agents, antimetabolites, plant alkyloids and terpenoids, vica alkyloids, podophyllotoxin, taxanes, topoisomerase inhibitors, and cytotoxic antibiotics. These drugs target rapidly dividing cells, including both cancerous and healthy tissues (such as hair, gastrointestinal, epithelium, and bone marrow).[9] Several of these classes will be discussed, after which an in depth presentation of the mechanisms most relevant to important metal based compounds with anticancer activities will be provided.

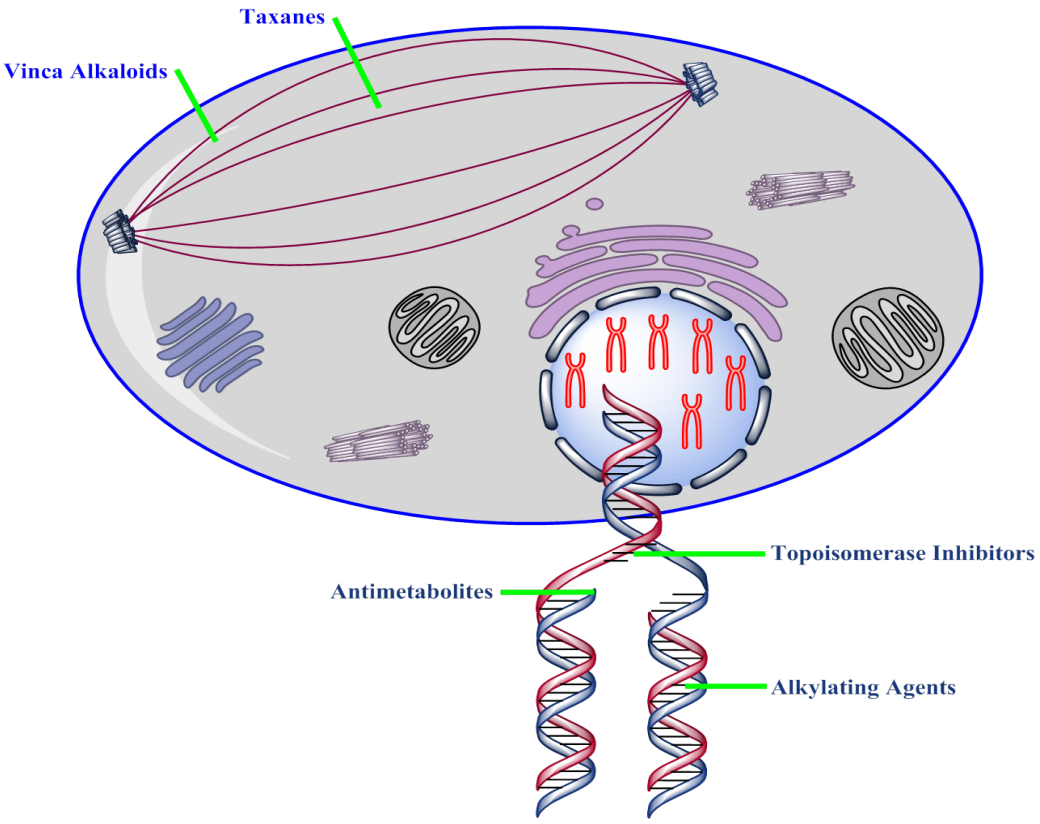

Figure I.1. Model of *in cellulo* drug targets (adapted from reference 8).

Antimetabolites work by inhibiting the ability of the cells to make or replicate DNA or RNA.[10] There are three types of antimetabolite drugs; those that work by impairing folic acid, mimicking purines, or mimicking pyrimidine.[10] Antifolates work by inhibiting the production of tetrahydrofolate, an essential compound in the synthesis of purines and pyrimidines. This leads to a decreased synthesis of DNA in these cells. Antifolates was one of the first classes of chemotherapy drugs used, first discovered in 1948 when folic acid was used to treat leukemia[11]. Purine and pyrimidine analogs work by being incorporated into the DNA before replication. This inhibits the ability of DNA to be replicated.[11] Antimetabolites are more effective in rapidly dividing cells. They affect the cell in the S phase; which is when the cell starts to make new DNA for replication (Figure I.2).[11]

Mitotic inhibitors encompass a large group of anticancer drugs, for example plant alkaloids and terpenoids, vinka alkaloids, as well as taxanes.[12] They work by inhibiting the ability of the cell to undergo mitosis. An example of how some mitotic inhibitors work (eg vinka alkaloids and plant alkaloids) is by preventing the formation of microtubules; while taxanes prevent the function of microtubules.[12] Microtubules are responsible for pulling the cell apart during reproduction, and so disrupting the function of microtubules prevents or slows cell reproduction. Mitotic inhibitors work during the M phase of the cell cycle (Figure I.2).[12]

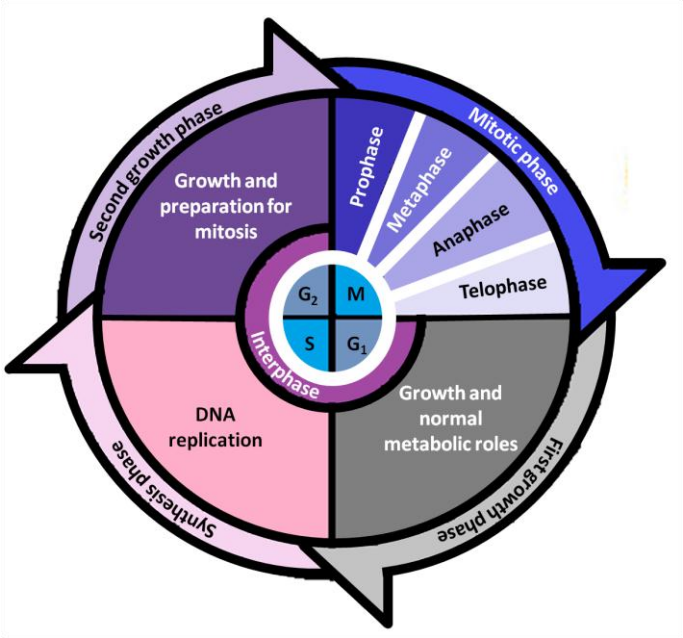

Figure I.2. Mitosis cell cycle.

Cytotoxic antibiotics work by affecting the DNA. One study showed that mytomycins work by cross linking DNA, causing a leasion that results in cell death.[13] The major class of cytotoxic antibiotics is anthracyclines; which have several known mechanisms of action.[14,15] The first is the ability to intercalate into DNA and RNA, which inhibits the replication of DNA and RNA. Anthracyclines also inhibit the function of topoisomerase, which is responsible for interconverting the topological isomers of DNA during replication.[14] Interfering with topoisomerase leads to cell death. Finally, these compounds can also create oxygen radicals with the assistance of iron.[14] These oxygen radicals can damage both the cell membrane and DNA. Anthracyclines are one

of the most affective chemotherapies, used for the treatment of many types of cancer.[15] The major problem with these compounds is their cardiac toxicity; which is so bad that a lifetime cap is put on the amount of many cytotoxic antibiotics a person can receive.[14]

While many cytotoxic antibiotics are considered topoisomerase inhibitors, there is a class of chemotherapy agents devoted to this mechanism of cell death.[16] There are two types of topoisomerase enzymes, namely type I and type II.[17] Both type I and type II can be further broken down, but in this section they will be discussed more generically. Topoisomerase I works by breaking the phosphodiester bond on one strand of the DNA in order to decrease the linking number, whereas topoisomerase II works by breaking the phosphodiester bond on both strands of DNA to decrease supercoiling. Topoisomerase inhibitors are classified based on whether they interfere with topoisomerase I or II. Topoisomerase inhibitors work by binding to topoisomerase, therefore preventing it from reanealing the break in the phosphodiester bond, and leading to cell death (Figure I.3).[17,18]

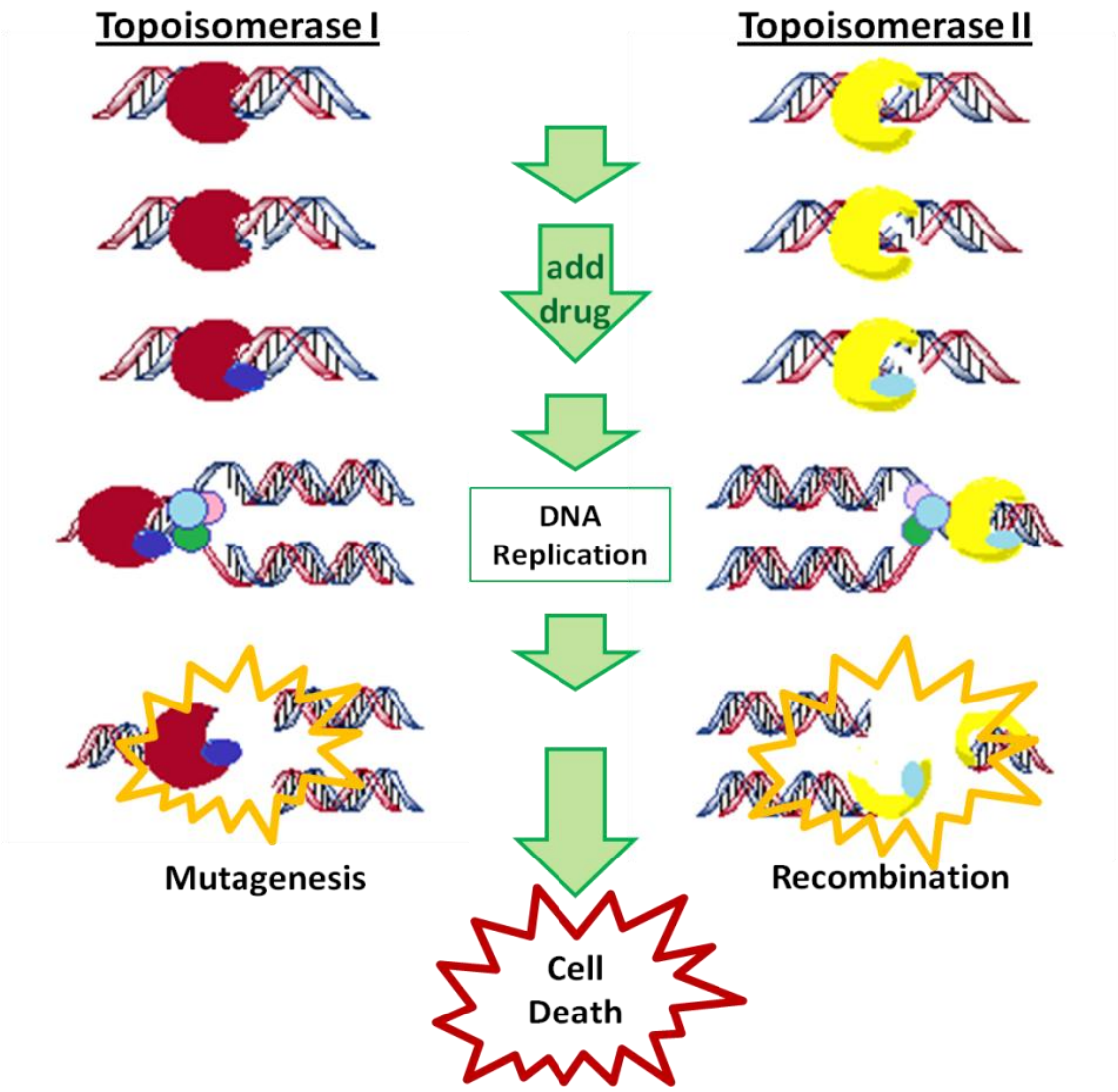

Figure I.3. Mechanism of topoisomerase inhibitors (adapted from reference 17).

Alkylating agents are electrophilic molecules that work by alkylating nucleophilic biomolecules – most importantly DNA bases. These compounds are capable of alkylating many sites on the DNA bases; such as the N1, N3, N^6 and N7 positions of adenine, N1, N^2, N3, N7, and O^6 positions on guanine, N3, N^4 and O^2 sites in cytosine, and N3, O^2, and O^4 positions in thymine (where the superscripted numbers indicate exocyclic atoms on the nucleobase) (Figure I.4).[19] These DNA base sites do not all have equal reactivity with alkylating agents. The electrophillicity of the compounds were calculated using the Swain-Scott equation, found in equation 1, where *s* is the substrate concentration, *n* is the nucleophilic constant for a nucleophile, *k* is the pseudo first order rate constant, and k_0 is the normalized rate constant. The Swain-Scott equation relates the rate constant with the normalized reaction rate (normalized to water as the nucleophile) to the nucleophilic constant and substrate constant. The less electrophilic compounds are the ones that react with the less nucleophilic oxygen sites – such as O^6 on guanine, and the oxygen atoms on the phosphodiester backbone of DNA.[19] However, the most active site of alkylation is the N7 of guanine, followed by the N3 site on adenine (Table I.1).[19]

$$sn = \log_{10} (k/k_0) \qquad (1)$$

Table I.1. Relative proportions of alkylation of base pairs (adapted from reference 19).

	% of total alkylation after reactions with:		
Adduct	**Dimethyl-nitrosamine, *N*-methyl-*N*-nitrosourea, 1,2-dimethylhydrazine**	**Methyl methane-sulfonate**	**Diethylnitrosamine, *N*-ethyl-*N*-nitrosourea**
N^1-Alkyladenine	0.7	1.2	0.3
N^3-Alkyladenine	8	11	4
N^7-Alkyladenine	1.5	1.9	0.4
N^3-Alkylguanine	0.8	0.7	0.6
N^7-Alkylguanine	68	83	12
O^6-Alkylguanine	7.5	0.3	8
N^3-Alkylcytosine	0.5		0.2
O^2-Alkylcytosine	0.1		3
N^3-Alkylthymine	0.3		0.8
O^2-Alkylthymine	0.1		7
O^4-Alkylthymine	0.1-0.7		1-4
Alkylphosphates	12	1	53

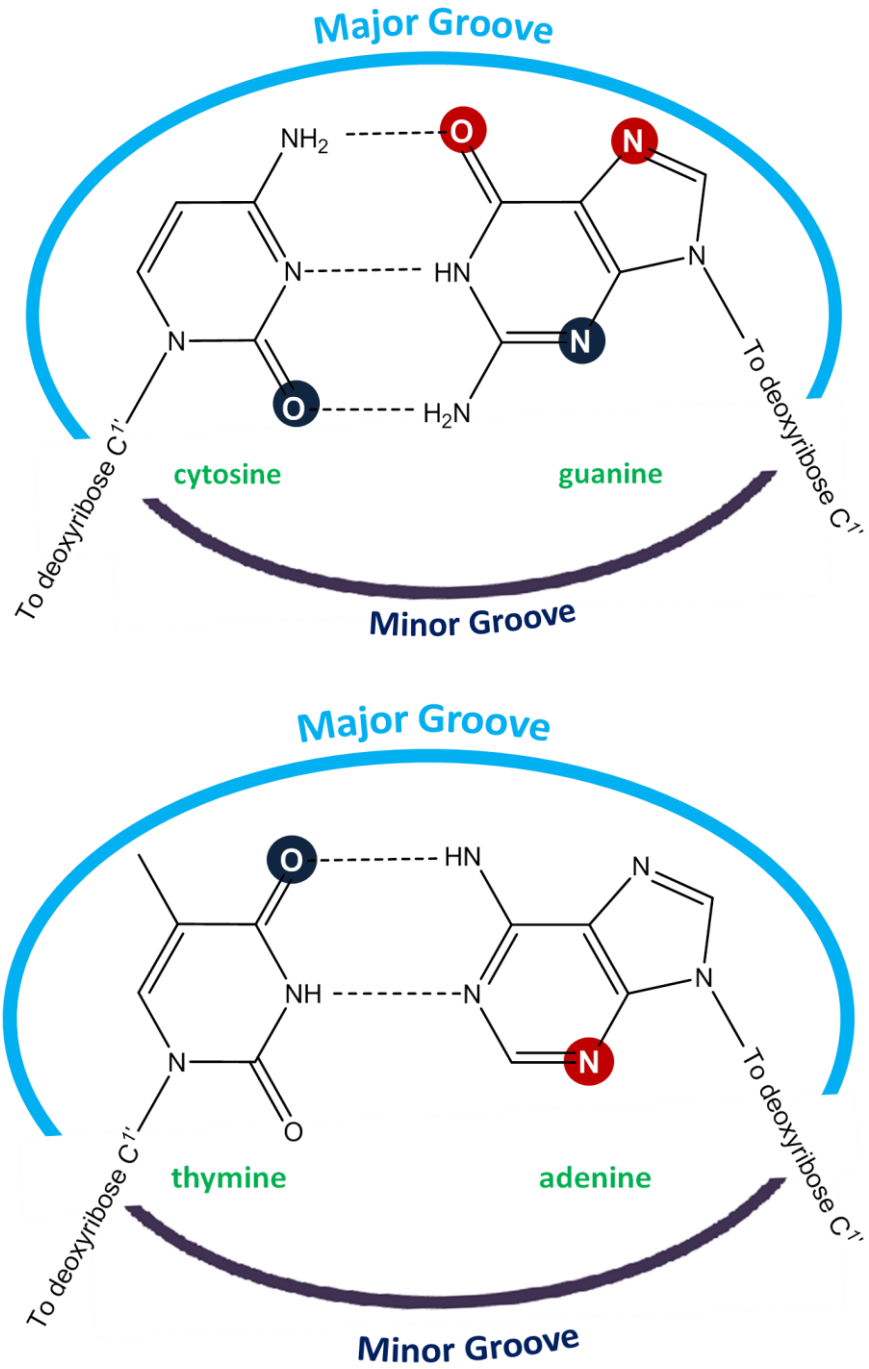

Figure I.4. Schematic figure of prominent alkylation sites on DNA base pairs (adapted from reference 19).

There has also been evidence that the position on DNA being alkylated is not random. The N7 position on guanine is more nucleophilic in a guanine rich sequence.[20] Sterics also affect the ability of a site to be alkylated. In B-DNA (which is the most common form), the N7 and O^6 of guanine are in the less sterically hindered major groove, whereas the N3 of adenine is in the minor groove (Figure I.4).[20] The steric properties change for the Z-DNA, a left-handed structure that is present in small fragments at biological conditions. In Z-DNA the major and minor groove have similar widths, allowing other sites such as C8 on guanine to become accessible.[20]

Alkylating agents are most commonly cell-cycle nonspecific, meaning they target cells at all phases of the cell cycle.[19,21] This category of drug is used to treat a wide variety of cancers, but is more active towards slow growing cancers such as solid tumors and leukemia.[21] These compounds also target cells that rapidly divide, such as cancer cells, but also the cells in the gastrointestinal tract, hair, bone marrow, ovaries, and testicles.[9,21] This leads to many side effects, including infertility and cancer. Alkylating agents can either be monofunctional, or difunctional. Monofunctional compounds can alkylate only one position, whereas difunctional compounds can react with two sites. Difunctional compounds can cause DNA cross-linking if the two reactive sites are on opposite strands of the DNA.[21]

Cisplatin

In the history of chemotherapy, the modern era began in 1965. This was an important year in cancer research, as well as medicinal inorganic chemistry, as this was the year that Dr. Barnett Rosenberg discovered the antibacterial effect of *Cis*-diamminodichloro platinum (II) (cisplatin).[22] Cisplatin was first discovered by Peyrone in 1845, and in 1983 Alfred Werner was able to structurally characterize the compound, and separate it from its *trans* isomer. In the 1970's cisplatin became the first inorganic anticancer drug, becoming the most important compound in modern medicinal inorganic chemistry.

In Dr. Barnett's study, cisplatin was inadvertently formed by the electrolysis of a platinum electrode during an experiment designed to study the effect of electromagnetic radiation on cell mitosis.[23] The experiment first used *Escherichia coli (E coli*), due to the fact that this bacteria is much easier to deal with than human cells. During this experiment Dr. Barnett wanted to use a platinum electrode due to the inert nature of the metal. However, the experiments showed that the reproduction of the bacteria was halted. This conclusion was based on the rod-like shape of the bacteria, a characteristic of bacteria that cannot replicate. After repeated experiments $(NH_3)_2Pt(Cl)_2$ was found to be the active compound responsible for the inhibition of binary fusion in *E coli*.[22] This species is formed from the platinum released from the electrode and the electrolyte, aqueous NH_4Cl, that was used. Further work examined the

most active platinum (II) analogue, comparing *cis*-$Pt(NH_3)_2Cl_4$, *cis*-$Pt(NH_3)_2Cl_2$, $Pt(NH_2CH_2CH_2NH_2)Cl_2$, and $Pt(NH_2CH_2CH_2NH_2)Cl_4$.[22] Rosenberg expanded this research to different late transition metal compounds to study their effect on the binary fusion of *E coli* (Table I.2).[22]

Table I.2. Compounds tested for biological activity (adapted from reference 22).

A. Caused bacterial death	B. No change	C. Caused elongation
$CoCl_2$	$Co(NH_3)_6]Cl_3$	K^+, NH_4^+, H^+ --$[PtCl_4]$=
$(NH_4)_2IrCl_6$	$K_2Ir(NO_2)_6$	$(NH_4)_2PtBr_6$
$NiCl_3$	$[Ni(NH_3)_6]Cl_2$	$(NH_4)_2PtI_6$
$(NH_4)_2OsCl_4$	*Cis* and *trans*	$[Pt(en)_3]Cl_4$
$(NH_4)_2PdCl_4$	$[Rh(en)_2Cl_2]NO_3$	$RhCl_3$
$[Rh(NH_3)_5Cl]Cl_2$		$(NH_4)_3RhCl_6$
$PdCl_2$		$[Ru(NH_3)_4ClOH]Cl$

Cisplatin is one of the most affective anticancer compounds to date. It is used to treat several types of cancer, including ovarian, head, neck, bladder, cervical, and lung.[23,24] Cisplatin is affective for many reasons; it is able to cross the cell membrane, or nonpolar regions due to its electronutrality. Once inside the cell, the chlorine ligands are easily replaced by water, making the compound active.[24,25] The cis position of the leaving groups makes it capable of binding interstrand, or intrastrand crosslinking of DNA, as well as DNA protein cross linking (Figure I.5).[24]

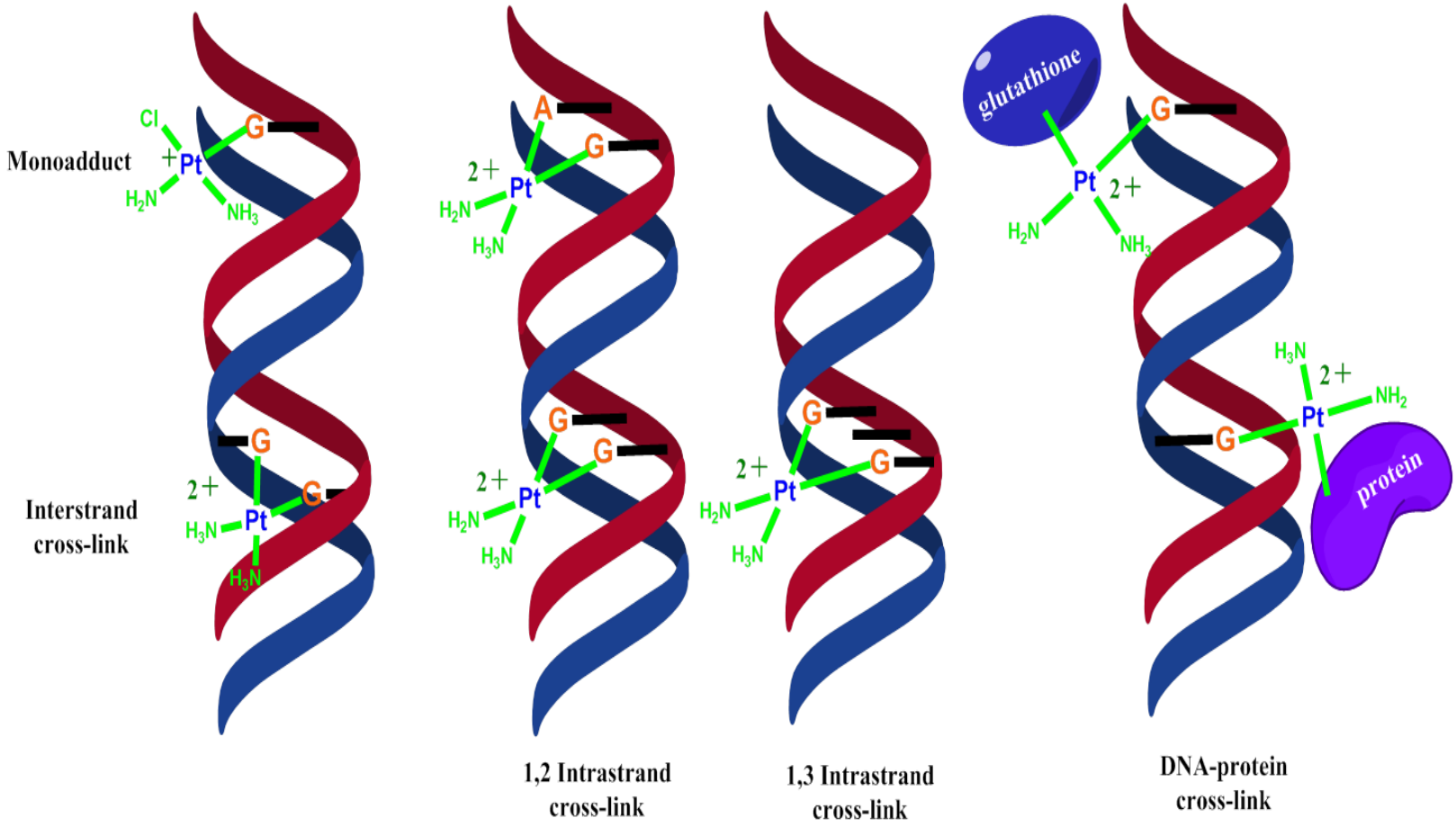

Figure I.5. Cisplatin binding modes to DNA and biomolecules.

Cisplatin is introduced to the body via several methods, depending on the form of cancer it is targeting. It is most typically given intravenously at a rate of 1mg/minute,[24-26] but for liver cancer, melanoma, or glioblastoma it is administered intraarterially.[26] For ovarian cancer it is an interparitoneal injection.[26,27] If there is a high chlorine concentration in the blood then the compound remains inert until it enters the cell, and so excess saline is administered with the drug.[26] If there is a low chlorine concentration in the blood the chlorine on the cisplatin will dissociate and the compound will become active in the blood stream, which interferes with its anticancer activity.[25] The first organs in which the concentration of cisplatin peaks are the kidneys. It takes a few days for concentrations to peak in the liver, testes, and intestines.[23,26]

Once the drug reaches the cell it enters through mechanisms, including Copper transporter 1, organic cation transporter, and passive diffusion.[24,25,28] Inside the cell cisplatin loses its chlorine ligands because of the low concentration of chlorine inside the cell (3-10 mM Cl^- concentration inside the cell versus 100 mM concentration outside the cell). They are replaced by water or hydroxyl groups, thereby activating the compound (Figure I.6).[25,29] Cisplatin is active towards many biomolecules, specifically thiol groups, RNA, mitochondrial DNA, and nuclear DNA (Figure I.7).[25] Only 1% of cisplatin has been shown to reach the nuclear DNA, but this interaction is believed to be the cause of cell death.

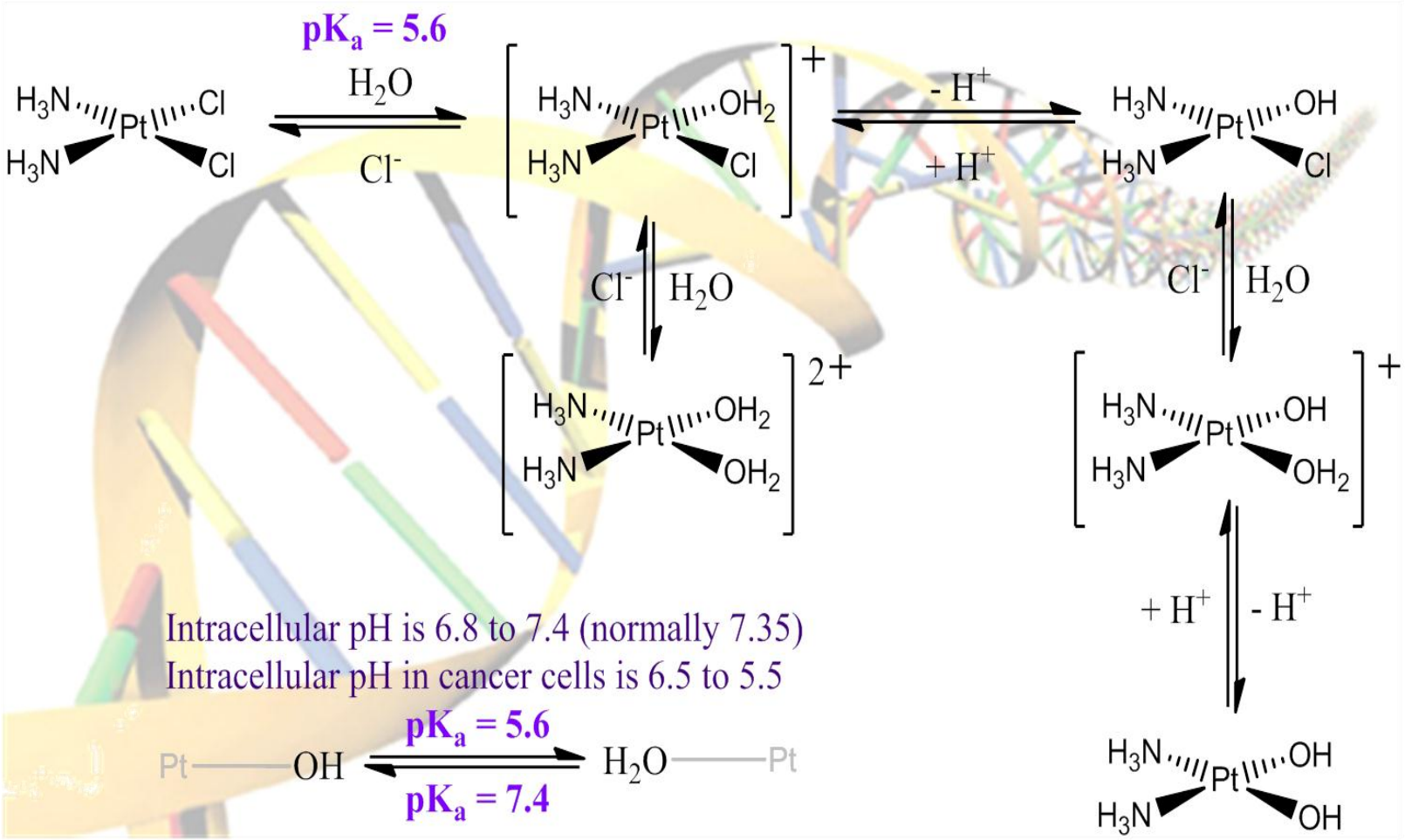

Figure I.6. Activation of cisplatin.

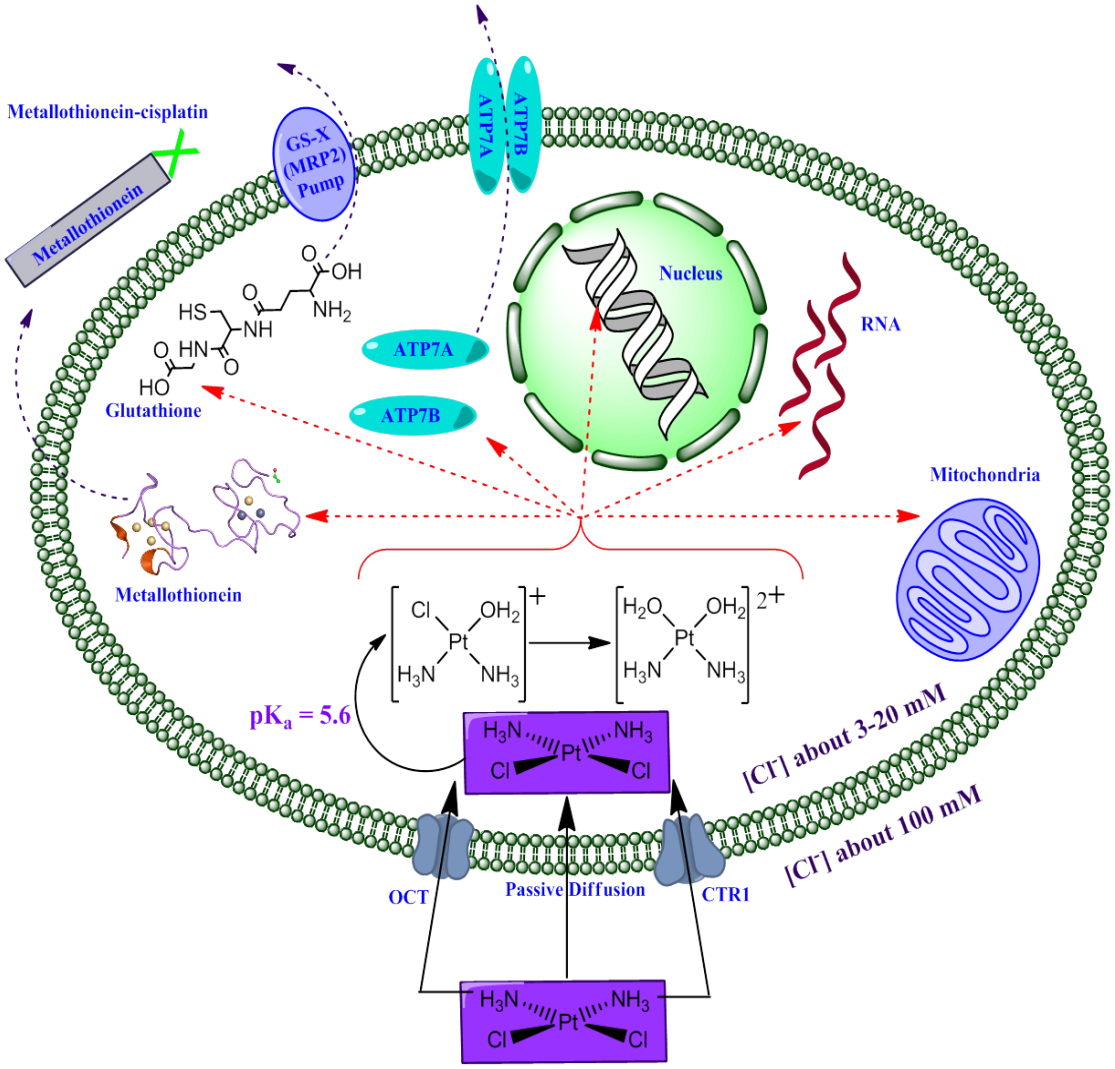

Figure I.7. Interactions of cisplatin *in cellulo.*

The active form of cisplatin is an electrophile, commonly targeting phosphate, amino, sulfhydryl, carboxyl, and hydroxyl groups. Therefore, cisplatin is classified as an “alkylating agent” (discussed above). Similar to other alkylating agents, cisplatins main target is the N7 of guanine and the N3 of adenine.[25,30] It has been found that the most common form of bonding is intrastrand cross-linking, with 65% 1,2-d (GpG), 25% 1,2-d (ApG), 5–10% 1,3-d (GpNpG).[31] These interactions comprise about 90% of the DNA-cisplatin lesions, and they induce a 26° bend toward the major groove, and unwind supercoiled DNA by 13°.[32] Interstrand adducts also exist, and exhibit more unusual properties such as the presence of cisplatin binding in the minor groove, DNA bending towards the minor groove, and major DNA unwinding.[31]

It is thought that the anticancer properties of cisplatin are due to their interactions with nuclear DNA, both intra- and interstrand cross-linking.[25] Much effort has been expended on elucidating the reason for cell death, either apoptosis or necrosis.[33] It was first posited that the reason for cell death was due to the inhibition of DNA synthesis.[34-36] Soon after, evidence emerged that dispelled this theory when DNA repair deficient cells underwent apoptosis at cisplatin concentrations too low to arrest DNA synthesis. It was also shown that

repair proficient cells were able to live at concentrations of cisplatin that should inhibit DNA synthesis.[35,36] It was clear that repair mechanisms were important to the survival or demise of cells treated with cisplatin, but research is still needed on the exact mechanisms responsible for apoptosis, necrosis, or survival of the cell. To this end the role of HMG1/2, mismatch repair (MMR), DNA-dependent protein kinase (DNA-PK), nucleotide excision repair (NER), and homologous recombination (HR) will be discussed.

The role of HMG1 and HMG2 proteins in conjunction with cisplatin has been studied. HMG1 and HMG2 are small proteins found in eukaryotic cells, and while their functions are not fully understood, they are thought to have a role in DNA replication, transcription and chromatin assembly.[37] HMG1 and HMG2 contain HMG box domains, which consists of three α-helical regions shown to bind to DNA. In a cancer infected cell treated with cisplatin these proteins have an affinity for binding to the kinked structure of DNA, which blocks other repair proteins from working. This leads to a slow repair, or more commonly, cell death (Figure I.8).[33]

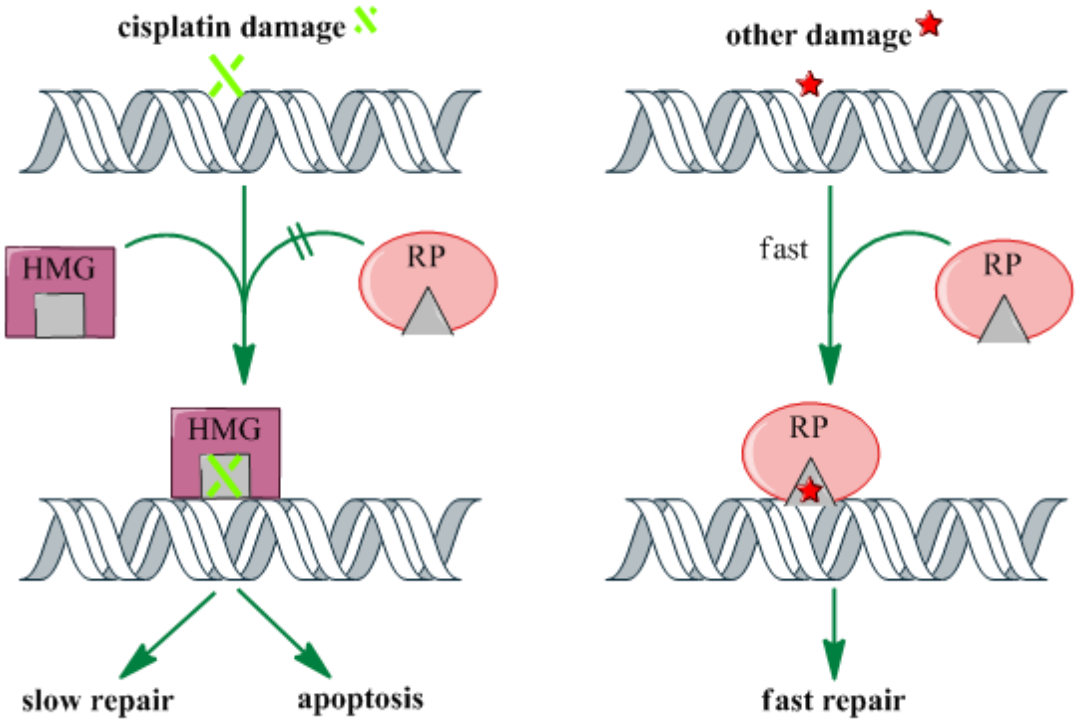

Figure I.8. DNA repair after being damaged by cisplatin (adapted from reference 33).

MMR has also been shown to interact with DNA bound cisplatin – leading to cell death independently of other repair mechanisms.[36,38,39] The exact mechanism has not yet been proven and there are a few theories as to exactly how MMR induces apoptosis.[36] What is known is that in cells treated with cisplatin, MMR causes intrinsic apoptitic pathways through an increase in cytochrome c in the cytoplasm, which promotes the cleavage and activation of caspase-9, which subsequently cleaves and activates caspase-3, an effector caspase that degrades intracellular proteins causing cell death.[36]

In normal cells there are repair mechanisms for double-strand breaks in nuclear DNA. The two mechanisms employed by the cell are recombination repair, and nonhomolougous end-joining (NHEJ).[40,41] NHEJ is the mechanism that has relevance in the toxicity of cells treated with cisplatin; more specifically DNA-PK has been implicated in pathways of cisplatin induced cell damage.[42] The protein DNA-PK is brought to a double-strand break by the heterodimer Ku70/Ku80, forming a multiprotein. In normal cells this functions to directly join double strand breaks, however, in cancer cells it is also responsible for cell-interdependent signaling in conjunction with gap junctions to send cytotoxic signals to cells surrounding the cisplatin treated cell.[42] One study showed that cisplatin had a reduced toxicity in cells lacking DNA-PK, Ku80, and gap junctions.[43,44] This same report also noticed that the confluency of the cells affected the toxicity of cisplatin. When cells are close together there is a higher cytotoxicity, than cells that are further apart. It is thought that cell-

interdependant mechanisms are responsible for one third of the toxicity of cisplatin (the other two thirds is a result of cell-autonomous pathways such as those mentioned above).[43] This result is dependent on the cell line being used as well. It has been shown in cisplatin sensitive laryngeal tumors that cell-interdependent mechanisms of cisplatin, specifically relating to gap junctions, reduce the motility of cancer cells.[43]

DNA repair pathways can also lead to DNA repair and cisplatin resistance. The main repair pathway implicated in cisplatin resistance is nucleotide excision repair (NER).[45] NER is responsible for repairing DNA that has major structural flaws, and there are two pathways by which this can happen, namely global genomic NER and transcription coupled NER.[46,47] TC-NER is the pathway that was shown to be active in repairing cisplatin damaged DNA.[48] The DNA lesion induced by cisplatin stalls RNA polymerase II, signaling NER to the repair site. NER is most efficient at repairing single strand breaks, and is used on bulky structural DNA damage – which makes it more effective on the 1,3 intrastrand binding mode of cisplatin.[36,48]

There are other DNA repair pathways that lead to cisplatin resistant cells, although to a lesser extent than the NER pathway. These include DNA polymerase beta, C-fos and C-myc, and p53 (a gene that is intended to suppress tumors). Along with DNA repair pathways, thiol rich biomolecules such as glutathione and metallothionein can cause resistance to cisplatin.[49]

Metallothione (MT) is a protein that has a low molecular weight and a high content of cysteine residues. Its exact purpose is not fully understood, but they are known to bind heavy metals, and are believed to play a role in both protecting cells against heavy metal toxicity and regulating the concentration of vital metals in the cell.[50-52] MT is shown to bind cisplatin *in vivo* through one of its SH moieties.[53] Upon binding, the MT-cisplatin adduct is exported from the cell, and can be seen in increased concentrations in the blood stream.[54] It has also been shown that as the MT concentration inside a cell increased, the effectiveness of cisplatin decreased.[55]

Aside from DNA repair mechanisms; there are other factors that induce acquired resistance to cisplatin in cells. Low concentrations of intracellular cisplatin cause have been postulated to cause resistance to cisplatin.[53] Low intracellular concentrations can be caused by down-regulation of the receptors that allow cisplatin to enter the cell.[53] When cisplatin does enter the cell, it can interact with biomolecules other than intended targets such as glutathione and metallothionein. These interactions can lead to the removal of cisplatin, and the resistance of cancer cells to this drug.[53] The role of glutathione in cisplatin

resistance has been debated for the last several decades; but recent evidence has led to strong indication that glutathione does indeed induce cisplatin resistance in cancer cells.[56] This study has looked at cisplatin resistant cells after inhibiting the reactivity of glutathione. The results showed that the cells which were resistant to the toxic effects of cisplatin before the inhibition of glutathione were now susceptible to the drug.[49]

In conjunction with cell resistance to cisplatin, the severe side effects attributed to the toxicity of cisplatin to healthy cells is a limitation of cisplatin. The dose limiting side effects of cisplatin include nefrotoxicity (damage to the kidneys), ototoxicity (damage to the ear – mainly the cochlea and auditory nerve), and nausea and vomiting.[23] Because of the severe side effects, and inherent and acquired resistance to cisplatin, there have been several generations of platinum and other inorganic analogues developed in an effort to improve upon the anticancer properties of cisplatin by minimizing the side effects, reducing the resistivity, and allowing for a more convenient method of delivery (Figure I.9).[23]

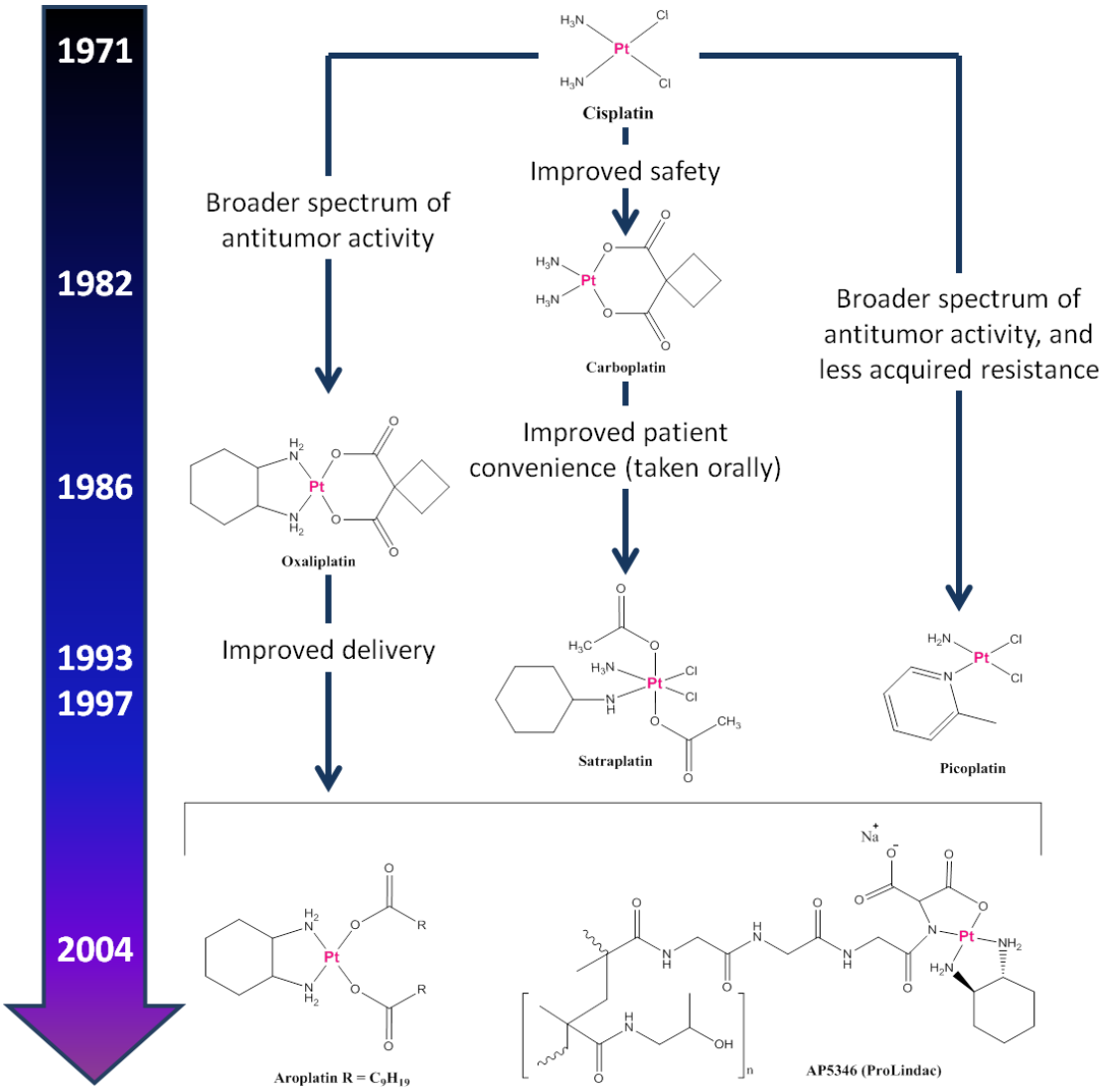

Figure I.9. New generations of platinum based drugs (adapted from reference 23).

New Generations of Cisplatin

New generations of platinum based anticancer drugs have been developed in an effort to improve upon cisplatin.[57,58] The first cisplatin analogue to be approved for use in the United States was carboplatin.[23] Carboplatin was first approved as a palliative treatment for ovarian cancer.[23] Carboplatin was developed in an attempt to reduce the toxicity of cisplatin, while maintaining its mechanism of action by making a more stable leaving group. The toxicity of carboplatin is less than that of cisplatin, with the main dose limiting toxicity being myelosuppression (bone marrow suppression) and thrombocytopenia (decrease in blood platelets); the nephrotoxicity that is the dose limiting side effect in cisplatin is greatly reduced. The nausea and vomiting associated with cisplatin is also reduced in carboplatin. The range of effectiveness for carboplatin is mainly ovarian cancer, but it is an adjunct therapy for other cancer types such as non-small-cell lung cancer (Figure I.10).[23]

New cisplatin analogues have a broader spectrum of antitumor activity with reduced resistance.[23] There are several platinum based drugs that have been approved by the FDA, or are currently under investigation, including: oxaliplatin, satraplatin, and picoplatin. Oxaliplatin was the third platinum based drug approved by the FDA, and has been shown to be effective against some cell lines that are resistant to cisplatin and carboplatin. This is thought to be caused by the ability of oxaliplatin to bind DNA via modes not observed with

cisplatin, or carboplatin. As a result of the different antitumor activities, oxaliplatin is active against some cisplatin resistant cell lines. satraplatin is another example of a cisplatin derivative that has shown to be active against cisplatin resistant cells.[23] In addition to overcoming resistance mechanisms, satraplatin has also improved methods of delivery.[23] As previously mentioned, cisplatin is given intra-venously, intra-arterially, or as an inter-paritoneal injection. New analogues, such as satraplatin, can be taken orally and still show similar levels of antitumor activity (Figure I.11).[23] These new derivatives have improved upon cisplatin disadvantages, and one of the most studied bioactivities of cisplatin which leads to acquired resistance is the interaction with glutathione. Picoplatin, one of the most recent analogues, has reduced interaction with glutathione, and other biomolecules that contain thiol groups. This reduced interaction is believed to be due to the bulky groups that protect the platinum core from interaction with the thiol groups of glutathione, therefore reducing the amount of drug that is rendered inactive (Figure I.12).[23]

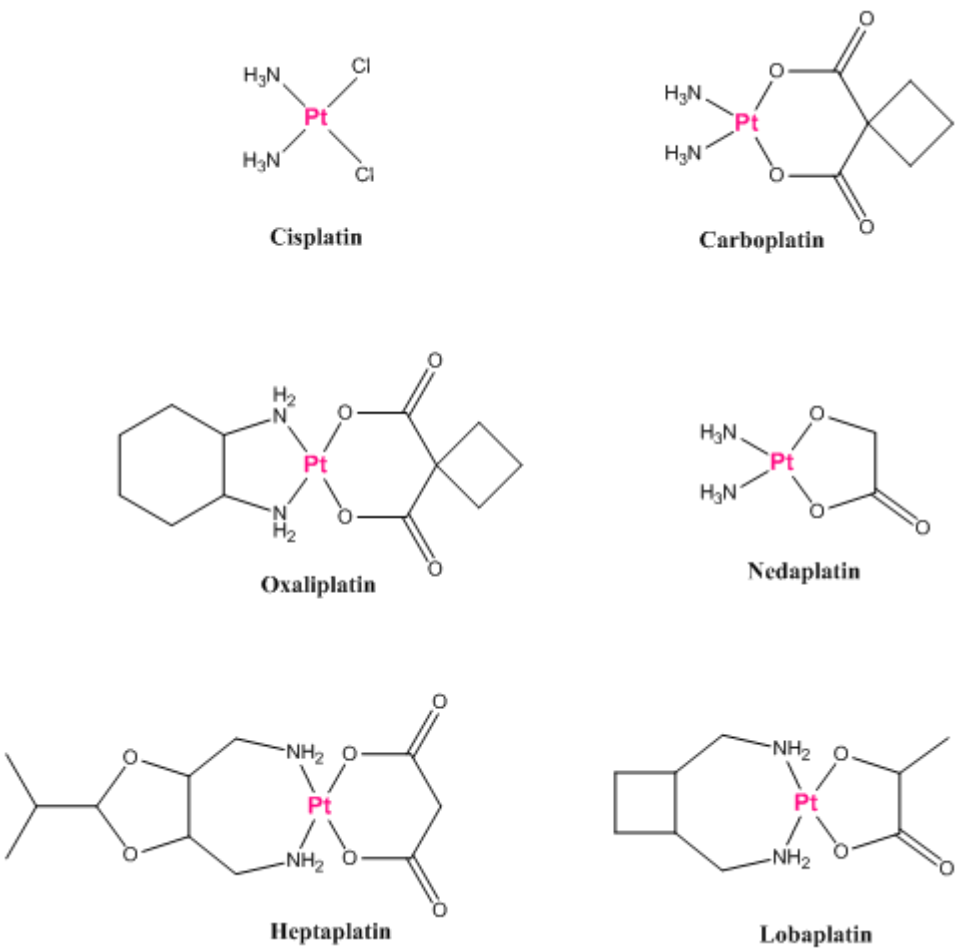

Figure I.10. Cisplatin drugs that are in, or are close to entering into, drug trials.

While these new platinum drugs have greatly improved the toxic side effects of cisplatin, efforts have been made to increase the specificity of platinum drugs to cancer cells.[23,57] To this end, there are drugs currently being tested by the FDA which use liposomes, or water soluble co-polymers, to target tumor cells. Aroplatin is the lead platinum based liposomal drug, and is being tested in colorectal cancer. The toxicity of aroplatin towards cancer cells is not as high as cisplatin, and further work is being carried out in an effort to improve anticancer properties. AP5346 is another platinum based drug which employs a water soluble polymer. This drug was developed to take advantage of the enhanced ability of tumors to take in and retain of macromolecules. The activation of this drug in more acidic environments could lead to enhanced ability to treat solid tumors which have a low pH.[23] Platinum based drugs have shown promising anticancer activity, particularly the platinum compounds with structures that differ from cisplatin, such as those with trans geometries or octahedral geometries, and also polynuclear platinum compounds, as well as compounds with ligands that are bulky or water soluble.[57] The success of these drugs has prompted research into the exploration of other metals that have promising anticancer properties as well.

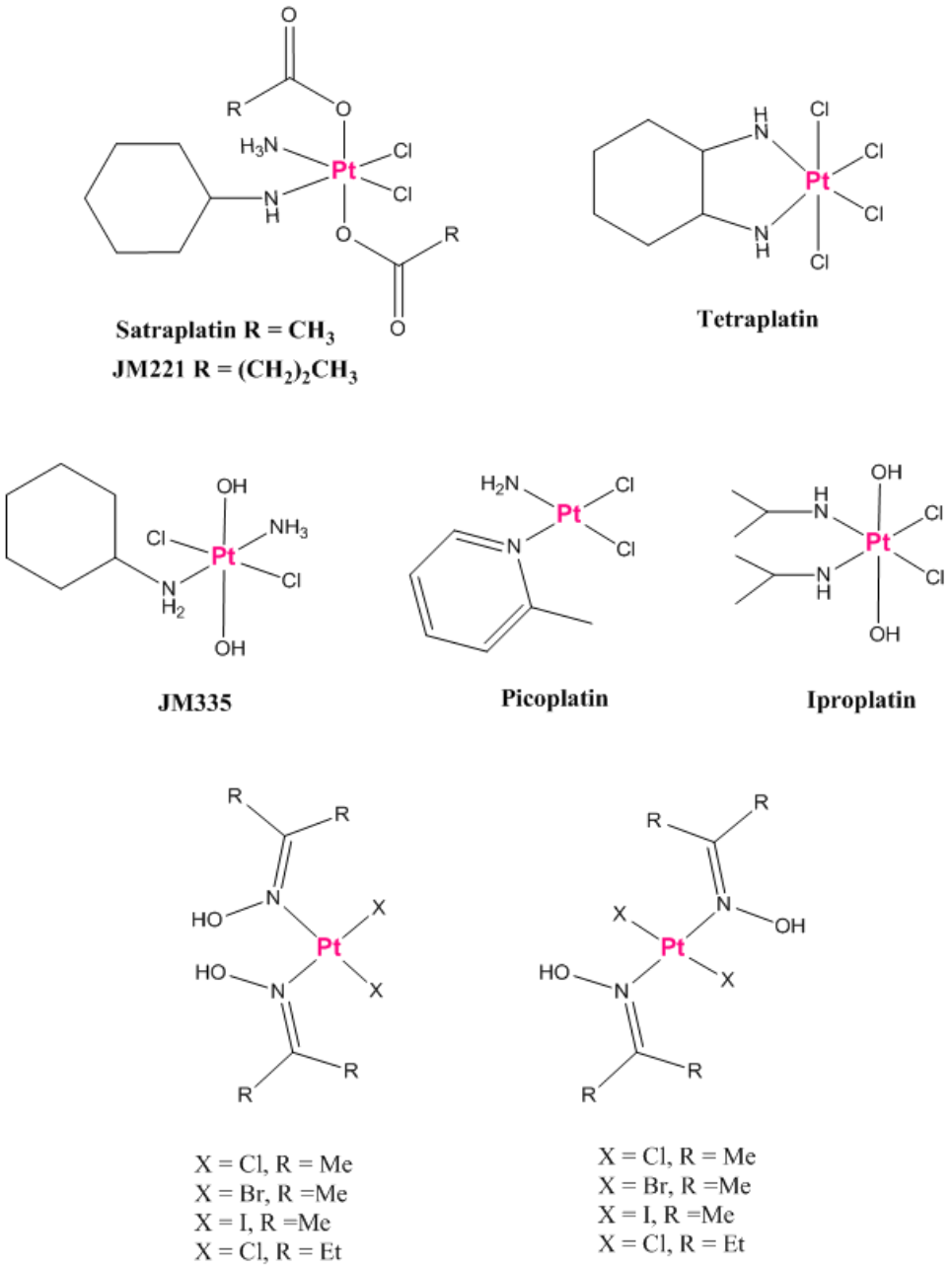

Figure I.11. Cisplatin and derrivatives that have been approved for use as a drug (not neccessarily in the United States).

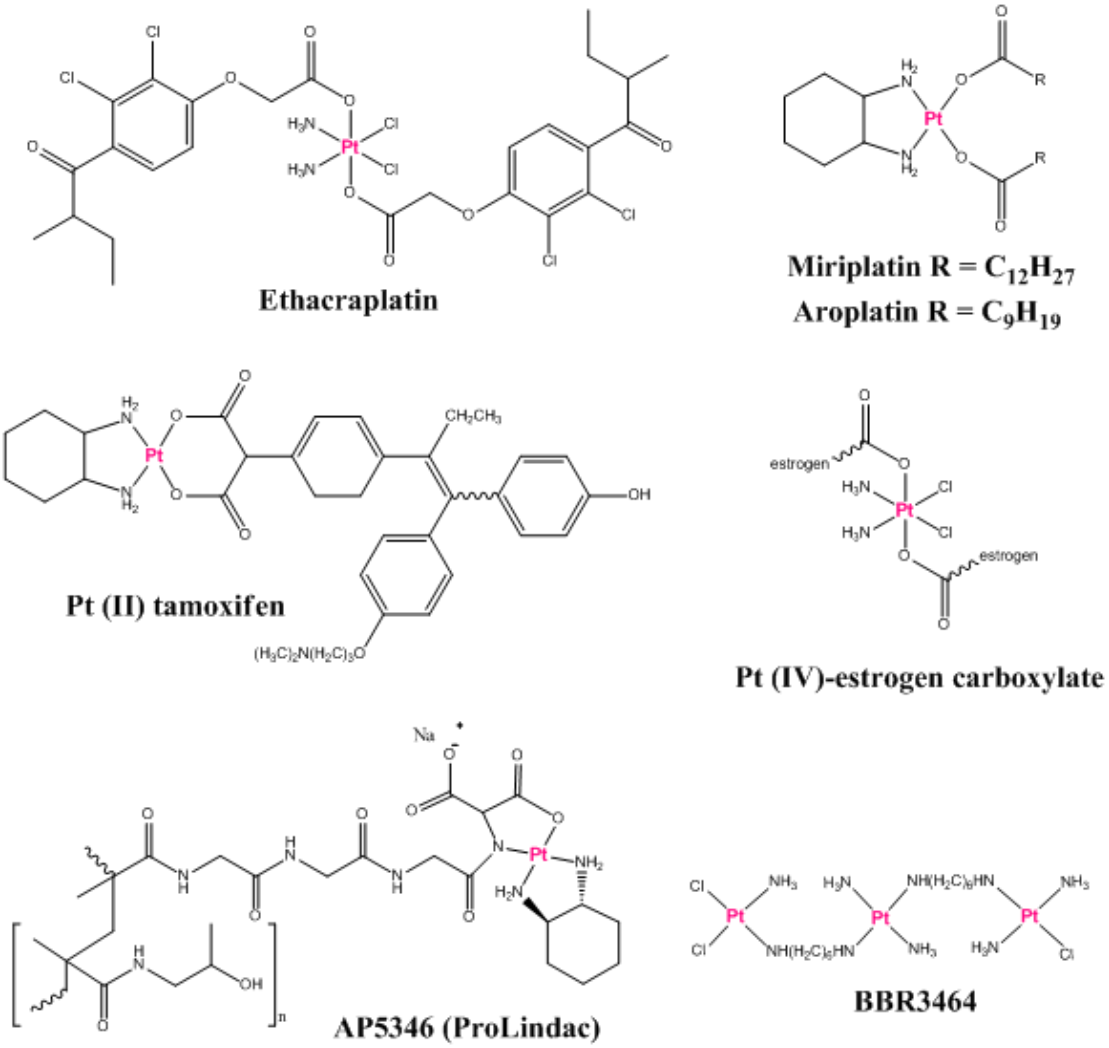

Figure I.12. Novel platinum based compounds

Inorganic Drugs

There are many metal based compounds that exhibit toxicity towards cancer cells. Metal centers such as vanadium, titanium, chromium, copper, iron, molybdenum, ruthenium, rhodium, osmium, rhenium, iridium, and gallium have been investigated.[58,59] The success of cisplatin opened the door for medicinal inorganic chemistry to develop, and the metal based compounds being explored have a range of activities from DNA intercalation to "trojan horse" clusters that house toxic compounds. Among the metal compounds that have shown biological activity are metallocenes, which are thought to be redox active towards biomolecules.[60] The redox potentials inside the cell are not known, and the mechanisms of these compounds are still under investigation. The most bioactive metallocene compounds to date are bent, with the two *cis* halide ligands. It is interesting to note that a derivative of ferrocene, ferroquine, is one of the metal complexes in the late stages of FDA testing (phase III); it has been shown to be active against malaria. Some of these ferrocene analogues have also been shown to cross the blood-brain barrier; something that most drugs cannot do.[60]

Ruthenium compounds have also shown promising activity that is dissimilar to cisplatin. Two ruthenium compounds, KP1019 and RuNAMI-A (Figure 1.13), were the first ruthenium compounds to enter clinical trials.[58,61] The compound KP1019 has activity against tumors, and RuNAMI-A is active against metastasized cancer cells. Another class of ruthenium compounds,

known as “RAPTA” compounds, have been probed for anticancer properties, and show similar activity to the RuNAMI-A. RAPTA compounds have a piano stool geometry, which allows for one side of the ruthenium compound to be hydrophobic (with respect to the aromatic group), with the other side containing ligands that are hydrophilic.

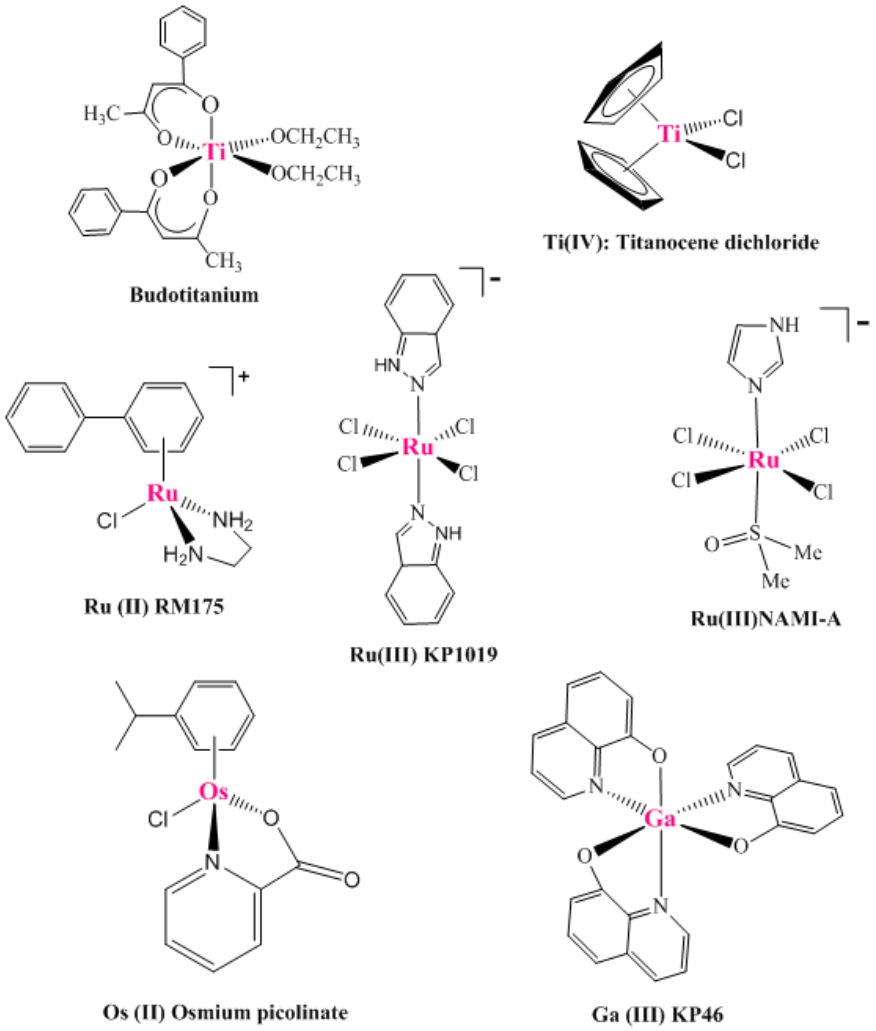

Figure I.13. Other metal based drugs that have shown anticancer properties.

Dirhodium Compounds

Dirhodium tetraacetate was first synthesized in 1963, and in 1970 the crystal structure was obtained. [62] This compound has a paddlewheel structure (Figure I.14), with the four acetate ligands binding in a bridging mode to the dirhodium core, with a Rh-Rh single bond of 2.40 ± 5 Å.[62] There are two different types of positions available for binding – the equatorial and the axial positions. The equatorial ligands bind more tightly to the dirhodium core, and are therefore more difficult to substitute. The axial positions are more weakly bound to the dirhodium core, and are usually occupied by the solvent in which the compound was las dissolved (commonly methanol, water, or acetonitrile).[62] An interesting property of this compound is that its color depends on its axial ligands. When water or other oxygen donating ligands are present, the molecule is a green-blue color. However, when nitrogen ligands occupy the axial positions the color is violet; sulfur causes a more burgandy color, and phosphorous bound axial ligands lead to an orange color. The spectroscopic changes introduced by the axial donor are caused by the fact that the LUMO is the σ* orbital, and thus the nucleophilic properties of the axial ligands effect the energy of this orbital. The Rh-Rh bond distance is not very dependent on the axial ligand (Figure I.14).[62]

The anticancer properties of dirhodium tetraacetate and some derivatives ($Rh_2(O_2C_2R)_4$, where R = CH_3, C_2H_5, and C_3H_7) were first reported in the late

1970's. This series was found to be active against Ehrlich ascites leukemia 1210, and sarcoma 180 and P388 cell lines.[63] While this series did not represent the properties of typical therapeutic agents they were shown to have good anticancer properties, and reduced side effects as compared to cisplatin. Further investigation into dirhodium compounds focused on paddlewheel compounds with varying electron donating properties.[64,65] It was found that dirhodium paddlewheel compounds with electron withdrawing groups, such as dirhodium tetrakis trifluoroacetate, exibit a higher toxicity against cancer cells.[9] The trifluoroacetic acid derivative was found to show activity against Ehrlich ascites tumors, and increased the lifetime of rats bearing this cancer. A similar derivative, trifluoroacetamide, (which binds rhodium through oxygen and nitrogen, as opposed to thrifluoroacetate which binds through only oxygen donors) was shown to have similar activity to cisplatin. This compound increased the lifetime of 90% of the rats bearing Ehrlich ascites tumors.[65,66]

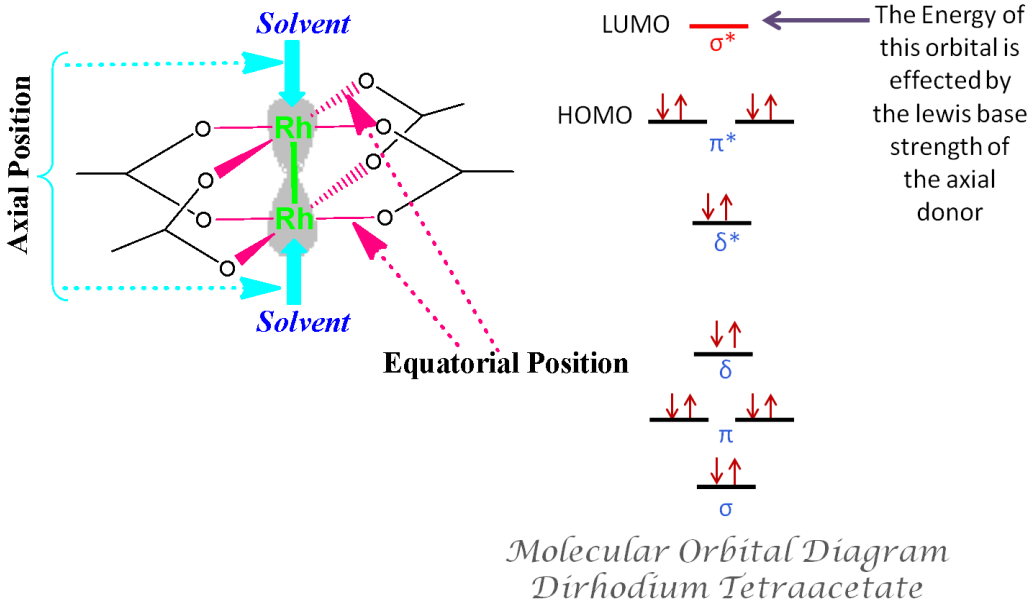

Figure I.14. Structure of dirhodium tetraacetate.

Other paddlewheel compounds, such as formamidinates which include the DTolF derivative (where DTolF is $((CH_3)C_6H_4)_2N_2CH$) have been tested for anticancer activity as well (Figure I.15). The tetraformamidinate derivatives do not show high toxicity in cancer cells, however, mixed paddlewheel compounds of formamidinate have toxicity towards cancer cells. An example of this is $Rh_2(DTolF)_2(O_2CCF_3)_2$, which show similar activity towards Yoshida ascites and T8 sarcomas as cisplatin. The promising anticancer properties of dirhodium paddlewheels lead to the need for further investigation into the mechanisms of biological activity.[67]

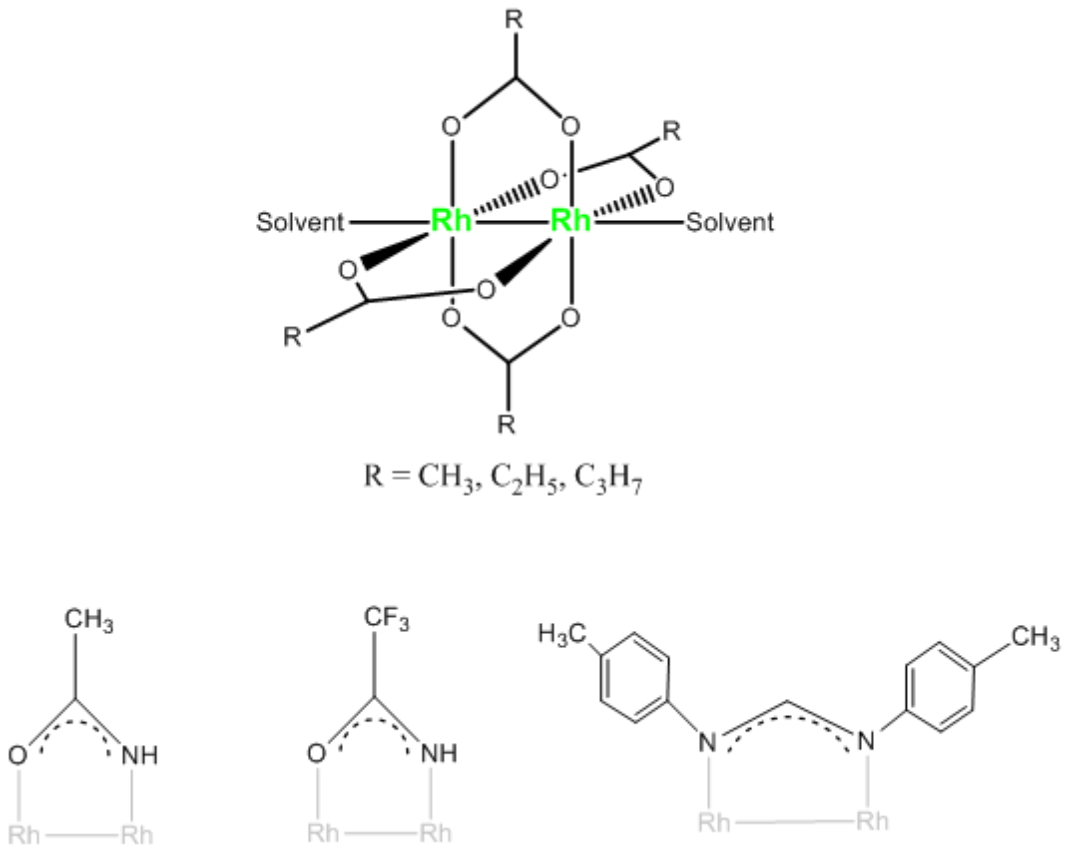

Figure I.15. Dirhodium paddlewheel derrivatives tested for anticancer properties.

Interactions Between Dirhodium Compounds and DNA

One of the first objectives towards determining the cause of cytotoxicity was to determine if dirhodium tetraacetate could bind to DNA, as was observed with cisplatin. It was shown early on by Bear and coworkers that the dirhodium compound was capable of binding 1-methyladenosine.[68] The aqueous dirhodium solution changed from blue/green to a pink color, which indicated that

the 1-methyladenosine was axially bound through a nitrogen atom. Similar reactions with guanine did not yield any adducts with dirhodium tetraacetate.[68] When a crystal structure of the axially bound 1-adenosine was obtained, it was shown that the oxygen atom from the acetate group was able to hydrogen bond with the amine group. This observation led to the hypothesis that guanine could not bind to dirhodium carboxylates because of the repulsive interaction between the O6 on guanine, and the oxygen of the acetate ligand. These interactions showed that dirhodium tetraacetate could interact with DNA, but it did not seem possible that the weak interaction between dirhodium and its axial ligands could cause the cytotoxicity exhibited by these compounds (Figure I.16).[69]

Later experiments revealed that dirhodium tetraacetate could bind 9-ethylguanine via a bridging mode. [69] Two of the acetate groups were replaced by the 9-ethylguanine, which is bound in the equatorial positions through O6/N7 positions on the purine. This results in both a head-to-head, and head-to-tail arrangement of the dirhodium 9-ethylguanine compound (Figure I.17). [69] Similar reactivity was found with the trifluoroacetic acid dirhodium derivative as well. Results of further studies indicated that 9-ethyladenine binds to the equatorial positions when reacted with the dirhodium compound $Rh_2(DTolF)_2(O_2CCF_3)_2$.[70] The adenine replaces the trifluoroacetate groups, binding via the O6/N6 positions. The ^1H NMR studies of this product revealed that the adenine was bound in the rare imido form, indicating that if this interaction occurs in dsDNA it could interfere with the hydrogen bonding of the base pairs (Figure I.17).[70]

Following the successful studies of cisplatin the binding mode of $[Rh_2(DTolF)_2(CH_3CN)_6]^{2+}$ with the dinucleotides d(GpG) and d(pGpG) was studied by 2D NMR experiments. After determining the binding motif of these compounds, molecular modeling was used to determine the probable structure of $Rh_2(CH_3CO_2)_2$(d(pGpG)). The calculated conformation of $Rh_2(CH_3CO_2)_2$(d(pGpG)) was overlaid with the crystal structure of $Pt(NH_3)$(d(pGpG)), revealing that the two binding modes are extremely similar. The interaction of $[Rh_2(DTolF)_2(CH_3CN)_6][BF_4]_2$ with the mixed adducts d(ApG) and d(GpA) were also studied by 2D NMR spectroscopy. This experiment provided evidence that dirhodium compounds are capable of binding mixed purine fragments. While it took longer for the dirhodium d(ApG) adduct to form, both of the dinucleoties reacted with the compound. Once again the adenine was found to be stabilized in its imido form.[71]

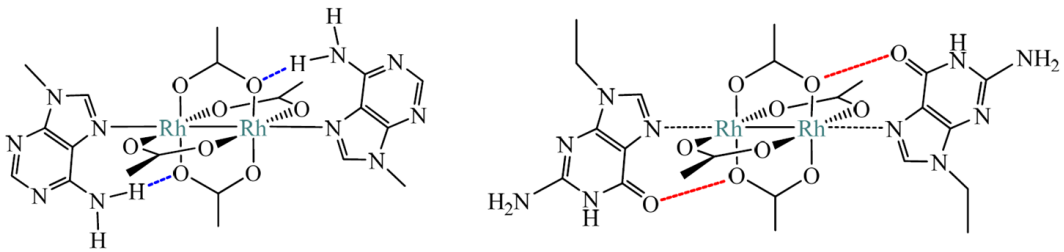

Figure I.16. a) Dirhodium tetraacetate axially binding to adenosine. b) Dirhodium tetraacetate with axial guanine.

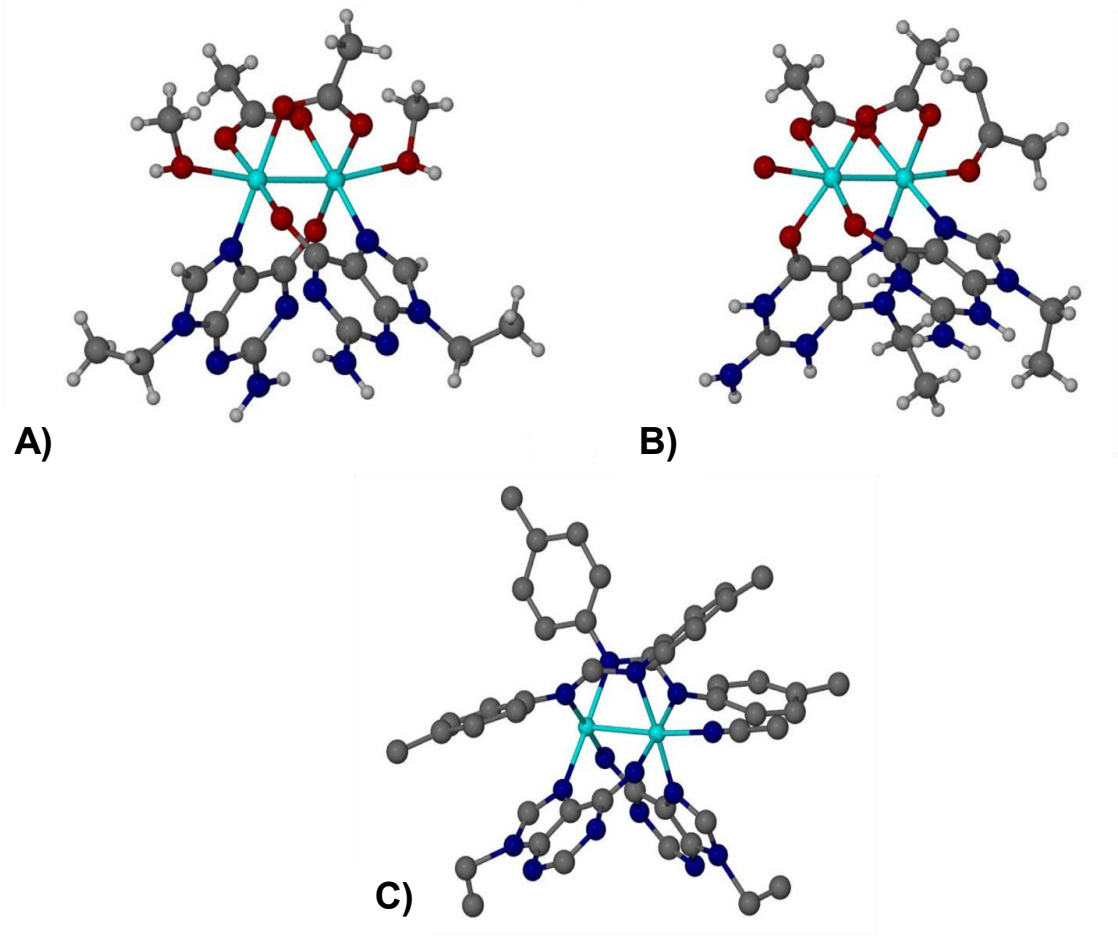

Figure I.17. Dirhodium equatorial binding to A) HT guanine B) HH guanine C) HT (adapted from reference 70).

The next step was to probe the ability of dirhodium compounds to bind to double stranded DNA. Matrix-assisted laser desorption ionization (MALDI) and nanoelectrospray (nanoESI) coupled to time-of flight mass spectrometry (TOF-MS) were used to determine the products of the interaction between $Rh_2(O_2CCH_3)_4$ and DNA fragments.[72,73] The duplex DNA strands were designed to have AA, GG, GA, and AG sequences in order to obtain insight into the favored purine arrangement for binding. It was shown that dirhodium preferentially binds to AA and GG sequences.[71,74] A subsequent detailed study was conducted to probe the interactions of $Rh_2(O_2CCH_3)_4$ with the DNA duplex, d(CTCTC*A*ACTTCC)·(GGAATTGAGAG).[75] The compound was first incubated with d(CTCTCAACTTCC), and then annealed to the other strand. The surprising results of this experiment showed that the compound $Rh_2(\mu\text{-}O_2CCH_3)2(\eta^1\text{-}O_2CCH_3)]^+$ formed an intrastrand adduct by binding to the C5 and A6 bases on the 5' strand. The 2D NMR data indicated that the dirhodium compound was bound to the exocyclic N4 of the cytosine, and the N7 of the adenosine; greatly destabilized the duplex DNA.[75]

Interaction of Dirhodium Compounds with Other Biomolecules

The process and logic used to develop an intimate understanding of the anticancer activity of cisplatin has helped guide the investigation of dirhodium compounds. To this end the biologically relevant interactions of several dirhodium comounds (Figure I.18) were investigated. This includes dirhodium compound activity towards transcription inhibition,[76] their interaction with glutathione,[77] the mechanism of cell death,[78] and the ability to reach nuclear DNA.[79] The interaction with glutathione was tested in solution with series 3 (as indicated in Figure I.18). EPR spectroscopy indicated that glutathione was able to reduce the dirhodium compounds, and that the reduction is reversible. After these studies a series of compounds (series 4 in Figure I.18) was tested in media that contained glutathione. The activity of the series of compounds remained very close to the control tests, which showed that the reactive radical species shown to be formed in previous tests were not responsible for cell death. This was also a promising preliminary result as glutathione is known to cause resistance in cancer cells treated with cisplatin.

Transcription inhibition experiments were carried out for series 1 and 2 (Figure I.18). For the first series the transcription inhibition is caused by the compounds binding to T7-RNA polymerase (T7-RNAP). The level of inhibition for these compounds is higher than that of cisplatin. The activity of the series that showed transcription inhibition is related to the redox activity of the

compounds. The redox chemistry can be controlled by changing the R groups at the distal end of the diimine ligand. Because the activity is related to the redox potential of the compounds, it was concluded that the dirhodium series interacts with exposed thiol groups in T7-RNAP.[76,77]

The mechanism of cell death was tested for compounds in series 5 (Figure I.18). All of the compounds in the series were shown to induce apoptosis, except for the dirhodium compound possessing two dppn (benzo[i]dipyrido[3,2-a:2',3'-c]phenazine) ligands. The morphology of the dead cells indicated that the mechanism for cell death wasnecrosis.[79] In addition to the mechanism of cell death, ongoing efforts are aimed at determining the localization of dirhodium compounds *in vitro*.[79] Studies indicated that compounds from series 5 were able to reach nuclear DNA, whereas series 1 was not. There is far too much work on these series to be thoroughly covered in this introduction, but suffice it to say the intricate nature of biological processes demands careful and systematic analysis of drugs to fully understand their *in vitro*, and *in vivo* mechanisms.[78]

Objectives

Dirhodium compounds have been studied for decades, and have shown promising results as anticancer agents. The ability to control the properties of these compounds based on the ligands allows for the rational development of dirhodium compounds with specific biological activities. The Dunbar group has been investigating dirhodium tetraacetate and its derivatives in an effort to understand and improve their anticancer properties. In addition to improved toxicity towards cancerous cells, it is important to decrease the toxicity to healthy cells in an effort to reduce the severe side effects seen in cisplatin.

My research has focused on characterizing and studying the cytotoxicity and photocytotoxicity of dirhodium series. Chapter II describes the series $[Rh_2(O_2CCH_3)(N\text{-}N)_2]^{2+}$, where N-N are the diimine ligands: 1,10-phenanthroline (phen), dipyrido[3,2-f:2',3'-h]quinoxaline (dpq), dipyrido[3,2a:2´,3´c]phenazine (dppz), and benzo[i]dipyrido[3,2-a:2',3'-c]phenazine (dppn). Because this series is composed of compounds that have been investigated before in various experiments, it was my goal to start assembling the pieces of the puzzle, and to fill in any missing information. The ultimate goal is to relate the structures to the activities of the dirhodium diimine compounds.

A second goal was to alter the electronic transitions of the dirhodium diimine series upon irradiation of light. Several of the compounds studied in the Dunbar group have been tested as possible photodynamic therapy (PDT)

agents.[80-82] PDT will be further discussed in the following chapters, but one important property of a useful PDT agent is to be able to be activated by low energy irradiation (the PDT window is 600 to 850 nm).[83] To this end, efforts in the Dunbar group are focusing on studying the effects that the bridging ligand has on the energy of light required to activate the compound. Chapter III describes the synthesis and characterization of a new series of orthometalated dirhodium compounds using the same diimine ligands. The cytotoxicity and photocytotoxicity properties were measured and compared to the analogous dirhodium carboxylate series.

The promising anticancer properties of several metal based compounds in conjunction with the benefits of metal-metal bonded systems has steered my research towards studying the biological activities of diiridium compounds. Diiridium (II, II) compounds are not well studied, presumably because they are much less easy to work with than their dirhodium (II,II) analogues. Chapter IV details a new synthesis of $[Ir_2(DTolF)_2(CH_3CN)_6]^{2+}$ and studies of its cytotoxicity and photocytotoxicity.

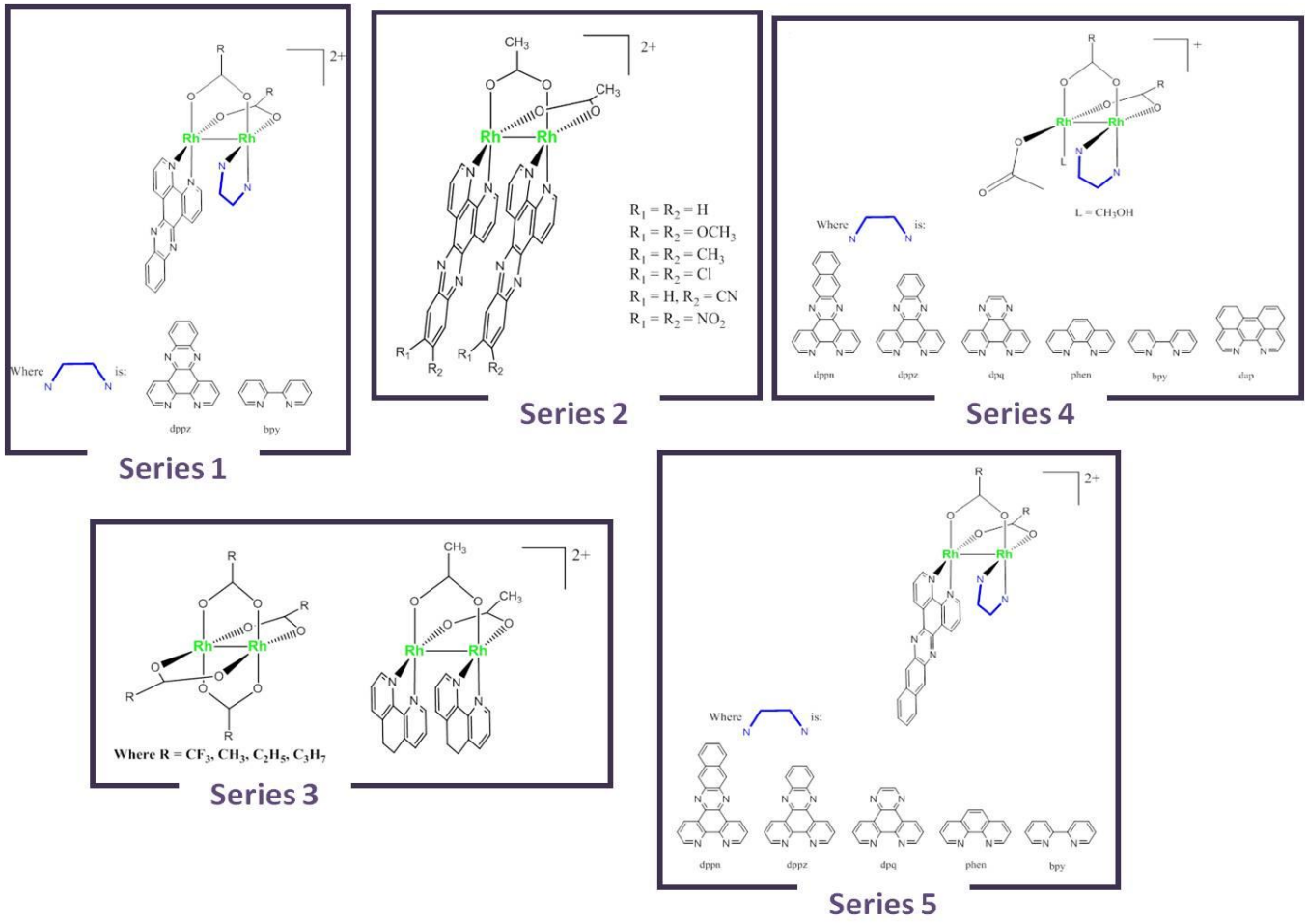

Figure I.18. Series of dirhodium partial paddlewheel compounds that have been explored for biological activity.

CHAPTER II

CARBOXYLATE BRIDGED DIRHODIUM PARTIAL PADDLEWHEELS: SYNTHESIS AND CYTOTOXICITY STUDIES

Introduction

Dirhodium compounds have been known to be cytotoxic towards cancer cells since the 1970's.[63] They present the possibility of tuning the anticancer activity based on the structure and properties of the ligands.[84] Knowing how the features of ligands affect the biological activity of these compounds is essential to designing drugs that have the desired properties. The Dunbar group has focused on the synthesis and biological activity of dirhodium partial paddlewheel compounds with extended π-conjugated bidentate diimine ligands.[76,78,79,85] Pruchnik was the first to investigate the anticancer properties of this type of compound in 1996, when $[Rh_2(O_2CCH_3)_2(phen)_2]^{2+}$ was shown to have cytostatic activity against the human oral carcinoma KB cell line.[86,87] Soon after the anticancer effect of the dirhodium phenantroline compound was found, Pruchnik reported the antibacterial effect of this compound, and its interactions with adenosine triphosphate.[88] In parallel studies, the Dunbar group reported the ability of this compound to inhibit RNA transcription.[77,89]

Many dirhodium compounds have been found to be cytotoxic – in some cases more so than cisplatin. The high cytotoxicity of cisplatin towards cancer cells has made it one of the most effective anticancer drugs, but the toxicity of

cisplatin extends to healthy cells as well. This leads to many negative side effects (such as the dose limiting nephrotoxicity).[23] Therefore it is necessary to find a way to limit the toxicity of these compounds towards healthy cells. There have been many methods of drug delivery reported in the literature which endeavor to limit the toxicity of drugs to healthy cells. Many of these approaches work by specifically targeting the delivery of toxic compounds to cancer cells, including the use of aptomers, cell penetrating peptides, and liposomes.[9] Photodynamic therapy (PDT) is another method aimed at reducing the toxicity of the drug to specific regions, that is to say tumors.[90]

Photodynamic therapy agents are non-toxic in the dark, and become cytotoxic upon irradiation with light. In a clinical use, the inert PDT agent is administered in the dark and the region of the tumor is irradiated in order to activate the drug. Therefore, PDT agents need to have some specific properties; first a high ratio between the cytotoxicity in the dark, and the cytoxicity upon irradiation (referred to as photocytotoxicity), and finally the wavelength of light needed to activate the compound should be in the near infrared range of 600-850 nm. This second property is required because red light is known to be able to more deeply penetrate tissue.[90]

The current PDT drug approved for use as an anticancer agent by the FDA is photofrin®, a drug that consists of oligomers of porphyrin units. The photocytotoxicity of this drug (LC_{50} is 3.8 ± 1 μM) is 5 times greater than the

cytotoxicity in the dark (LC_{50} is 21 ± 0.2 μM). The wavelength needed to activate the compound is 630 nm, which is inside the PDT window. Photofrin®, and most other PDT agents, works by sensitizing singlet oxygen, which is known to damage DNA and other biomolecules. The quantum yield of sensitized singlet oxygen for photofrin® is 0.17 (found in methanol). The disadvantage of using singlet oxygen as the mechanism of photocytotoxicity is that many of the most malignant and drug resistant tumors are hypoxic. The prolonged cutaneous sensitivity is another negative aspect of current PDT drugs. For these reasons new classes of PDT agents with improved properties are being sought.

Dirhodium compounds were first investigated for their photoactivity in biological systems because of the ability of these compounds to exhibit long-lived excited states with lifetimes of 3.5 - 5 μs. Also, the neutral or positive charges of these compounds prevent electrostatic repulsion with DNA.[91] It was found that both $Rh_2(O_2CCH_3)_4$ and $[Rh_2(O_2CCH_3)_2(phen)_2]^{2+}$ could photocleave DNA in the presence of an electron acceptor.[81] The potential of dirhodium diimine compounds to act as PDT agents was further investigated for dirhodium dppz compound, where dppz is dipyrido [3,2a:2´,3´c]phenazine. The ligand dppz was chosen because of the dearth of metal-dppz compounds that are photoactive.[80,92] This includes the series $[Ru(L)_2(dppz)]^{2+}$, where L is 2,2'-bipyridine (bpy), or 1,10-phenantroline (phen), which exhibit luminescence in the presence of DNA, and the bpy derivative was shown to be able to photocleave

DNA.[93] The dirhodium dppz compounds explored are the di-substituted and mono-substituted compounds, $[Rh_2(O_2CCH_3)_2(dppz)_2]^{2+}$ and $[Rh_2(O_2CCH_3)_2(dppz)(\eta^1\text{-}O_2CCH_3)(CH_3OH)]^{+}$ respectively, and their photo-activity with DNA, and LC_{50} values in the dark and light were investigated.[80,81,85,94] Both compounds were found to photocleave DNA upon irradiation with visible light, $\lambda_{irr} \geq 375$ nm. The analysis of the cytotoxicity of these compounds in a human skin cell culture revealed LC_{50} values of 135 ± 8 μM and 27 ± 2 μM, and the photocytotoxicity resulted in LC_{50} values of 39 ± 1 μM and 21 ± 3 μM (for $[Rh_2(O_2CCH_3)_2(dppz)_2]^{2+}$ and $[Rh_2(O_2CCH_3)_2(dppz)(\eta^1\text{-}O_2CCH_3)(CH_3OH)]^{+}$ respectively). It can be seen that the LC_{50} values for the dirhodium compounds with one coordinated dppz ligand did not change, which is attributed to the ability of these compounds to intercalate into DNA. The LC_{50} values of the homoleptic dirhodium dppz compound showed a 3.5 fold decrease in the LC_{50} values (135 ± 8 μM in the dark to 39 ± 1 μM upon irradiation).[94]

The photoactivity of a related series, namely the cations $[Rh_2(O_2CCH_3)_2(dppz)(L)]^{2+}$, was subsequently studied (where L is bpy, phen, dpq (dipyrido[3,2-f:2',3'-h]quinoxaline), dppz, or dppn (benzo[i]dipyrido[3,2-a:2',3'-c]phenazine).[78,95] Because the toxicity of PDT agents is often caused from the creation of singlet oxygen upon irradiation, the quantum yield of singlet oxygen was determined for each compound in the series. The quantum yield of singlet oxygen ranged from 0.9 for the phen derivative to 0.4 to the homoleptic dppn derrivative.[95] Other studies aimed at finding the biological activity of these

compounds upon irradiation include the ability to photocleave DNA, and the cytotoxicity and photocytotoxicity. The most interesting results were observed for the homoleptic dppz and dppn compounds. For both compounds the photocleavage of DNA was not as high as other compounds in this series, and the cytotoxicites were low (355 ± 18 and 384 ± 24 for the dppz and dppn derivatives respectively). The photocytotoxicities of these compounds revealed LC_{50} values of 17 ± 3 μM and 16 ± 4 μM respectively. This is a 21 and 24 fold increase in cytotoxicities upon irradiation.[80]

While much work has been carried out on the compounds $[Rh_2(O_2CCH_3)_2(L)_2]^{2+}$, where L is phen, dpq, dppz, and dppn, but they have never been studied systematically as a series. This chapter reports the synthesis, structural characteristics, and biological relevance of these compounds. The data on these compounds are compiled to asses how the structural characteristics relate to the biological properties of these compounds, and evaluated according to their potential to be used in photodynamic therapy.

Experimental Section

Materials

The reagents 1,10-phenanthroline, 1,2 phenylene diamine, and 2,3 diaminonapthalene were purchased from Acros, and used as received. The starting material $Rh_2(\mu\text{-}O_2C_2H_3)_4$ was purchased from Pressure Chemicals and used as received. The HeLa cell line was obtained from the American Type Culture Collection.

The starting material 1,10 phenanthroline 5,6 dione was used to synthesize the ligands dipyrido[3,2-f:2',3'-h]quinoxaline (dpq),[96] dipyrido[3,2a:2´,3´c]phenazine (dppz),[97] benzo[i]dipyrido[3,2-a:2',3'-c]phenazine (dppn);[98] all according to published procedures. The dirhodium compounds $[Rh_2(CH_3CO_2)_2(phen)_2][CH_3CO_2]_2$ **(1)**, $[Rh_2(CH_3CO_2)_2(dppz)_2][CH_3CO_2]_2$ **(3)**, and $[Rh_2(CH_3CO_2)_2(dppn)_2][CH_3CO_2]_2$ **(4)** were synthesized according to published procedures.[78,81,89,94]

Synthesis of $[Rh_2(CH_3CO_2)_2(dpq)_2][CH_3CO_2]_2$ **(2)**

Solid dpq (0.380 g, 2.00 mM) was added to a solution of (0.100 g, 10.0 mM) dirhodium tetraacetate in 20 mL of distilled acetonitrile. The mixture was heated to reflux for 24 hours under a dinitrogen atmosphere, during which time it turned from purple/brown color to a brown/red color. At this time the solution

was cooled to room temperature, and the resulting precipitate was collected by vacuum filtration, and washed with cold acetonitrile. The product was obtained in an 82% yield. ^{1}H NMR (300 MHz) $CDCl_3/CD_3OD$ (1:1, v:v) ɗ/ppm (mult./ integral/ assignment): 1.71 (s, 6H, CH_3CO_2), 2.65 (s, 6H, CH_3CO_2), 7.62 (m, 4H), 8.50 (d, 4H), 8.81 (m, 4H), 8.90 (d, 4H). UV-vis in H_2O λ/nm (ε/$M^{-1}cm^{-1}$): 362 (10500), 483 (3000), 580 (1300).

Instrumentation

The ^{1}H NMR spectra of the new complexes were recorded on a Varian spectrometer at 300 MHz and referenced to the residual proton impurities in the deuterated solvents. Absorption measurements of solutions were performed on a Shimadzu UV 1601PC spectrophotometer, and 96 well plate measurements were performed on a GloMax® Multi Detection System.

Methods

Cell Culture

The HeLa cell line was cultured in Dulbecco's modified Eagle medium with 4.5 mg/mL glucose, and 4 mM L-glutamine (Invitrogen), and was modified to include 10% fetal bovine serum (Atlanta Biologicals), 50 μg/mL gentamicin.

Cell cultures were incubated in a humidified atmosphere at 37 °C which contained 5% CO_2.

In Vitro Cytotoxicity and Photocytotoxicity

The LC_{50} concentrations in HeLa cells of the compounds under investigation were determined using the 3-(4,5-dimethylthiazol-2-yl)-d,5-diphenyltetrazolium bromide (MTT) assay (invitrogen).[99] A 100% confluent monolayer of cells in sterile 96 well plates were used for this experiment. The cells were plated at a concentration of 24-36 cell/μL using 100 μL per well, they were and incubated for 48 hours. Once confluent, the media was replaced with 100 μL of Lebovitz-15 (L15) media (containing no phenol red). The compounds were incubated for 2 hours, then the wells were washed with 1% dibasic phosphate buffer and the compound solution was replaced with L15 media. The plates that were used to determine photocytotoxicity were then irradiated for 20 minutes with λ_{irr} = 350 nm. The plates used for cytotoxicity and photocytotoxicity were incubated for 24 hours from the time the compounds were added. Then 10 μL of fresh MTT solution was added to each well. After 4 hours of incubation, 100 μL of fresh SDS solution in 0.01M HCl was added to each well. The plates were incubated for another 4 hours, then the plates were read at 570 nm using a GloMax® Multi Detection System. Each concentration of compound had six wells per plate, and three plates were run per compound.

Results and Discussion

Synthesis and Characterization of the Series $[Rh_2(O_2CCH_3)_2(N\text{-}N)_2][O_2CCH_3]_2$

The synthesis and characterization of the compounds in this series, $[Rh_2(CH_3CO_2)_2(phen)_2][CH_3CO_2]_2$ **(1)**, $[Rh_2(CH_3CO_2)_2(dppz)_2][CH_3CO_2]_2$ **(3)**, and $[Rh_2(CH_3CO_2)_2(dppn)_2][CH_3CO_2]_2$ **(4)**, have all been reported with the exception of $[Rh_2(CH_3CO_2)_2(dpq)_2][CH_3CO_2]_2$ **(2)**. This series results from the substitution of two bridging acetate groups from the starting matierial $Rh_2(O_2CCH_3)_4$ for bidentate diimine ligands under refluxing conditions in the presence of the diimine ligand (Figure II.1).

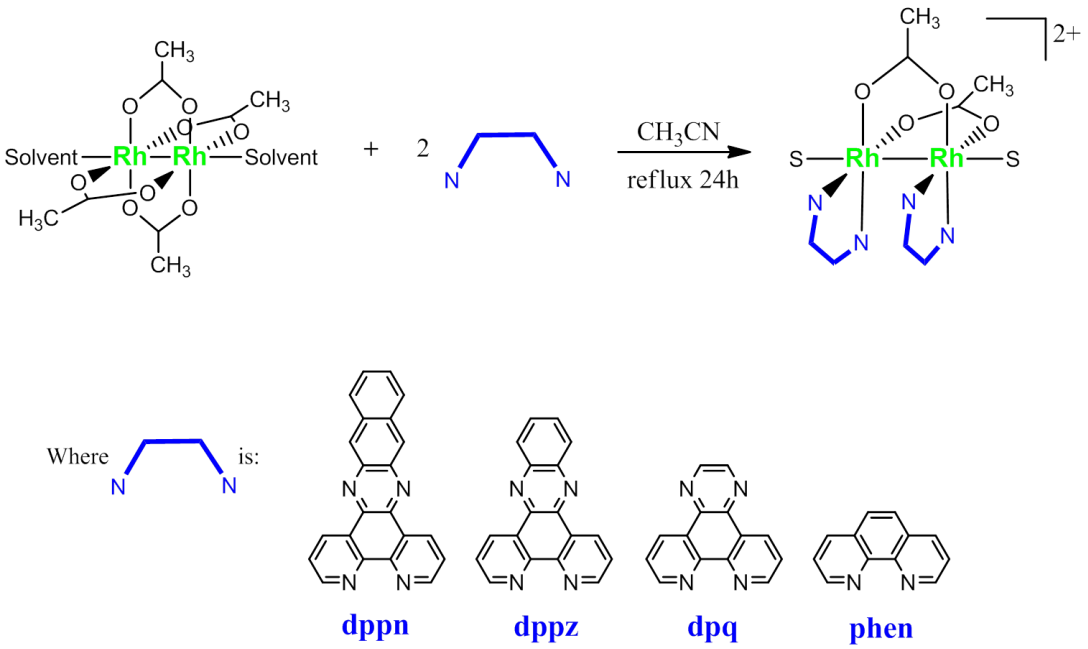

Figure II.1. Synthesis of the compounds **1-4**.

The series was characterized by a combination of methods, including X-Ray crystallography and spectroscopic methods, namely ^{1}H NMR and electronic absorbtion spectroscopy. For the compounds characterized by X-Ray crystallography, the Rh-Rh bond distances are 2.525(7) Å, and 2.551(9) Å for $[Rh_2(CH_3CO_2)_2(phen)_2][BF_4]_2$ and $[Rh_2(CH_3CO_2)_2(dppz)_2][BF_4]_2$ respectively.[94] The crystal structure of the dirhodium dppz derivative reveals a splaying of the dppz ligands and an internal twist angle of 13°, which helps to reduce the repulsive forces the dppz ligands would otherwise experience.[94] The distance at the distal end of the dppz ligands in the dirhodium structure was found to be 3.494(7) Å. The ^{1}H NMR of the compounds in the series all show coordinated and free acetate ligands at 2.6 and 1.7 ppm respectively.[94] For compound **3**, the protons on the aromatic rings of the diimine ligands (dpq) are between 7.62 and 8.90 ppm. The electronic absorbance of the compounds in the series have similar properties, namely a transition between 325 - 377 nm – believed to be ligand based π to π* transitions, and a transition in the range 373 - 483 nm – which are assigned to charge transfer transitions involving the diimine ligand.

Cytotoxicity and Photocytotoxicity

The cytotoxicity and photocytotoxicity properties of the dirhodium bisacetate diimine series (compounds **1-4**) in HeLa cells were determined by the MTT (3-(4,5-dimethylthiazol-2-yl)-d,5-diphenyltetrazolium bromide) assay. The MTT assay is a colorimetric assay that is used to quantify the number of living cells. In the presence of living cells the yellow tetrazole compound is reduced to the purple formazan form by the mitochondrial reductase. The concentration of purple formazan is measured at 570 nm, and can be plotted against the concentration of compound added to find the equation for the linear trend line. From these data the concentration of compound needed to kill half of the cells (lethal concentration of 50%, LC_{50}) can be extrapolated.[99]

The range of concentrations used to measure the cytotoxicity of compounds **1-4** were chosen based on previous data for similar compounds. The range of concentrations measured for this series was 50 μM to 800 μM. For all off the MTT assays, both light and dark, the amount of ambient light was limited as much as possible, and experiments used to determine the photocytotoxicity exposed the cells to light for 20 minutes. The results are summarized in Table II.1.

The values reported in Table II.1 represent the μM concentration of compounds **1-4** needed to kill 50% of HeLa cells. In the dark, compounds **2**, **3**, and **4** have similar *in vitro* cytotoxicities ranging from 126 μM to 152 μM, while

compound **1** is less cytotoxic, with and LC_{50} of 446 ± 16 μM. The photocytotoxicity values show more deviation between compounds with compound **4** being the most photocytotoxic, and compound **1** is the least photocytotoxic. Compounds **2** and **3** have similar photocytotoxicities. When comparing the cytotoxicity and photocytotoxicity of the series the major difference is that the photocytotoxicity of compound **4** is no longer similar to compounds **2** and **3**, as was seen in the cytotoxicity.

To further explore this trend the ratio of cytotoxicity to photocytotoxicity of each compound was found. For compound **1** the ratio between cytotoxicity and photocytotoxicity is 1, indicating that irradiation has no effect on the toxicity of the compound towards HeLa Cells. Compounds **2** and **3** have similar ratios of toxicity in the dark and light, 1.5 and 1.2 respectively. It is possible that irradiation affects the LC_{50} concentrations of these compounds; yet, if this is true it is only slightly. Compound **4** differs from the others in that its ratio of toxicity in dark and light is **2**, meaning that the photocytotoxicity of compound **4** is twice that of its cytotoxicity. The change in toxicity upon irradiation indicates that light induces a toxic change in the compound. It is reasonable sense that compound **4** would have a greater toxicity upon irradiation, as dppn is known to produce singlet oxygen, and to have a long lived excited state.[95]

Table II.1. Cytotoxicity and photocytotoxicity of compounds 1-4 in HeLa cells.

	Compound	LC_{50} (μM)	LC_{50}* (μM)	Ratio
(1)	$[Rh_2(O_2CCH_3)_2(phen)_2][O_2CCH_3]_2$	446 ± 16	424 ± 8	1.1
(2)	$[Rh_2(O_2CCH_3)_2(dpq)_2][O_2CCH_3]_2$	150 ± 9	102 ± 6	1.5
(3)	$[Rh_2(O_2CCH_3)_2(dppz)_2][O_2CCH_3]_2$	152 ± 6	126 ± 8	1.2
(4)	$[Rh_2(O_2CCH_3)_2(dppn)_2][O_2CCH_3]_2$	126 ± 5	63 ± 5	2.0

LC_{50} ± SD, LC_{50} is the value upon irradiation with light for 20 minutes.*

Compilation of Data

Several compounds in this series have been previously studied,[79,94,95] so one of the goals was to compile past and current experimental data in an effort to fully understand the properties of these compounds that lead to their biological activity. The first dirhodium diimine compounds studied by the Dunbar group were $[Rh_2(O_2CCH_3)_2(phen)_2]^{2+}$ (**1**) and $[Rh_2(O_2CCH_3)_2(dppz)_2]^{2+}$ (**3**). The compound $[Rh_2(O_2CCH_3)_2(dppn)_2]^{2+}$ was studied as a part of series 5, shown in Figure I.18. The physical and electronic properties of these compounds have been measured, and the relevant information is reported here. The goal is to deduce the effect that the length of aromatic ligand has on the biological activity.

As the length of the aromatic ligand increases, the metal to ligand charge transfer undergoes a general trend of hyperchromicity, and a bathochromic shift

Table II.2. Compilation on all LC_{50} and LC^*_{50} values found for this series.

Rhodium series:		Cytotoxicity vs. Photocytotoxicity			
		Cell Line	LC_{50}	LC_{50}*	Ratio
$[Rh_2(O_2CCH_3)_2(phen)_2]^{2+}$	**(1)**	HS-27	290 ± 15	294 ± 15	1.0
		HeLa	446 ± 16	424 ± 8	1.1
$[Rh_2(O_2CCH_3)_2(dpq)_2]^{2+}$	**(2)**	HeLa	150 ± 9	102 ± 6	1.5
$[Rh_2(O_2CCH_3)_2(dppz)_2]^{2+}$	**(3)**	HS-27	135 ± 8	39 ± 1	3.5
		HeLa	152 ± 6	126 ± 8	1.2
$[Rh_2(O_2CCH_3)_2(dppn)_2]^{2+}$	**(4)**	Hs-27		384 ± 24	*NA*
		HeLa	126 ± 5	63 ±5	2.0

in the MLCT tail. The λ_{max} for the transitions in this series does not follow a noticeable trend. In an effort to fully understand the effect of the bidentate ligands, the results found on the compounds in this series have been compiled in several tables (Table II.2, Table II.3, and Table II.4). Based on the results found for compounds **1-4**, it can be seen that as the diimine ligand progresses from phen to dppn the reduction potentials are increasingly negative. The dirhodium phen derivative is not able to cleave DNA unless an electron acceptor is present, while the dppz and dppn derivatives are able to cleave DNA in the absence of an electron acceptor. It was found that the dppn derivative sensitizes singlet oxygen (which is known to cleave DNA), but it was still able to cleave DNA under anaerobic conditions as well. The compounds that were tested for transcription inhibition were found to inhibit transcription through the inhibition of T7RNAP.[76,89]

Table II.3. Experimental data compiled for the dirhodium series, including electronic absorption data.

Rhodium series:		FW (g/mole)	Rh-Rh bond distance (Å)	E_{red} (V)	UV bands					log *P*
					Counter Ion	ππ* LC (dppz)	Rh-Rhπ* to Rh-Oσ* (MLCT)	Rh-Rhπ* to Rh-Rhσ* (MC)	tail to	
$[Rh_2(O_2CCH_3)_2(phen)_2]^{2+}$	(1)	802.44	2.526(7)	-0.83 (reversible, vs. $[Fe(Cp)_2]/[Fe(Cp)_2]^+$ in CH_3CN)	2[Cl⁻]	371 (350000)	397 (4660)	444 (4660)		
					2[BF_4^-]	362 (47600)	408 (3050)	514 (292)		
$[Rh_2(O_2CCH_3)_2(dpq)_2]^{2+}$	(2)	906.52			2[CH_3COO^-]	356 (6800)	373 (5400)	547 (300)	600	
					2[CH_3COO^-]	362 (10500)	483 (3000)	580 (1300)	620	
$[Rh_2(O_2CCH_3)_2(dppz)_2]^{2+}$	(3)	1006.64	2.551(9)	-1.06 (reversible, vs. Ag/AgCl in dry DMF)	2[CH_3COO^-]	363 (15170)	434 (5459)	510 (350)		
						377 (14600)	450 (3000)	562 (1000)	640	
$[Rh_2(O_2CCH_3)_2(dppn)_2]^{2+}$	(4)	1106.76			2[CH_3COO^-]	397 (16570)*	410 (13200)	621 (2000)		0.4 (in methanol)
					2[CH_3COO^-]	325 (37300)	420 (16700)	614 (4700)	660	1.02 ± 0.03

Solvents = water, methanol, and acetonitrile

Table II.4. Cell studies compiled for the dirhodium series.

Rhodium series:		*In Vitro* DNA interactions (interactions with DNA, glutathione, photoreactivity towards DNA, and transcription inhibition)	*In Cellulo* interactions (annexin V and commet assay)
$[Rh_2(O_2CCH_3)_2(phen)_2]^{2+}$	(1)	Does not photocleave DNA directly, requires the presence of an electron acceptor. Transcription inhibition via interaction with T7-RNAP	
$[Rh_2(O_2CCH_3)_2(dpq)_2]^{2+}$	(2)		
$[Rh_2(O_2CCH_3)_2(dppz)_2]^{2+}$	(3)	Can photocleave DNA, however, the presence of glutathione inhibits this interaction. Has similar viscosity to a groove binder. Transcription inhibition via interaction with T7-RNAP	
$[Rh_2(O_2CCH_3)_2(dppn)_2]^{2+}$	(4)	Can photocleave DNA with viscosities similar to groove binders	The mechanism of cell death is necrosis, and the compound does not reach nuclear DNA

Concluding Remarks

Several compounds in this series have been investigated by the Dunbar group. When all of the information is compiled, it is clear that there are some promising findings. Compound **1** is able to inhibit transcription, but it is not shown to have phototoxic effects – such as an increase in cytotoxicity upon irradiation, or ability to photocleave DNA. Compounds **3** and **4** exibit the most promising results, especially in regards to the potential use as PDT agents. Based on all of the information known on this series, it can be proposed that the progression from phen to dpq changes the electronic properties of the compound. This is significant because the redox properties of these dirhodium diimine compounds affected their anticancer activity. Although it is still unclear where these compounds localize in the cell, and what their targets are.

Future work on this series needs to include studes of *in cellulo* activity of these compounds, namely where these compounds are localizing in the cell, their effect on biological processes, and the mechanism of cell killing. Further experiments in the Dunbar group are being carried out on this series to improve the possibility of these compounds to be used in PDT. When compared to photophrin®, the lead PDT agent on the market, the ratio between LC_{50} values in the dark and light is found to be about 3.5 for the dirhodium compound $[Rh_2(CH_3COO)_2(dppn)_2]^{2+}$, and 5 fold for photophrin. The energy needed to induce the increase in toxicity for photophrin is at a λ = 630 nm, whereas the

dirhodium compound is irradiated at wavelengths from 400-700 nm, with a MLTC shown at 410 nm. The high energy light needed to activate compounds **1** through **5** prompted a need to alter the dirhodium series in order to lower the energy needed to induce the MLCT, shifting it into the PDT window.

CHAPTER III

ORTHOMETALATED DIRHODIUM PARTIAL PADDLEWHEELS: SYNTHESIS AND CYTOTOXICITY STUDIES

Introduction

Useful PDT agents are activated by light in the range of 600-850 nm.[90] Dirhodium compounds have shown promising results as potential PDT agents, including the derivatives with bidentate diimine (ligands dpq, dppz and dppn). There have been several derivatives of the homoleptic diimine series studied in an effort to shift the wavelength of the MLCT into the PDT window. Reducing the energy gap between the metal based HOMO and ligand based LUMO can be accomplished via several methods, including raising the energy of the HOMO. One way to shift the energy of metal orbitals is by changing the bridging ligands on the dirhodium core.[84]

The Lewis base strength of the equatorial ligands can be used to control the electronic profile of dirhodium compounds.[84] There are been many examples of dirhodium compounds with various bridging ligands, including those of types (N, O), (S, O), (N, S), (N, N), (S, S), (P, O), and (P, C).[62] Weak field ligands lead to more electrophillic compounds, whereas strong field ligands reduce the electrophilicity.[84] It is also known that the more electron withdrawing bridging ligands of dirhodium compounds are more labile. An example of this is the binding strength of acetate versus trifluoracetate, with the latter being more

labile.[62] The ability to tune the properties of dirhodium compounds through bridging ligands has lead to the investigation of the effect of several types of bridging ligands on the anticancer properties of dirhodium compounds. One that was previously mentioned is the mixed paddlewheel compound $Rh_2(DTolF)_2(O_2CCF_3)_2$, which show similar activity towards Yoshida ascites and T8 sarcomas as cisplatin.[67]

Orthometalated dirhodium compounds of the types ortho-C and ortho-O-metalated have been studied for their anticancer properties as well.[100] The compounds include $[Rh_2(\mu\text{-}O_2CCH_3)_2((C_6H_3\text{-}3\text{-}OCH_3)P(C_6H_4\text{-}3\text{-}OCH_3)_2)_2(O_2CCH_3)_2]$ – where the methoxyphenylphosphine is bridging through carbon and phosphorous (C, P), and $[Rh_2(\mu\text{-}O_2CCH_3)_2((C_6H_4\text{-}2\text{-}O)P(C_6H_4\text{-}2\text{-}OCH_3)_2)_2(O_2CCH_3)_2]$ – where the methoxyphenylphosphine is bridging through the oxygen of the methoxy group and phosphine atom (O, P). The ID_{50} (dose needed to inhibit 50% of cellular proliferation) for the cell lines KB (oral carcinoma), HU1703 (bladder cancer), SW707 (colon adenocarcinoma), and T47D (breast cancer) was investigated. It was found that the (O, P) derivative was the most active, with ID_{50} values comparable to cisplatin.[100]

It has been shown that orthometalated bridging ligands affect the dirhodium core, and previous studies indicated that these compounds could have significant anticancer activity.[100,101] Therefore, it was of interest to use diimine derivatives (where the diimine ligand is phen, dpq, dppz, and dppn) of

orthometalated tris(p-methoxyphenyl)phosphine (PMP) compounds are toxic towards cancer cells, and if they have the potential to be used as PDT agents. As previously stated, electron donating ligands reduce the electrophilicity, and bond more strongly to the dirhodium core. This situation could lead to an increase in the energy of the HOMO orbital, thereby reducing the energy gap between the HOMO and LUMO.

Experimental Section

Materials

The reagents tris(p-methoxyphenyl)phosphine (PMP), 1,10 phenanthroline, 1,2 phenylene diamine, 2,3 diaminonapthalene, and 1,10 phenanthroline 5,6 dione were purchased from Acros, and used as received. The starting material $Rh_2(\mu\text{-}O_2C_2H_3)_4$ was purchased from Pressure Chemicals and used as received. The HeLa cell line was obtained from the American Type Culture Collection.

The starting material 1,10 phenanthroline 5,6 dione was used to synthesize the ligands dipyrido[3,2-f:2',3'-h]quinoxaline (dpq),[96] dipyrido[3,2a:2´,3´c]phenazine (dppz),[97] benzo[i]dipyrido[3,2-a:2',3'-c]phenazine (dppn);[98] all according to published procedures. The dirhodium compound

$Rh_2(PMP)_2(CH_3CO_2)_2][CH_3CO_2]_2$ was synthesized according to published procedures.[100]

Synthesis of $[Rh_2((C_6H_3\text{-}OCH_3)P(C_6H_3\text{-}OCH_3)_2)_2(CH_3CN)_6][\ BF_4]_2$ **(5)**

A sample of (0.050 g, 0.024 M) $[Rh_2(PMP)_2(CH_3CO_2)_2][CH_3CO_2]_2$ was dissolved in 2 mL of distilled acetonitrile, and (0.012 g) $NOBF_4$ was added in a slight excess of a 1:2 ratio. The solution was stirred in air for two hours at room temperature, and then evaporated the solvent under a N_2 stream. The solid was washed with diethylether, and then redissolved in 1 mL of acetonitrile. The product was precipitated with 3 mL of diethylether. The product was recovered by filtration in a 67% yield and characterized by ^1H NMR spectroscopy (300 MHz) CD_3CN ɗ/ppm (mult./ integral/ assignment): 2.02 (s, 18H, CH_3CN) 3.24 (s, 6H, OMe), 3.71 (s, 6H, OMe), 3.74 (s, 6H, OMe), 6.41 – 7.65 (aromatic region).

Synthesis of $[Rh_2((C_6H_3\text{-}OCH_3)P(C_6H_3\text{-}OCH_3)_2)_2(phen)_2][\ BF_4]_2$ **(6)**

Solid phenanthroline (5.5 mg, 6.10 mM) was added to a solution of (0.020 g, 3.01 mM) $[Rh_2((C_6H_3\text{-}OCH_3)P(C_6H_3\text{-}OCH_3)_2)_2(CH_3CN)_6][\ BF_4]_2$ in 5 mL of dry acetonitrile in an N_2 atmosphere. The mixture was heated to reflux for 24 hours, during which time it changed from a purple/brown to bright red color. At this time the solution was cooled to room temperature and diethyl ether was added to the

solution to precipitate the product. The resulting solid was collected by filtration and washed with cold acetonitrile. The reaction afforded a 77% yield. ^{1}H NMR (300 MHz) d^6-benzene ɗ/ppm (mult./ integral/ assignment): 3.23 (s, 6H, OMe), 3.70 (s, 6H, OMe), 3.73 (s, 6H, OMe), 6.48 – 7.65 (aromatic PMP) 7.51 (dd, 4H), 7.62 (s, 4H), 8.18 (m, 4H), 8.39 (d, 4H).

Synthesis of $[Rh_2((C_6H_3\text{-}OCH_3)P(C_6H_3\text{-}OCH_3)_2)_2(dpq)_2][\ BF_4]_2$ **(7)**

Solid dpq (7.10 mg, 6.11 mM) was added to a solution of (0.020 g, 3.01 mM) $[Rh_2((C_6H_3\text{-}OCH_3)P(C_6H_3\text{-}OCH_3)_2)_2(CH_3CN)_6][\ BF_4]_2$ in 5 mL of dry acetonitrile under an N_2 atmosphere. The mixture was heated to reflux for 24 hours, during which time it changed from purple/brown to a bright red color. At this time the solution was cooled to room temperature, and diethyl ether was added to the solution to precipitate the product. The resulting solid collected by filtration and washed with cold acetonitrile. The reaction afforded an 76% yield. ^{1}H NMR (300 MHz) d^6-benzene ɗ/ppm (mult./ integral/ assignment): 3.22 (s, 6H, OMe), 3.68 (s, 6H, OMe), 3.72 (s, 6H, OMe), 6.50 – 7.65 (aromatic PMP) 7.60 (m, 4H), 8.53 (d, 4H), 8.76 (m, 4H), 8.89 (d, 4H).

Synthesis of $[Rh_2((C_6H_3\text{-}OCH_3)P(C_6H_3\text{-}OCH_3)_2)_2(dppz)_2][BF_4]_2$ **(8)**

Solid dppz (8.80 mg, 6.19 mM) was added to a solution of (0.020 g, 3.01 mM) $[Rh_2((C_6H_3\text{-}OCH_3)P(C_6H_3\text{-}OCH_3)_2)_2(CH_3CN)_6][BF_4]_2$ in 5 mL of dry acetonitrile in an N_2 atmosphere. The mixture was heated to reflux for 24 hours, during which time the color changed from purple/brown to a bright red color. At this time the solution was cooled to room temperature, and diethyl ether was added to the solution to precipitate the product. The resulting solid was collected by filtration and washed with cold acetonitrile. The reaction afforded an 86% yield. ^{1}H NMR (300 MHz) d^6-benzene ɗ/ppm (mult./ integral/ assignment): 3.21 (s, 6H, OMe), 3.68 (s, 6H, OMe), 3.71 (s, 6H, OMe), 6.50 – 7.65 (aromatic PMP) 7.39 (m, 4H), 7.70 (d, 8H), 8.59 (d, 4H), 8.81 (d, 4H). UV-vis in H_2O λ/nm (ε/$M^{-1}cm^{-1}$): 362 (10500), 483 (3000), 580 (1300).

Synthesis of $[Rh_2((C_6H_3\text{-}OCH_3)P(C_6H_3\text{-}OCH_3)_2)_2(dppn)_2][BF_4]_2$ **(9)**

Solid dppn (10.2 mg, 6.10 mM) was added to a solution of (0.020 g, 3.01 mM) $[Rh_2((C_6H_3\text{-}OCH_3)P(C_6H_3\text{-}OCH_3)_2)_2(CH_3CN)_6][BF_4]_2$ in 5 mL of dry acetonitrile in an N_2 atmosphere. The mixture was heated to reflux for 24 hours, during which time the color changed from purple/brown to a bright red color. At this time the solution was cooled to room temperature, and diethyl ether was added to the solution to precipitate the product. The resulting solid was filtered off and washed with cold acetonitrile. The reaction afforded an 82% yield. ^{1}H

NMR (300 MHz) d^6-benzene ɗ/ppm (mult./ integral/ assignment): 3.21 (s, 6H, OMe), 3.68 (s, 6H, OMe), 3.71 (s, 6H, OMe), 6.50 – 7.65 (aromatic PMP) 7.35 (dd, 4H), 7.58 (d, 4H), 7.70 (t, 4H), 8.06 (s, 4H), 8.62 (d, 4H), 9.01 (d, 4H).

Instrumentation

The ^{1}H NMR spectra of the new complexes were recorded on a Varian spectrometer at 300 MHz and referenced to the residual proton impurities in the deuterated solvents. Absorption measurements of solutions were performed on a Shimadzu UV 1601PC spectrophotometer, and 96 well plate measurements were performed on a GloMax® Multi Detection System.

X-ray diffraction data were collected on a Apex II diffractometer equipped with a CCD detector. The data sets were recorded as four ω–scans of 600 frames each, at 0.3° step width. The frames were integrated with the Bruker SAINT software, and the absorption correction was based on fitting a function to the empirical transmission surface as sampled of multiple-measured reflections applied by using SADABS. The structures were solved and refined using X-SEED, a graphical interface to SHELX97.

Methods

X-Ray Structural Study of $[Rh_2((C_6H_3\text{-}OCH_3)P(C_6H_3\text{-}OCH_3)_2)_2(dppz)_2][\ BF_4]_2$

For X-ray crystallographic analysis, a bright red/orange block crystal of **8** was selected, with approximate dimensions of 0.10 x 0.12 x 0.06 mm^3. The crystal was formed spontaneously upon precipitation with diethyl ether from the reaction solution in acetonitrile. The crystal was coated with Paratone oil, and transferred to a cold stream (110(2) K) of N_2 on a nylon loop. Indexing of preliminary diffraction patterns indicated the crystal was triclinic. In the final cycles of refinement all atoms were refined anisotropically. Hydrogen atoms were placed at calculated positions. The structure was solved and refined in the space group P-1.

Cell Culture

The HeLa cell line was cultured in Dulbecco's modified Eagle medium with 4.5 mg/mL glucose, and 4 mM L-glutamine (invitrogen), and was modified to include 10% fetal bovine serum (Atlanta Biologicals), 50 µg/mL gentamicin. Cell cultures were incubated in a humidified atmosphere at 37 °C which contained 5% CO_2.

In Vitro Cytotoxicity and Photocytotoxicity

The LC50 concentrations in HeLa cells of the compounds under investigation were determined using the 3-(4,5-dimethylthiazol-2-yl)-d,5-diphenyltetrazolium bromide (MTT) assay (invitrogen).[99] An overconfluent (100% confluent) monolayer of cells in sterile 96 well plates was used for this experiment. The cells were plated at a concentration of 24-36 cell/μL – using 100 μL in each well – and incubated for 48 hours. Once the cells were confluent, the media was replaced with 100 μL of Lebovitz-15 (L15) media (containing no phenol red). The compounds were incubated for 2 hours, and then the wells were washed with 1% dibasic phosphate buffer and the compound solution was replaced with fresh L15 media. The plates that were used to determine photocytotoxicity were then irradiated for 20 minutes with λ_{irr} 375 nm. The plates used for cytotoxicity and photocytotoxicity were then placed in the incubator until it 24 hours had passed since the time the compounds were added. At this point 10 μL of fresh MTT solution was added to each well. After 4 more hours of incubation, 100 μL of fresh SDS solution in 0.01M HCl was added to each well. The plates were incubated for another 4 hours, and then the plates were read at 570 nm using a GloMax® Multi Detection System. Each experiment contained six wells for one concentration of one compound, and each compound was tested three different times.

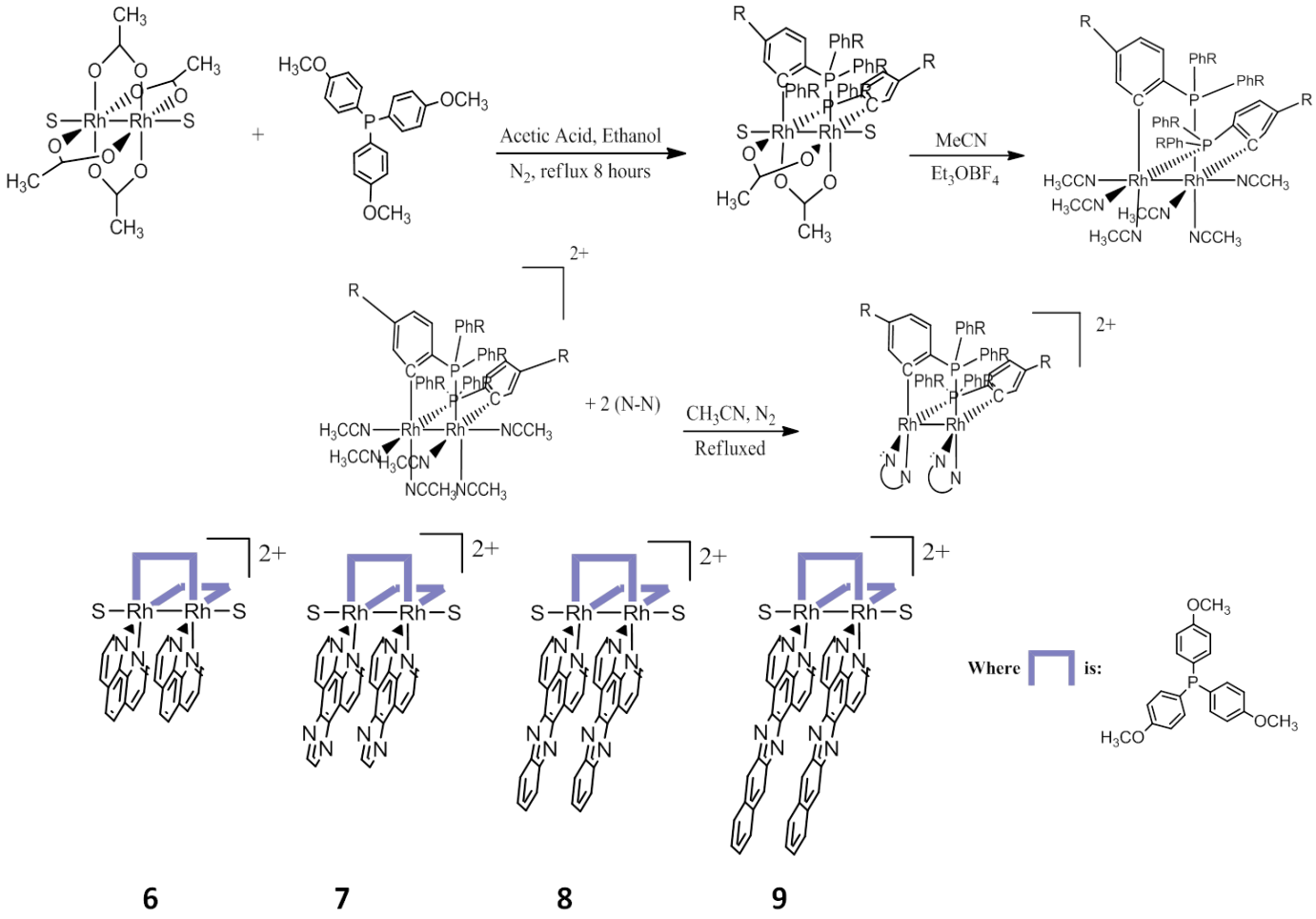

Figure III.1. Synthetic scheme to prepare the series $[Rh_2(PMP)_2(N\text{-}N)_2]^{2+}$.

Results and Discussion

Synthesis and Characterization of the Series $[Rh_2(PMP)_2(N\text{-}N)_2][CH_3CO_2]_2$

The dirhodium analogues of the "homoleptic series" discussed in chapter II: $[Rh_2(PMP)_2(phen)_2][BF_4]_2$ **(6)**, $[Rh_2(PMP)_2(dpq)_2][BF_4]_2$ **(7)**, $[Rh_2(PMP)_2(dppz)_2][BF_4]_2$ **(8)**, and $[Rh_2(PMP)_2(dppn)_2][BF_4]_2$ **(9)**, were synthesized using the starting material $[Rh_2(PMP)_2(CH_3CN)_2][BF_4]_2$ **(5)**. Compound **5** was prepared from the known compound $Rh_2(PMP)_2(CH_3CO_2)_2$ (where PMP is tris(p-methoxyphenyl)phosphine). The acetate bridging ligands were removed by the alkylating agent triethyloxonium tetrafluoroborate ($[(CH_3CH_2)3O][BF_4]$) in acetonitrile. The labile equatorial acetonitrile ligands on the compound $[Rh_2(PMP)_2(CH_3CN)_2][BF_4]_2$ were easily substituted by two equivalents of the diimine ligands phen, dpq, dppz, and dppn (compounds **6**, **7**, **8**, and **9** respectively) upon refluxing for 24 hours (Figure III.1).

The crystal structure of **8** was determined (Figure III.2), and the bond distances and angles are provided (Table III.1 and Table III.2). The results can be compared to the structure of compound **3** (the *μ*-acetate analogue), to

determine the effect of the bridging ligand on the structure. The Rh-Rh bond distance of compound **8** is 2.723 Å, and for **3** it is 2.551 Å. The same splaying of the dppz ligands that occurs in **3** is observed in **8**, which is attributed to the fact that the dppz ligands are brought too close together by the dirhodium bond for π-π stacking, and so they splay to reduce the repulsion between them. The compound is similar to the acetate analogue in that there is internal twist, breaking away from an eclipsed conformation in an attempt to reduce repulsive interactions.[94]

Table III.1. Crystal data and structure refinement for compound **8**.

Empirical formula	C41 H28 B F4 N5 O3 P Rh2
Formula weight	859.39
Crystal system	Triclinic
Space group	P-1
Unit cell dimensions	a = 13.8706 Å α= 87.832
	b = 14.0849 Å β= 79.113°
	c = 23.8704 Å γ = 66.225°
Volume	4662.923 Å3
Z	4
Density (calculated) Mg/m^3	1.843
Crystal size	0.10 x 0.12 x 0.06 mm^3
Reflections collected	24689
Independent reflections	5224 [Rint = 0.0385]
Goodness-of-fit on F^2	1.03
Final R indices [I>2sigma(I)][a]	R1 = 0.0552, wR2 = 0.074
R indices (all data)[a]	R1 =0.0385 , wR2 = 0.203

aR1 = Σ ||Fo| - |Fc|| /Σ |Fo| ; wR2 = [Σ[w(F02-Fc2)2]/Σ[w(F02)2]]1/2

Table III.2. Bond distances for $[Rh_2(PMP)_2(dppz)_2][BF_4]_2$.

Bond type	Bond distance (Å)
Rh2-Rh1	2.723(1)
Rh2-P1	2.252(1)
Rh2-C26	2.028(4)
Rh2-N1	2.197(4)
Rh2-N8	2.125(3)
Rh2-N7	2.182(3)
Rh1-P2	2.252(1)
Rh1-C13	2.043(4)
Rh1-N3	2.126(3)
Rh1-N4	2.195(3)
Rh1-N2	2.182(4)

Table III.3. Dihedral angle for the structure of $[Rh_2(PMP)_2(dppz)_2][BF_4]_2$.

Dihedral Angle	
P1-Rh2-Rh1-P2	-94.62(4)
P1-Rh2-Rh1-C13	-10.3(1)
P1-Rh2-Rh1-N3	81.68(8)
P1-Rh2-Rh1-N4	158.51(8)
P1-Rh2-Rh1-N2	174.5(8)
C26-Rh2-Rh1-P2	-10.9(1)
C26-Rh2-Rh1-C13	73.4(2)
C26-Rh2-Rh1-N3	165.5(1)
C26-Rh2-Rh1-N4	-117.7(1)
C26-Rh2-Rh1-N2	-101.7(8)
N1-Rh2-Rh1-P2	174.0(7)
N1-Rh2-Rh1-C13	-101.7(7)
N1-Rh2-Rh1-N3	-9.7(7)
N1-Rh2-Rh1-N4	67.2(7)
N1-Rh2-Rh1-N2	83(1)
N8-Rh2-Rh1-P2	82.44(8)
N8-Rh2-Rh1-C13	166.7(1)
N8-Rh2-Rh1-N3	-101.3(1)
N8-Rh2-Rh1-N4	-24.4(1)
N8-Rh2-Rh1-N2	-8.4(8)
N7-Rh2-Rh1-P2	159.19(8)
N7-Rh2-Rh1-C13	-116.5(1)
N7-Rh2-Rh1-N3	-24.5(1)
N7-Rh2-Rh1-N4	52.3(1)
N7-Rh2-Rh1-N2	68.3(8)

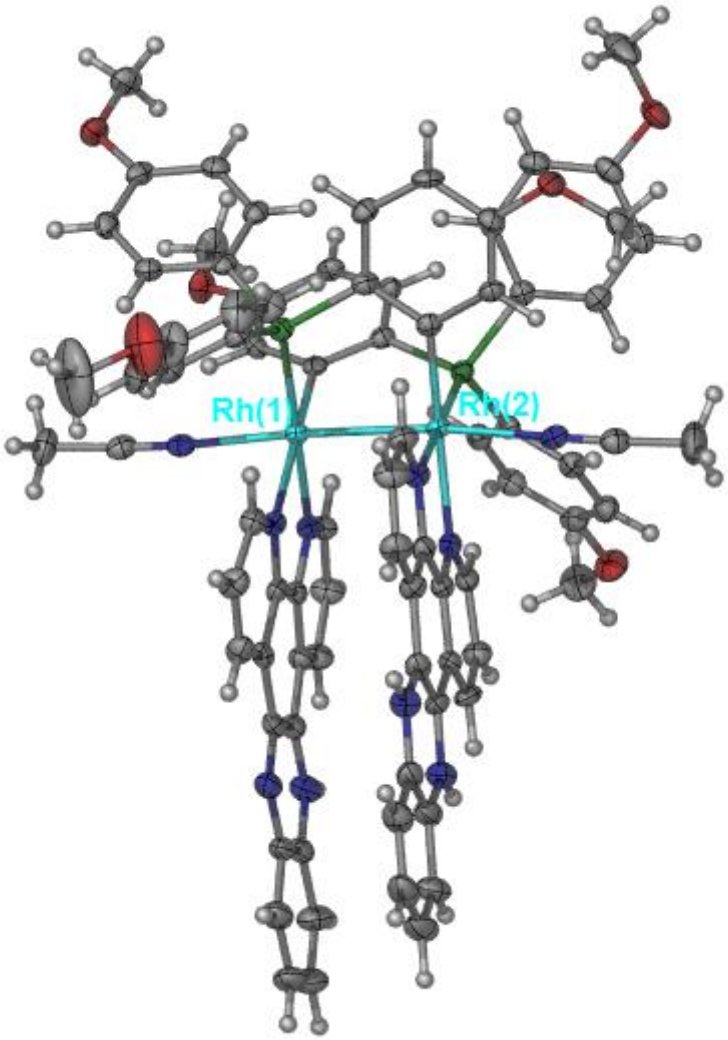

Figure III.2. X-ray crystal structure of $[Rh_2(PMP)_2(dppz)_2][BF_4]_2$.

This series was also characterized by ^{1}H NMR spectroscopy (Figure III.3). In the spectra there is an upfield shift in some of the proton resonances in the aromatic region as compared to the dirhodium acetate analogues. This could be caused by an increase in shielding due to the stronger trans effect of the orthometalated phosphine ligand. This theory is further corroborated by the bond distances seen in the crystal structure.[102] The Rh-N bond distance between the rhodium and the nitrogen of dppz for compound **3** is approximately 2.00 Å, whereas the corresponding bond distance in **8** is approximately 2.10 Å. Elongation of the Rh-N bond is evidence of the trans effect, and explains the upfield shift in the dppz resonances for compound **8**. The downfield shift in the aromatic resonances of the PMP ligand as compared to the known structure $Rh_2(PMP)_2(CH_3CO_2)_2$ is also observed. The electronic absorption spectrum for **8** was found in pH 7 tris buffer. It is seen that there is a strong absorption at wavelengths lower than 400 nm. The tail of the lowest energy band tails off above 600. This represents a bathochromic shift as compared to the acetate analogue, compound **3**, which has a metal centered band at about 560 nm.

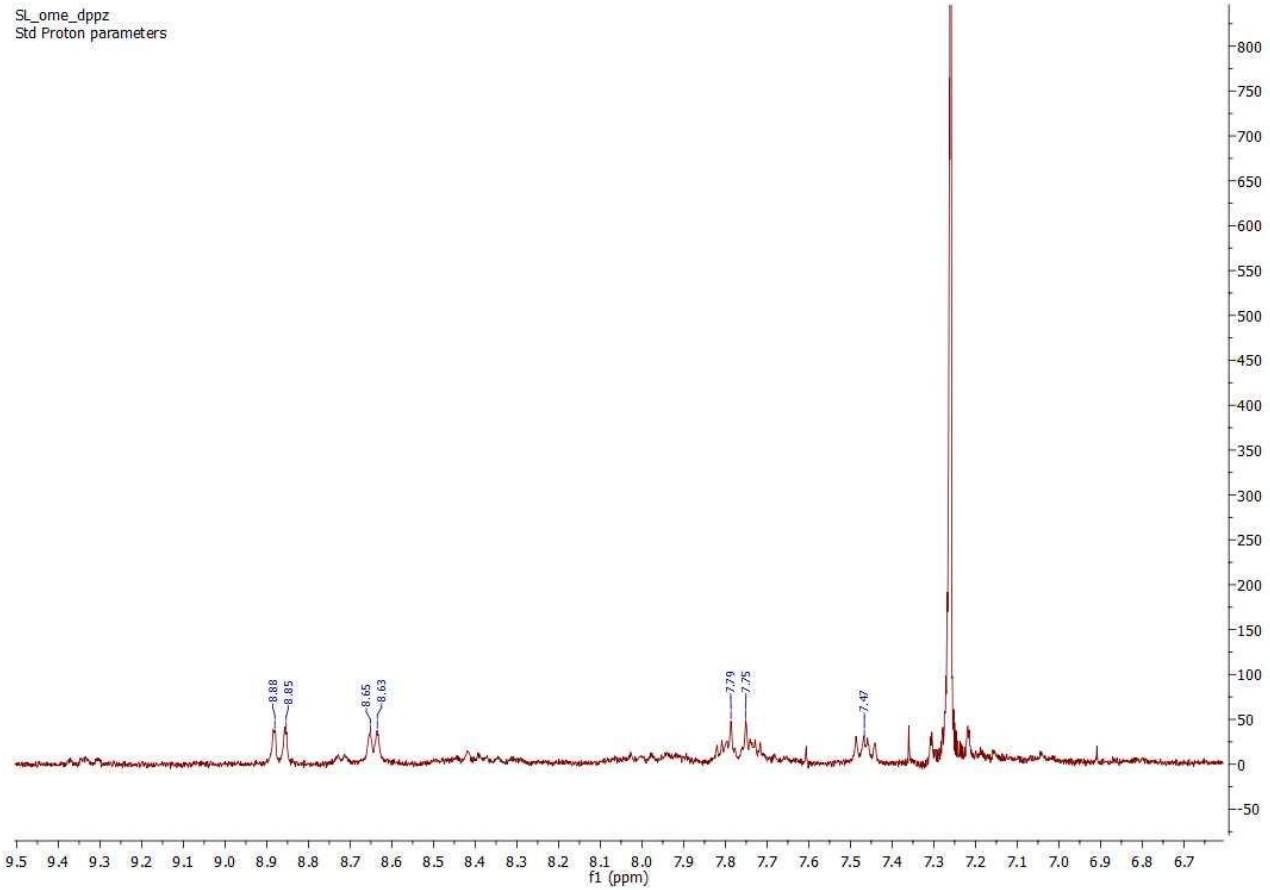

Figure III.3. ^{1}H NMR spectrum of $[Rh_2(PMP)_2(dppz)_2][BF_4]_2$.

Cytotoxicity and Photocytotoxicity

The cytotoxicity and photocytotoxicity of compounds **5**, **6**, **7**, **8**, and **9** were determined using the MTT assay and the LC_{50} of the compounds were determined in the dark and after irradiation. The range of concentrations used in the assay for compounds **5**, **6**, **7**, **8**, and **9** were 50 μM to 800 μM; concentrations that are based on the results of previous series. For all of the MTT assays, both in light and in the dark, the amount of ambient light was limited as much as possible, and experiments used to determine the photocytotoxicity exposed the cells to light for 20 minutes. The results are summarized in Table III.3.

It can be seen that compounds **7** and **9** are the most cytotoxic in the dark, while compound **8** is the least cytotoxic in the dark. The extreme difference in the progression of cytotoxicity from the dpq **(7)** to dppz **(8)** to dppn **(9)** derivatives is surprising, but when considering the properties of the compounds, it seems plausible. The solubility of the compounds in aqueous solutions dramatically decreases from dpq to dppz, which may reduce the cytotoxic effects of dppz to dppn. However the dppn compound is very cytotoxic in the dark, which could be caused by the redox properties of the compound. The photocytotoxicity could lend some further insight into this.

The toxicities of **5**, **6**, **7**, **8**, and **9** were determined after irradiation with light for 20 minutes. Compound **9** has an LC^*_{50} of 71 ± 3 μM, which is very

close to its LC_{50} value in the dark (85 ± 5 μM). The ratio of LC_{50} values in the dark and light is 1.2, which indicates that irradiating the compound for 20 minutes does not cause an increase in cytotoxicity. It is known that dppn compounds (such as compound **4**) are able to produce singlet oxygen, and photocleave DNA in the presence and absence of oxygen upon irradiation with light. Therefore, it could be that the redox activity of this compound seen upon irradiation of compound **4** readily occurs in the dark for compound **9**. In order to conclusively determine the mechanism of cytotoxicity for **9** more experimentation is needed; including electrochemistry experiments and further analysis of photoactivity.

The photocytotoxicity of **7** and **8** show an increase in toxicity upon irradiation with light. Compound **7** has a two fold increase in cytotoxicity in the dark and light upon irradiation. Compound **8** has an LC_{50} value of 901 ± 6 μM, and an LC^*_{50} value of 126 ± 6 μM; which is a 7 fold increase in cytotoxicity. This is a better ratio than that found in photofrin®, indicating that this compound has the potential to be used as a PDT agent.

Compounds **5** and **6** have not yet been discussed. Neither of these compounds shows an increase in toxicity upon irradiation. The LC_{50} values are greater than the other compounds in the series, with **5** being around 250 μM and **6** being just under 600 μM. The results for **6** are expected, based on the results found for compound **2** in the previous chapter. Both of these dirhodium phen

derivatives have high LC_{50} values, with the LC_{50} in the dark having a slightly higher toxicity than the LC^*_{50} value. The results of compound **5** are somewhat surprising because it is known that the acetonitrile ligands in both the axial and equatorial ligands are labile, especially upon irradiation. It is possible that the compound is not able to easily enter the cell, or perhaps the less electrophilic dirhodium core is not as active without an aromatic ligand that is capable of being easily reduced.

One of the reasons for studying this series of compounds was to see how the bridging ligand affects the biological properties of the compound. When comparing the cytotoxicity and photocytotoxicity of these compounds it is clear that the PMP bridging ligand enhances the toxicity of compounds **7** and **9** in the dark and upon irradiation. The cytotoxicity in the dark for compound **8** is dramatically lower than that of **3**, and has exactly the same photocytotoxicity as compound **3** (Table III.4). This indicates the mechanism of activity upon irradiation is similar for both compounds and so is likely to be due to the dppz ligand. More work needs to be done to truly understand the results found.

Table III.4. Cytotoxicity and photocytotoxicity data for compounds **5-9**.

	Compound	LC_{50}* (μM)	LC_{50} (μM)	Ratio
(5)	$[Rh_2((C6H3OCH3)P(C6H4OCH3)_2)_2(CH3CN)_6][BF_4]_2$	258 ± 4	245 ± 5	1.0
(6)	$[Rh_2((C_6H_3OCH_3)P(C_6H_4OCH_3)_2)_2(phen)_2][BF_4]_2$	571 ± 10	592 ± 5	1.0
(7)	$[Rh_2((C_6H_3OCH_3)P(C_6H_4OCH_3)_2)_2(dpq)_2][BF_4]_2$	44 ± 3	76 ± 10	1.7
(8)	$[Rh_2((C_6H_3OCH_3)P(C_6H_4OCH_3)_2)_2(dppz)_2][BF_4]_2$	126 ± 6	901 ± 6	7.2
(9)	$[Rh_2((C_6H_3OCH_3)P(C_6H_4OCH_3)_2)_2(dppn)_2][BF_4]_2$	71 ± 3	85 ± 5	1.2

LC50 ± SD is the value upon radiation with light for 20 minutes*

Concluding Remarks

The results found from these experiments represent promising steps forward in the pursuit of understanding the structure-function relationship of dirhodium compounds, and the pursuit of discovering potential PDT agents. The ratio of cytotoxicity in the dark and upon irradiation for compound **8** makes it a good candidate for PDT. The 7-fold increase in toxicity is a higher ratio than the 5.5 fold increase observed in the clinical PDT agent photofrin®. It should be noted, however, that **8** was irradiated at a wavelength of 350 nm, where it absorbs strongly. Further studies need to be done to determine the ratio of toxicity upon irradiation with light in the PDT window (greater than 600 nm).

It is interesting to observe the effect that changing the bridging ligand had on the homoleptic dirhodium diimine series. Compounds **6-9** had similar or

higher toxicity than their counterparts (**1-4**), and a slight bathochromic shift in the tail of the MC band observed in the electronic absorption spectrum. In the cell studies detailed in the introduction to this chapter an orthometalated bridging ligand bound through an oxygen atom showed greater cytotoxicity than the ortho-c analogue. It should be mentioned that the preliminary studies of the cytotoxicity and photocytotoxicity of a known ortho-o dirhodium compound, [Rh2(O2CCF3)3(TMPP)] (where TMPP is (2,4,6-trimethoxyphenyl)phosphine), was examined for anticancer activity.[103] However, there was no change in cytotoxicity upon irradiation, and the LC_{50} concentrations were almost 500 μM. This is likely due to the poor solubility of the compounds in water, thus further efforts in developing more water soluble analogues is of high interest.

CHAPTER IV

SYNTHESIS, CHARACTERIZATION, AND BIOLOGICAL PROPERTIES OF $[Ir_2(DTolF)_2(CH_3CN)_6][BF_4]_2$

Introduction

Iridium compounds have been gaining in popularity for use as anticancer drugs.[104] Research into the biological propterties of iridium compounds have focused on Ir(III) and Ir(I) oxidation states to date.[104,105,106] A primary area of interest has been iridium(III) compounds with diimine ligands that are able to intercalate between DNA base pairs.[107] In 2001, Barton and coworkers showed that Ir(III) phi complexes were capable of intercalating DNA.[92,108] The negative reduction potential of $[Ir(bpy)(phen)(phi)]^{3+}$ made it possible to investigate the properties of the reduced phi complexes intercalated in DNA without interference from Ir =(II) (where phi is 9,10-phenanthrenequinone diimine).[108]

Other known Ir(III) intercalators include $[Ir(ppy)_2(pp)][PF_6]$ (where ppy is 2-phenylpyridine, and pp is dpq, dppz, or dppn),[109] $[(\eta^5\text{-}C_5Me_5)Ir(dppz)(peptide\text{-}\kappa S)]^{n+}$,[110] and $[(\eta^5\text{-}C_5Me_5)IrCl(pp)][CF_3SO_3]$ and $[(\eta^5\text{-}C_5Me_5)Ir((NR_2)_2CS)pp][CF_3SO_3]_2$ (where R is H or Me, and pp is dpq, dppz, or dppn).[104] The compound $[Ir(ppy)_2(pp)][PF_6]$ was studied for its luminescent properties in the presence and absence of DNA; revealing that the luminescence of the compounds intercalated in DNA can be up to 40 times greater (depending on the analogue) than the luminescence of the compound in aqueous media.[109]

The increase in luminescence of the iridium(III) compound in the presence of DNA is due to the fact that the luminescence is ligand-based, and when the compound is able to hydrogen bond, it decreases the luminescence, but when the ligand intercalates into DNA it is protected from any interactions with water. Upon intercalation the diimine ligand is in a more hydrophobic and rigid environment, which also helps to increase the luminescent properties.[109] The half sandwich Ir(III) compound, $[(\eta^5\text{-}C_5Me_5)Ir(dppz)(peptide\text{-}\kappa S)]^{n+}$, was found to bind DNA through intercalation with K_b values of 1.3 - 3.3 X 10^6.[107] It was also observed that the peptide was eventually cleaved, leaving the iridium core to bind to DNA. This same research later published work on the other half sandwich compounds listed above, $[(\eta^5\text{-}C_5Me_5)Ir(L)(pp)][CF_3SO_3]_x$ (where L is Cl, $(NH_2)_2CS$, and $(N(CH_3)_2)_2CS$).[104] The analogue where L = Cl was shown to intercalate DNA, and the slow substitution of the chloride ligand results in the iridium(III) center binding to N7 on the DNA. In the thiourea derivative, sterics lead to side-on intercalation of dppz, and partial intercalation of dpq; however, dppn is too large to intercalate in any manner. The tetramethylthiourea derivative shows strong binding of the dppn derivative to DNA via intercalation, which is in opposition to the results shown for the thiourea compound. This fact is thought to be caused by the tetramethylthiourea compound to change the conformation of DNA from B to A.[104]

Iridium(III) partial sandwich compounds have recently been investigated for potential cytotoxicity towards cancer cells.[106] In 2010, the compound $[(\eta^5\text{-}$

C_5Me_5)Ir(pyTz)Cl]$^+$ (where pyTz is 2-(pyridine-2-yl)thiazole) was tested in the ovarian cancer cell lines A2780 and A2780cisR (A2780cisR being cisplatin resistant).[111] The IC_{50} (the concentration required to inhibit 50%) for the iridium(III) compound exibits greater than 300 μM after 72 hours, showing that it was not very cytotoxic. Its rhodium (III) counterpart had similar cytotoxicity values after 72 hours of exposure.[111]

Another partial sandwich compound, [(η^5-C_5Me_5)IrCl(XY)]^n (where XY is either 2,2'-bipyridine – n is 1+, or 2-phenylpyridine – n is 0), has been probed for its anticancer activity.[112] The bidentate ligand, XY, was shown to greatly affect the IC_{50} value. When introduced to the A2780 cell line for 24 hours, the bpy derivative has an IC_{50} value greater than 100 μM, whereas the phpy derivative has an IC_{50} value of about 11 μM. These compounds can also undergo substituting of the chloride ligand for 9-ethylguanine, or 9-methyladenine. It was shown that the bidentate ligand used affects the equalibrium of binding of 9-EtG or 9-MeA, where the bpy derivative binds to only 9-EtG, and the phpy derivate binds both bases, but it binds 9-MeA more strongly. This is an excellent example of how the chelating ligands affect the anticancer properties of Iridium (III) compounds.[112]

Recently, more work has been carried out to determine the effect that the bidentate ligand has on the cytotoxicity of iridium (III) half sandwich compounds. To this end a series of compounds, [(η^5-C_5Me_5)IrCl(phen*)]$^+$ (where phen* is 5,6-

methylphen, 5-Clphen, or 5-NO_2phen), has been studied.[104] It was shown that the more electron withdrawing the phen derivative is, the more cytotoxic the compound is. The cytotoxicity was found for several cell lines, including MCF-7 (breast cancer), HT-29 (colon cancer), and immortalized HEK-293, when the cells were incubated with the compounds for 48 hours. For all cell lines, the 5,6-methylphen derivative was the least cytotoxic derivative (with IC_{50} values between 50 and 60 μM), and the 5-Clphen and 5-NO_2phen were about half as cytotoxic. The ability to drastically tune the cytotoxicity iridium (III) compounds based on the ligand field lends great potential for designing anticancer drugs.[104]

In addition to Ir(III) compounds, Ir(I) compounds have been shown to have anticancer activity as well.[105] However, few, if any, examples of iridium (II) compounds have been investigated for their biological activities. More specifically, diiridium (II,II) compounds have not been studied as anticancer agents, but the redox properties of these compounds are proving to be useful in photocatalytic H_2 production, photochemistry, bond activation, and other chemistry.[113] The first examples of diiridium (II,II) compounds were reported in the 1970's and 80's.[114,115] The exploration of the properties of diiridium compounds have been compared to the better understood properties of dirhodium compounds. In comparison the diiridium sigma bond is stronger than its dirhodium counterpart, and it was found that similarly to dirhodium, the axial ligands do not greatly affect the iridium-iridium bond distance.[116]

The reactivity, and properties of diiridium (II,II) compounds are still less known than dirhodium (II,II) compounds, which is understandable as diiridium (II,II) compounds are very stable, and therefore tend to be relatively inert.[117] Taking a cue from dirhodium chemistry, we decided to synthesize diiridium compounds with more labile ligands, such as acetonitrile. In this vein the compound $[Ir_2(DTolF)_2(CH_3CN)_6][BF_4]_2$ was synthesized.[117] The Ir-Ir bond distance is 2.601(1) Å, the equatorial Ir-$NCCH_3$ bond distance is approximately 2.00 Å, and the axial Ir-$NCCH_3$ bond distance is approximately 2.20 Å.[117] As compared to the dirhodium analogue that was reported a few years later, $[Rh_2(DTolF)_2(CH_3CN)_6][BF_4]_2$, the Rh-Rh bond distance is 2.5594(8) Å, the equatorial Rh-$NCCH_3$ bond distance is approximately 2.02 Å, and the axial Rh-$NCCH_3$ bond distance is about 2.23 Å.[117-119] While the dirhodium bond distance is shorter than that of the diiridium compound, the metal-$NCCH_3$ bond distances are shorter for the diiridium compound than the dirhodium compound.

The compound $[Rh_2(DTolF)_2(CH_3CN)_6][BF_4]_2$ was later investigated for biological activity, and was found to bind dsDNA in its equatorial positions.[73,74,120] Because of this result it was of interest to study the biological activity of the compound $[Ir_2(DTolF)_2(CH_3CN)_6][BF_4]_2$. This chapter details new synthetic routes to the diiridium partially solvated compound, and characterization of the structure. The cytotoxicity and the photocytotoxicity in HeLa cells was studied; the partition coefficient was found to lend insight into a possible contributor the toxicity of the compound.

Experimental Section

Materials

The reagents $NOBF_4$, p-toluidine, triethyl orthoformate, and cyclooctadiene (COD) were purchased from Acros, and used as received. The starting material $[Ir(COD)Cl]_2$ was purchased from Pressure Chemicals and used as received. The HeLa cell line was obtained from the American Type Culture Collection.

The starting materials ditolylformamidinate and $[Ir(DTolF)COD]_2$ (where DTolF is formamidine and COD is 1,8-cyclooctadiene) were synthesized according to literature procedures.[121,122]

Synthesis of $[(DTolF)_2Ir(COD)Ir(CH_3CN)_3][BF4]_2$ ***(10)***

The oxidizing agent $NOBF_4$ (0.022 g) was added to a solution of (0.100 g) $[Ir(DTolF)COD]_2$ in 8 mL of distilled acetonitrile under an N_2 atmosphere. The mixture was stirred for 24 hours, during which time the color turned from purple/brown to brown. The solution was reduced in volume, and diethylether was added to precipitate the product. The reaction afforded a 92% yield. ^1H NMR (300 MHz) CD_3CN ɗ/ppm (mult./ integral/ assignment): 1.96 (s, free acetonitrile), 2.32 (s, 24H), 2.50 (s, 10H, H_2O), 2.70 (s, 3H) 2.81 (s, 8H), 4.75 (s,

2H), 5.2 (s, 2H), 6.92 (t, 5H), 7.05 (m, 6H), 7.17 (m, 9H), 7.28 (s broad, 4H), 7.90 (s, 2H).

Synthesis of $[Ir_2(DTolF)_2(CH_3CN)_6][BF4]_2$ ***(11)***

The compound $[(DTolF)_2Ir(COD)Ir(CH_3CN)_3][BF4]_2$ (0.061 g) was refluxed in 10 mL of acetonitrile under an N_2 atmosphere for 2 hours, and then the reaction was stirred under N_2 overnight at room temperature. The solvent was reduced in volume to about 4 mL under vacuum, and a small amount of $NaBF_4$ was added to help precipitate the product. Diethyl ether was then added to precipitate the product, and it was left at 5 °C overnight. The product was collected by filtration in air, and 84% was recovered. ^{1}H NMR (300 MHz) CD_3CN ɗ/ppm (mult./ integral/ assignment): 1.96 (s, free acetonitrile), 2.26 (s, 6H, tolyl), 2.72 (s, 12H, MeCN), 6.93 (d, 8H) 7.02 (d, 8H), 7.75 (s, 2H).

Instrumentation

The ^{1}H NMR spectra of the new complexes were recorded on a Varian spectrometer at 300 MHz and referenced to the residual proton impurities in the deuterated solvents. Absorption measurements of solutions were performed on a Shimadzu UV 1601PC spectrophotometer, and 96 well plate measurements were performed on a GloMax® Multi Detection System. Mass spectra were

acquired on a PE SCIEX QSTAR Pulsar electrospray ionization mass spectrometer at Texas A & M University.

Methods

Cell Culture

The HeLa cell line was cultured in Dulbecco's modified Eagle medium with 4.5 mg/mL glucose, and 4 mM L-glutamine (Invitrogen), and was modified to include 10% fetal bovine serum (Atlanta Biologicals), 50 µg/mL gentamicin. Cell cultures were incubated in a humidified atmosphere at 37 °C which contained 5% CO_2.

In Vitro Cytotoxicity and Photocytotoxicity

The LC_{50} concentrations in HeLa cells of the compounds under investigation were determined using the 3-(4,5-dimethylthiazol-2-yl)-d,5-diphenyltetrazolium bromide (MTT) assay (Invitrogen).[99] An overconfluent (100% confluent) monolayer of cells in sterile 96 well plates was used for this experiment. The cells were plated at a concentration of 24-36 cell/µL – using 100 µL in each well – and incubated for 48 hours. Once the cells were confluent the media was replaced with 100 µL of Lebovitz-15 (L15) media (containing no phenol red). The compounds were incubated for 2 hours, and then the wells

were washed with 1% dibasic phosphate buffer and the compound solution was replaced with fresh L15 media. The plates that were used to determine photocytotoxicity were then irradiated for 20 minutes with λ_{irr} 350 nm**.** The plates used for cytotoxicity and photocytotoxicity were then placed in the incubator until it 24 hours had passed since the time the compounds were added. After this time 10 µL of fresh MTT solution was added to each well. After 4 additional hours of incubation, 100 µL of fresh SDS solution in 0.01M HCl was added to each well. The plates were incubated for another 4 hours, and then the plates were read at 570 nm using a GloMax® Multi Detection System. Each experiment contained six wells for one concentration of one compound, and each compound was tested three different times.

Results and Discussion

Synthesis and Characterization of $[Ir_2(DTolF)_2(CH_3CN)_6][BF_4]_2$

The synthesis and characterization of $[Ir_2(DTolF)_2(COD)(CH_3CN)_3][BF_4]_2$ and $[Ir_2(DTolF)_2(CH_3CN)_6][BF_4]_2$ were first reported by Dunbar and coworkers in 1995. After examining the anticancer effects of various dirhodium series of compounds we were interested in determining the anticancer activity of analogous diiridium compounds. In pursuit of this goal a problem was encountered, namely that color of $[Ir_2(DTolF)_2(CH_3CN)_6][BF_4]_2$ would change from a pale yellow to a dark purple/grey when exposed to light over a short

period of time. The best hypothesis for this occurrence is that the silver (in the silver trifluoroacetate required to synthesize the precursor for this compound) was not fully removed. In order to test the toxicity of these compounds, and be sure that silver did not interfere in the results it was necessary to find an alternate synthesis that did not require silver (Figure IV.1).

In the original synthesis the compound $[Ir(DTolF)(COD)]_2$ was reacted with silver trifluoroacetate in toluene. The silver acts as an oxidizing agent, forming the mixed valence iridium (I,III) compound, $[(DTolF)_2Ir(COD)Ir(CF_3COO)_2(H_2O)]$. This compound is then refluxed for three hours in acetonitrile (using Schlenk-line techniques) to first form the intermediate $[Ir_2(DTolF)_2(COD)(CH_3CN)_3][BF_4]_2$. After three more hours of refluxing the hexaacetonitrile compound, $[Ir_2(DTolF)_2(CH_3CN)_6][BF_4]_2$, is formed. In several instances it was found that the product degraded in light. The obvious cause for this would be silver contamination, and an effort was made to find evidence for this hypothesis. The ESI mass spectra of the freshly made pale yellow $[Ir_2(DTolF)_2(CH_3CN)_6][BF_4]_2 + H^+$ at m/z is 1081. Upon turning to a purple/brown color the ESI mass spec was performed on the same batch of $[Ir_2(DTolF)_2(CH_3CN)_6][BF_4]_2 + H^+$ and the m/z was 1051. Efforts to find the identity of the species formed using ^1H NMR are still underway.

In order to circumvent the use of silver, another oxidizing agent needs to be used. Because the mixed valence compound is not necessary, a one step

reaction from $[Ir(DTolF)(COD)]_2$ to $[Ir_2(DTolF)_2(CH_3CN)_6][BF_4]_2$ was attempted in acetonitrile using two equivalents of the oxidizing agent $NOBF_4$. This oxidizing agent was chosen in hopes that it would not coordinate to the iridium compound. It was found that upon reacting $[Ir(DTolF)(COD)]_2$ with $NOBF_4$ in acetonitrile at room temperature, the compound $[Ir_2(DTolF)_2(COD)(CH_3CN)_3][BF_4]_2$ was formed. When refluxing this compound in acetonitrile, the partially solvated compound was successfully prepared.

The identities of the compounds $[Ir_2(DTolF)_2(COD)(CH_3CN)_3][BF_4]_2$ (Figure IV.2) and $[Ir_2(DTolF)_2(CH_3CN)_6][BF_4]_2$ (Figure IV.3) were confirmed via ^1H NMR spectroscopy, and mass spectrometry. From the ^1H NMR spectrum of $[Ir_2(DTolF)_2(CH_3CN)_6][BF_4]_2$ it can be seen that there is a peak at 7.75 ppm and 7.02 to 6.96 ppm, which is indicative of the formamidinate bridge-head and aromatic region (respectively).[117] The ESI mass specrum of the hexaacetonitrile compound has a peak at m/z 1081, which indicates that the axial acetonitrile ligands remain intact. As previously stated, Ir-Ir bond distance is 2.601(1) Å, the equatorial Ir-$NCCH_3$ bond distance is approximately 2.00 Å, and the axial Ir-$NCCH_3$ bond distance is approximately 2.20 Å. As compared to the dirhodium analogue of this compound, the Ir-N bond distances are shorter, which indicates a strong interaction.

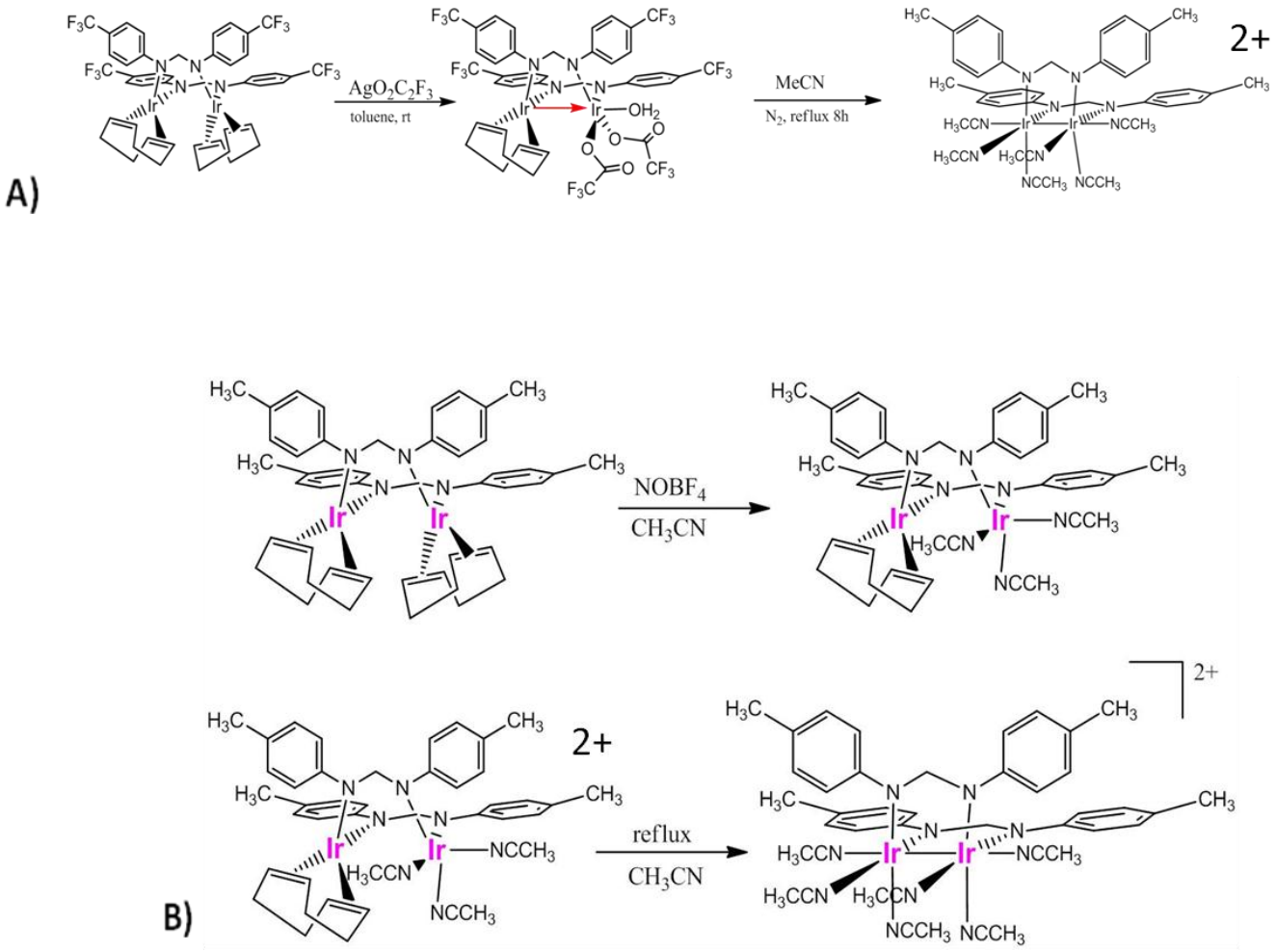

Figure IV.1. A) Reported synthesis for $[Ir_2(DTolF)_2(CH_3CN)_6][BF_4]_2$ B) New synthesis of $[Ir_2(DTolF)_2(CH_3CN)_6][BF_4]_2$

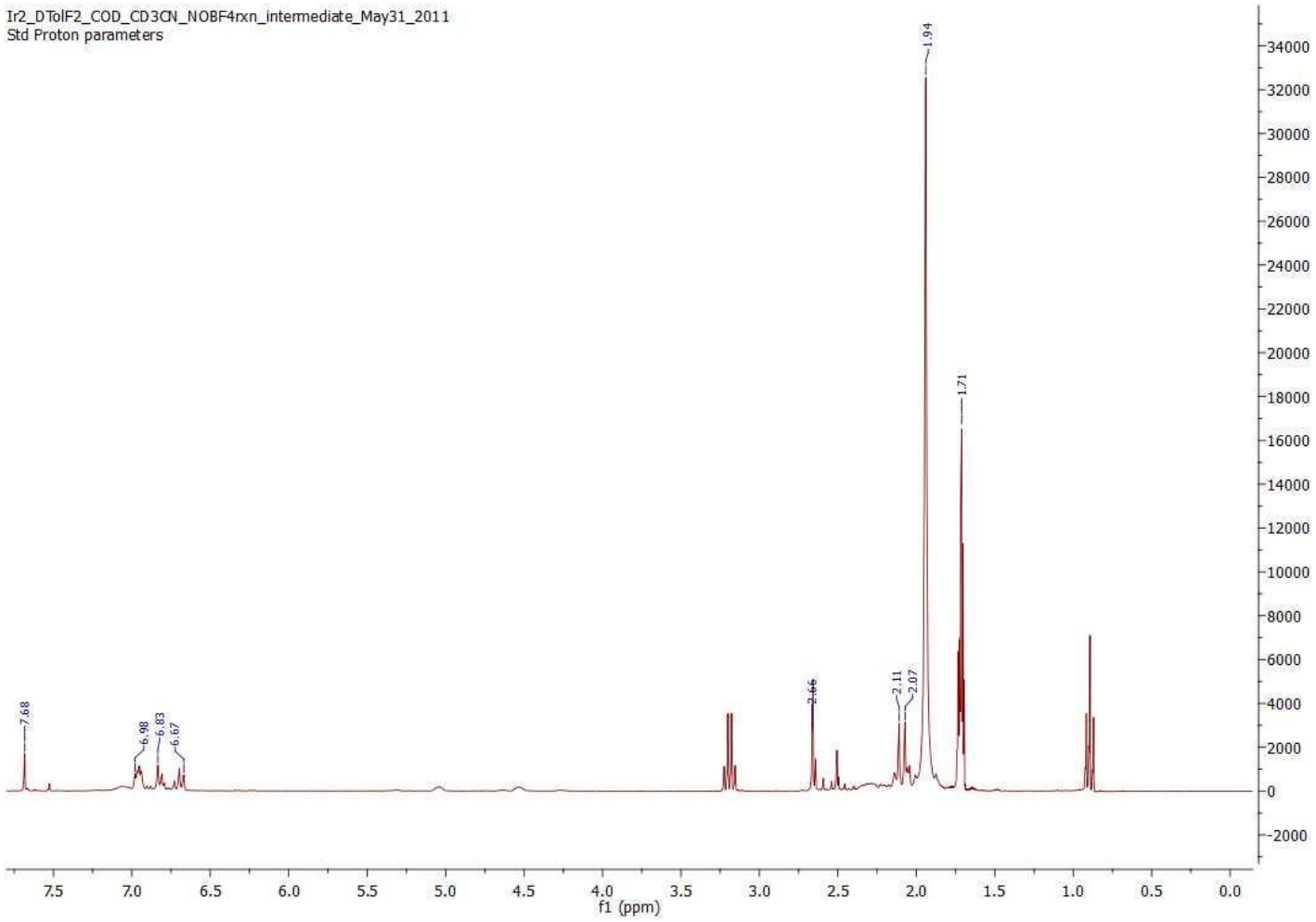

Figure IV.2. ^{1}H NMR spectrum of (COD)Ir(DTolF)$_2$Ir(CH$_3$CN)$_3$.

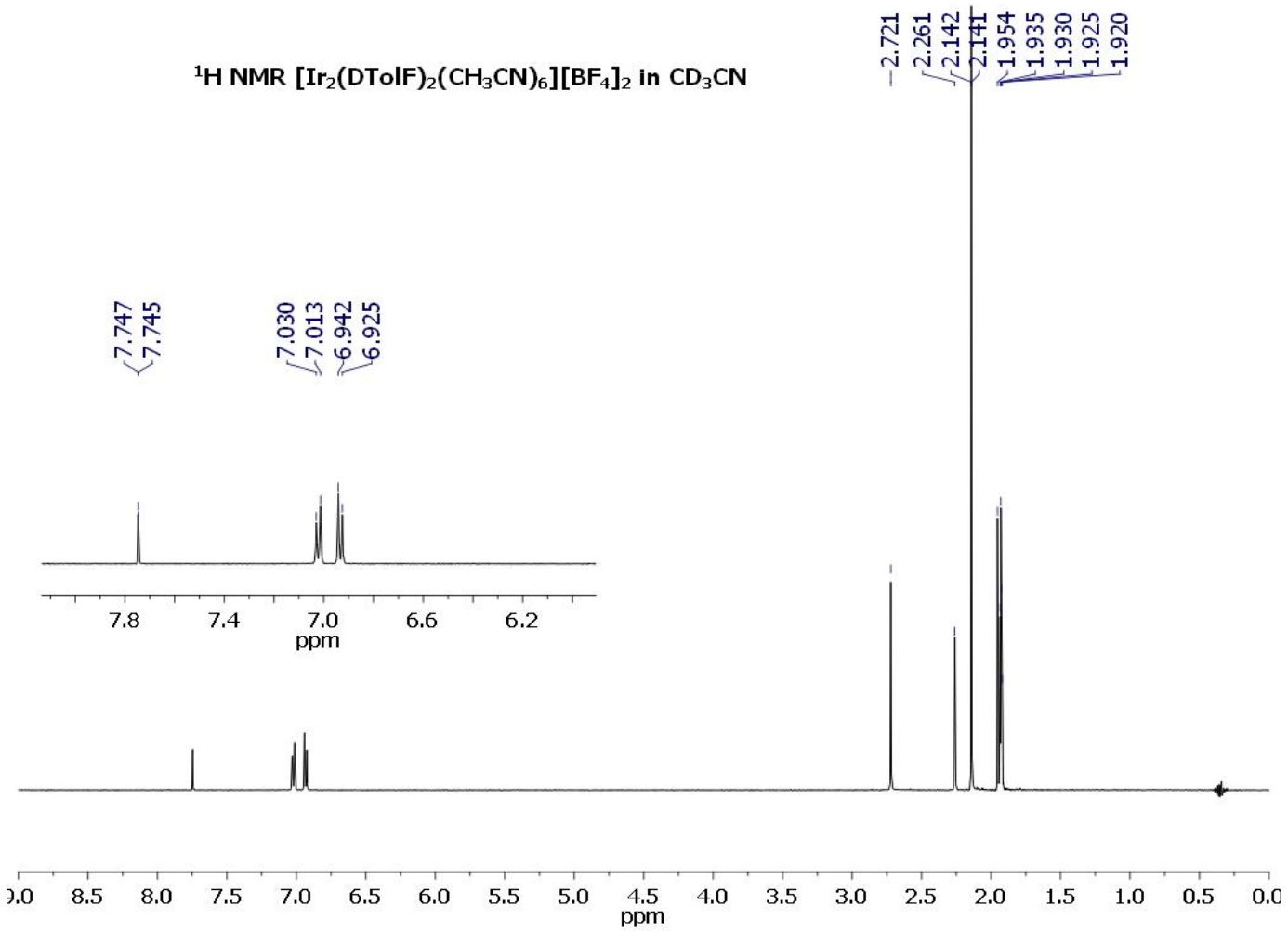

Figure IV.3. ^{1}H NMR spectrum of $[Ir_2(DTolF)_2(CH_3CN)_6][BF_4]_2$.

Cytotoxicity and Photocytotoxicity

Table IV.1. Cytotoxicity and photocytotoxicity of $[Ir_2(DTolF)_2(CH_3CN)_6][BF_4]_2$.

Compound	LC_{50}* (μM)	LC_{50} (μM)	Ratio
$[Ir_2(form)_2(CH3CN)_6][BF_4]_2$	105 ± 9	83 ± 4	0.8

LC_{50} ± SD is the value upon radiation with light for 20 minutes*

The cytotoxicity and photocytotoxicity of $[Ir_2(DTolF)_2(CH_3CN)_6][BF_4]_2$ was determined in HeLa cells (Table IV.1). The cytotoxicity was determined to be 83 ± 4 μM and the photocytotoxicity was determined to be 105 ± 9 μM. These values were found after an incubation period of 2 hours. The LC_{50} value (in the dark) after incubation of HeLa cells with the partially solvated compound for 24 hours is 54 ± 4 μM. The low LC_{50} values are somewhat surprising based on the stability of the diiridium compound, and its full coordination sphere. In the dirhodium series studied it was proven that the toxicity of the compounds was related to having an open axial position that could bind to biomolecules.[123] The importance of the axial position to dirhodium toxicity was shown when the LC_{50} values of a series of compounds were studied. The series is composed of $[Rh_2(CH_3CO_2)_2(np)_2]^{2+}$ (where np is 1,8-naphthyridine), $[Rh_2(CH_3CO_2)_2(np)_2]^{2+}$ (where pynp is 2-(2-pyridil)1,8-naphthyridine), and $[Rh_2(CH_3CO_2)_2(pynp)_2]^{2+}$. It was shown that when both of the axial positions were blocked the compound is

not cytotoxic, meaning that the compounds were not capable of binding to DNA, and the LC_{50} values were above 500 μM (which is considered to be non-toxic).[123]

This hypothesis was carried over into the diiridium chemistry, but these results called that assumption into question. Because of the evidence seen in the mass specrum it was assumed that the axial acetonitrile were inert to substitution. However, a color change from pale yellow to purple/brown was observed when the compound was dissolved in octanol. Further studies showed that the diiridium partially solvated compound was dark purple in acetone, green in glycerol, and bright yellow in DMSO (dimethylsulfoxide). When the diiridium compound is dissolved in acetone, only a small quantity of acetonitrile will cause the solution to return to a pale yellow. These observations call into question the idea that the axial ligands would not be displaced. To test this concept even further the solubility and color change of $[Ir_2(DTolF)_2(CH_3CN)_4(CNCH_3)_2][BF_4]_2$ was tested in octanol and acetone. This compound is known to have very strongly bound isonitrile ligands, which will not be displaced easily. When dissolved in both octanol and acetone a decrease in solubility was observed as compared to compound **11**, and there was no color change. These results indicate that it is likely the axial positions of **11** that are labile, and therefore are able to interact with biomolecules *in vivo*. This could be the reason for the high cytotoxicity of compound **11**.

Concluding Remarks

Iridium compounds are not well studied, but more emphasis is being placed on research into iridium (III) partial sandwich compounds. There are few, if any, reports on the biological activity of diiridium (II,II) compounds, and so this is an important study. The findings that this inorganic diiridium compound has a high cytotoxicity that is independent of photoactivation opens the door to further studies of diiridium compounds. It is even more interesting that this is a very stable compound, and yet has a low LC_{50} concentration.

The success of the silver-free synthesis is also relevant, as diiridium (II,II) compounds are be difficult to work with. The partially solvated diiridium compound was originally of interest because of an effort to make another homoleptic diimine series with a different metal. The substitution of the equatorial acetonitrile ligands has proven very difficult. Even after refluxing for over 5 days, there is no substitution observed. The diimine series is still being actively pursued, as it has been observed for iridium (III) compounds that the diimine derivatives can be very active. It will be exciting to see how this will translate to the diiridium (II,II) compounds.

CHAPTER V

CONCLUSIONS

This thesis details the synthesis, cytotoxicity, and photocytotoxicity of rhodium and iridium metal-metal bonded compounds. The diimine ligands used in the dirhodium compounds (dpq, dppz, and dppn) exibit cytotoxic behavior when irradiated with light. The most interesting compounds are the dppz and dppn derivatives, which have the highest ratio between the LC_{50} values in the dark and upon irradiation. Further exploration in this area is needed to understand the cellular targets of these compounds, and their mechanism of cytotoxicity. Previous results have shown that compound **4** is not capable of reaching the nucleus, and kills the cell via a non-programmed cell death pathway. The next step for determining the cellular localization of compounds would be to tag the compounds with a fluorescent dye, or use ICP mass spectroscopy to see if the compounds enter the nucleus. If these experiments could be repeated over a period of time it would be possible to see how long it takes the drugs to reach their target.

The series of compounds **1-4** are of interest as potential PDT agents. The best candidates for this therapy are compounds **3** and **4**, which exhibit an increase in cytotoxicity upon irradiation with 350 nm light. This is not the optimal wavelength for use in PDT therapy, and in an attempt to shift the energy of light needed to activate the compound to a lower energy, different bridging ligands

are being explored. This thesis details the synthesis of a completely new series of compounds **5-9**. When the electronic absorption spectrum was measured, a bathochromic shift in the tail of the MC band into the PDT window is seen. That coupled with the 7-fold increase in cytotoxicity between the dark and the light for compound 8 makes it a potential PDT agent. Further studies need to be performed on the photoactivity of the compound to test if it is capable of sensitizing singlet oxygen. Also, DNA cleavage studies in the dark and upon irradiation would indicate the ability of this compound to cleave DNA. These studies can be performed in a low oxygen environment, which would reveal the ability of these compounds to be toxic without producing singlet oxygen (this is a character of the series **1-4**). Many of the most aggressive tumor cells are hypoxic, making this a desirable trait in a PDT agent.

Future work will focus on new bridging ligands that could further improve the potential for these dirhodium diimine compounds to be used as PDT agents. Further studies of ortho metalated compounds (bound through oxygen and phosphorous atoms) would be a good series to study. While the TMPP ligand was not immediately successful, perhaps a more water soluble version would prove valuable. It would also be interesting to investigate how the bridging ligand effects the localization and mechanism of cell death in the cell.

Finally, the diiridium project proved to be the most challenging, but the most rewarding. The new synthetic path to compound **11** will prove useful in

using any of its derivatives in biological studies. It should also be noted that the new synthetic pathway eliminates a step from the synthetic process, which is advantageous. Future work will also focus on the substitution of the acetonitrile ligands for the diimine ligands (phen, dpq, dppz, and dppn).

REFERENCES

(1) Murphy, S. L.; Xu J, Kochanek, K. D. *National Vital Statistics Report*. **2012** 60(4).

(2) American Cancer Society. *Cancer Facts & Figures, 2010*. American Cancer Society: Atlanta, GA, 2010.

(3) American Cancer Society. *The History of Cancer*. American Cancer Society: Atlanta, GA, 2012.

(4) Olson, J. S. *Bathsheba's Breast : Women, Cancer & History*; Johns Hopkins University Press: Baltimore, MD, 2002.

(5) Bosch, F.; Rosich, L. *Pharmacology.* **2008**, *82*, 171.

(6) Chabner, B. A.; Roberts, T. G. *Nat Rev Cancer.* **2005**, *5*, 65.

(7) Papac, R. *Yale Journal of Biology and Medicine.* **2001**, *74*, 391.

(8) DeVita, V. T.; Chu, E. *Cancer Res.* **2008**, *68*, 8643.

(9) Gerber, D. E. *American Family Physician.* **2008**, *77*, 311.

(10) Walsh, D. *Palliative Medicine*; 1st ed.; Philadelphia, PA: Saunders, 2009.

(11) Kaye, S. B. *Brit J Cancer.* **1998**, *78*, 1.

(12) Schmidt, M.; Bastians, H. *Drug Resist Update.* **2007**, *10,* 162.

(13) Sartorelli, A. C.; Tomasz, M.; Rockwell, S. *Advances in Enzyme Regulation.* **1993**, *33*, 3.

(14) Abdella, B. R. J.; Fisher, J. *Environmental Health Perspectives.* **1985**, *64*, 3.

(15) Rabbani, A.; Finn, R. M.; Ausio, J. *Bioessays.* **2005**, *27*, 50.

(16) Li, Q.; Mitscher, L. A.; Shen, L. L. *Medicinal Research Reviews.* **2000**, *20*, 231.

(17) Salerno, S.; Da Settimo, F.; Taliani, S.; Simorini, F.; La Motta, C.; Fornaciari, G.; Marini, A. M. *Curr Med Chem.* **2010**, *17*, 4270.

(18) Rothenberg, M. L. *Ann Oncol.* **1997**, *8*, 837.

(19) Pegg, A. E. *Cancer Invest.* **1984**, *2*, 223.

(20) Neidle; S. *Cancer Drug Design and Discovery.* 1st ed.; Academic Press, 2008: New York, 2008.

(21) Reddy, L. H., Couvreur, P. *Macromolecular Anticancer Therapeutics*. Springer Science and Business Media: Springer, New York, 2009.

(22) Rosenberg, B; Vancamp, L.; Krigas, T. *Nature.* **1965**, *205*, 698.

(23) Kelland, L. *Nat Rev Cancer.* **2007**, *7*, 573.

(24) Dhar, S.; Lippard, S. J. *Bioinorganic Medicinal Chemistry*. Wiley-VCH: New York, 2011, p 79.

(25) Dabrowiak, J. C. *Metals in Medicine*. John Wiley & Sons, Ltd: New York, 2009, p 73.

(26) Treatment with Cisplatin. cisplatin.org/treat.htm. (accessed March 12, 2012).

(27) Gonzalez, M. J. E.; Green, R.; Muggia, F. M. *Oncology.* **2011**, *25*, 156.

(28) Palm-Espling, M. E.; Wittung-Stafshede, P. *Biochem Pharmacol.* **2012**, *83*, 874.

(29) Berners-Price, S. J.; Ronconi, L.; Sadler, P. J. *Progress in Nuclear Magnetic Resonance Spectroscopy.* **2006**, *49*, 65.

(30) Eastman, A. *Biochemistry.* **1986**, *25*, 3912.

(31) Wozniak, K.; Blasiak, J. *Acta Biochim Pol.* **2002**, *49*, 583.

(32) Bellon, S. F.; Coleman, J. H.; Lippard, S. J. *Biochemistry.* **1991**, *30*, 8026.

(33) Gonzalez, V. M.; Fuertes, M. A.; Alonso, C.; Perez, J. M. *Mol Pharmacol.* **2001**, *59*, 657.

(34) Hoffmann, R. L. *Toxicological and Environmental Chemistry.* **1988**, *17*, 139.

(35) Diggle, C. P.; Bentley, J.; Knowles, M. A.; Kiltie, A. E. *Nucleic Acids Res.* **2005**, *33*, 2531.

(36) Siddik, Z. H. *Oncogene.* **2003**, *22*, 7265.

(37) Stros, M. *Biologia.* **1986**, *41*, 1229.

(38) Topping, R. P.; Wilkinson, J. C.; Scarpinato, K. D. *J Biol Chem.* **2009**, *284*, 14029.

(39) Shimodaira, H.; Yoshioka-Yamashita, A.; Kolodner, R. D.; Wang, J. Y. J. *P Natl Acad Sci.* **2003**, *100*, 2420.

(40) Jasin, M.; Rouet, P.; Smih, F. *J Cell Biochem.* **1995**, 328.

(41) Rassool, F. V. *Cancer Lett.* **2003**, *193*, 1.

(42) Jensen, R.; Glazer, P. M. *P Natl Acad Sci.* **2004**, *101*, 6134.

(43) Zhao, W.; Lin, Z. X.; Zhang, Z. Q. *Cell Res.* **2004**, *14*, 60.

(44) Paduch, R.; Rzeski, W.; Klatka, J. *Folia Histochemica Et Cytobiologica.* **2009**, *47*, 75.

(45) Kelland, L. R. *Drugs.* **2000**, *59*, 1.

(46) Rouillon, C.; White, M. F. *Research in Microbiology.* **2011**, *162*, 19.

(47) Sczepanski, J.; Jacobs, A.; Van Houten, B.; Greenberg, M. M. *Chem Res Toxicol.* **2010**, *23*, 284.

(48) Furuta, T.; Ueda, T.; Aune, G.; Sarasin, A.; Kraemer, K. H.; Pommier, Y. *Cancer Res.* **2002**, *62*, 4899.

(49) Wang, C. H.; Wu, H. T.; Cheng, H. M.; Yen, T. J.; Lu, I. H.; Chang, H. C.; Jao, S. C.; Shing, T. K. M.; Li, W. S. *J Med Chem.* **2011**, *54*, 8574.

(50) Perez, R.P.; Hamilton, T. C.; Ozols, R. F. *Parmac Ther.* **1990**, *48*, 19.

(51) Kelly, S.L.; Basu, A.; Teicher, B. A.; Hacker, M. P.; Hamer, D. H.; Lazo, J. S. *Science.* **1988**, *241*, 1813.

(52) Brady, F. O. *Trends in Biochemical Sciences.* **1982**, *7*, 143.

(53) Kartalou, M.; Essigmann, J. M. *Mutat Res-Fund Mol M.* **2001**, *478*, 23.

(54) Florea, A.-M.; Büsselberg, D. *Cancers.* **2011**, *3*, 1351.

(55) Smith, D. J.; Jaggi, M.; Zhang, W.; Galich, A.; Du, C.; Sterrett, S. P.; Smith, L. M.; Balaji, K. C. *Urology.* **2006**, *67*, 1341.

(56) Galluzzi, L.; Senovilla, L.; Vitale, I.; Michels, J.; Martins, I.; Kepp, O.; Castedo, M.; Kroemer, G. *Oncogene.* **2012**, *31*, 1869.

(57) Bloemink, M. J.; Reedijk, J. *Metal Ions in Biological Systems.* **1996**, *32*, 641.

(58) Fricker, S. P. *Dalton. T* **2007**, 4903.

(59) Bratsos, I.; Gianferrara, T.; Alessio, E.; Hartinger, C. G.; Jakupec, M. A.; Keppler, B. K. In *Bioinorganic Medicinal Chemistry*. Wiley-VCH: New York, 2011, p 151.

(60) Gasser, G.; Ott, I.; Metzler-Nolte, N. *J Med Chem.* **2011**, *54*, 3.

(61) Yan, Y. K.; Melchart, M.; Habtemariam, A.; Sadler, P. J. *Chem Commun.* **2005**, 4764.

(62) Cotton, F. A. *Abstr Pap Am Chem S.* **1978**, *176*, 129.

(63) Reibscheid, E. M.; Zyngier, S.; Maria, D. A.; Mistrone, R. J.; Sinisterra, R. D.; Couto, L. G.; Najjar, R. *Brazilian Journal of Medical and Biological Research.* **1994**, *27*, 91.

(64) Esposito, B. P.; de Oliveira, E.; Zyngier, S. B.; Najjar, R. *Journal of the Brazilian Chemical Society.* **2000**, *11*, 447.

(65) Zyngier, S. B.; Esposito, B. P.; Souza, A. R.; Najjar, R. *N-S Arch Pharmacol.* **1998**, *358*, R530.

(66) Esposito, B. P.; Faljoni-Alario, A.; de Menezes, J. F. S.; de Brito, H. F.; Najjar, R. *J Inorg Biochem.* **1999**, *75*, 55.

(67) Fimiani, V.; Ainis, T.; Cavallaro, A.; Piraino, P. *J Chemotherapy.* **1990**, *2*, 319.

(68) Bear, J. L.; Gray, H. B.; Rainen, L.; Chang, I. M.; Howard, R.; Serio, G.; Kimball, A. P. *Cancer Chemotherapy Reports Part 1.* **1975**, *59*, 611.

(69) Crawford, C. A.; Folting, K.; Christou, G.; Matonic, J. H.; Dunbar, K. R. *Abstr Pap Am Chem S.* **1994**, *208*, 557.

(70) Phillips, S. L.; Huffman, J. C.; Christou, G.; Dunbar, K. R. *Abstr Pap Am Chem S.* **1994**, *208*, 460.

(71) Chifotides, H. T.; Dunbar, K. R. *Chem Eur J.* **2008**, *14*, 9902.

(72) Chifotides, H. T.; Koomen, J. M.; Kang, M. J.; Tichy, S. E.; Dunbar, K. R.; Russell, D. H. *Inorg Chem.* **2004**, *43*, 6177.

(73) Chifotides, H. T.; Dunbar, K. R. *J Am Chem Soc.* **2007**, *129*, 12480.

(74) Chifotides, H. T.; Dunbar, K. R. *Chem Eur J.* **2006**, *12*, 6458.

(75) Kang, M.; Chifotides, H. T.; Dunbar, K. R. *Biochemistry Us.* **2008**, *47*, 2265.

(76) Aguirre, J. D.; Chifotides, H. T.; Angeles-Boza, A. M.; Chouai, A.; Turro, C.; Dunbar, K. R. *Inorg Chem.* **2009**, *48*, 4435.

(77) Chifotides, H. T.; Fu, P. K. L.; Dunbar, K. R.; Turro, C. *Inorg Chem.* **2004**, *43*, 1175.

(78) Aguirre, J. D.; Angeles-Boza, A. M.; Chouai, A.; Turro, C.; Pellois, J. P.; Dunbar, K. R. *Dalton T.* **2009**, 10806.

(79) Aguirre, J. D.; Angeles-Boza, A. M.; Chouai, A.; Pellois, J. P.; Turro, C.; Dunbar, K. R. *J Am Chem Soc.* **2009**, *131*, 11353.

(80) Angeles-Boza, A. M.; Bradley, P. M.; Fu, P. K. L.; Shatruk, M.; Hilfiger, M. G.; Dunbar, K. R.; Turro, C. *Inorg Chem.* **2005**, *44*, 7262.

(81) Bradley, P. M.; Angeles-Boza, A. M.; Dunbar, K. R.; Turro, C. *Inorg Chem.* **2004**, *43*, 2450.

(82) James, C. A.; Morris, D. E.; Doorn, S. K.; Arrington, C. A.; Dunbar, K. R.; Finnis, G. M.; Pence, L. E.; Woodruff, W. H. *Inorg Chim Acta.* **1996**, *242*, 91.

(83) Yano, S.; Hirohara, S.; Obata, M.; Hagiya, Y.; Ogura, S.; Ikeda, A.; Kataoka, H.; Tanaka, M.; Joh, T. *Journal of Photochemistry and Photobiology C-Photochemistry Reviews.* **2011**, *12*, 46.

(84) Trindade, A. F.; Coelho, J. A. S.; Afonso, C. A. M.; Veiros, L. F.; Gois, P. M. P. *Acs Catalysis.* **2012**, *2*, 370.

(85) Angeles-Boza, A. M.; Chifotides, H. T.; Aguirre, J. D.; Chouai, A.; Fu, P. K. L.; Dunbar, K. R.; Turro, C. *J Med Chem.* **2006**, *49*, 6841.

(86) Pasternak, H.; Pruchnik, F. P. *Transition Metal Chem.* **1996**, *21*, 305.

(87) Pruchnik, F.; Dus, D. *J Inorg Biochem.* **1996**, *61*, 55.

(88) Wajda-Hermanowicz, K.; Pruchnik, F. P.; Zuber, M.; Ciunik, Z. *Polyhedron.* **2005**, *24*, 1577.

(89) Sorasaenee, K.; Fu, P. K. L.; Angeles-Boza, A. M.; Dunbar, K. R.; Turro, C. *Inorg Chem.* **2003**, *42*, 1267.

(90) Lane, N. *Scientific American.* **2008**, *18*, 84.

(91) Lutterman, D. A.; Turro, C.; Fu, P. K. L.; Liu, Y. *Abstr Pap Am Chem S.* **2005**, *230*, U2225.

(92) Happ, B.; Winter, A.; Hager, M. D.; Schubert, U. S. *Chemical Society Reviews.* **2012**, *41*, 2222.

(93) Jenkins, Y.; Friedman, A. E.; Turro, N. J.; Barton, J. K. *Biochemistry Us.* **1992**, *31*, 10809.

(94) Angeles-Boza, A. M.; Bradley, P. M.; Fu, P. K. L.; Wicke, S. E.; Bacsa, J.; Dunbar, K. R.; Turro, C. *Inorg Chem.* **2004**, *43*, 8510.

(95) Joyce, L. E.; Aguirre, J. D.; Angeles-Boza, A. M.; Chouai, A.; Fu, P. K. L.; Dunbar, K. R.; Turro, C. *Inorg Chem.* **2010**, *49*, 5371.

(96) Delgadillo, A.; Romo, P.; Leiva, A. M.; Loeb, B. *Helvetica Chimica Acta.* **2003**, *86*, 2110.

(97) Lehtonen, K.; Summers, L. A. *Aust J Chem.* **1970**, *23*, 1699.

(98) Yam, V. W. W.; Lo, K. K. W.; Cheung, K. K.; Kong, R. Y. C. *J Chem Soc, Chem Commun.* **1995**, 1191.

(99) Fotakis, G.; Timbrell, J. A. *Toxicol Lett.* **2006**, *160*, 171.

(100) Pruchnik, F. P.; Starosta, R.; Ciunik, Z.; Opolski, A.; Wietrzyk, J.; Wojdat, E.; Dus, D. *Can J Chem.* **2001**, *79*, 868.

(101) Pruchnik, F. P.; Starosta, R.; Lis, T.; Lahuerta, P. *J Organomet Chem.* **1998**, *568*, 177.

(102) Gilaberte, J. M.; López, C.; Alvarez, S. *J Organomet Chem.* **1988**, *342*, C13.

(103) Dunbar, K. R.; Matonic, J. H.; Saharan, V. P. *Inorg Chem.* **1994**, *33*, 25.

(104) Geldmacher, Y.; Splith, K.; Kitanovic, I.; Alborzinia, H.; Can, S.; Rubbiani, R.; Nazif, M. A.; Wefelmeier, P.; Prokop, A.; Ott, I.; Wolfl, S.; Neundorf, I.; Sheldrick, W. S. *J Biol Inorg Chem.* **2012**, *17*, 631.

(105) Rajput, J.; Moss, J. R.; Hutton, A. T.; Hendricks, D. T.; Arendse, C. E.; Imrie, C. *J Organomet Chem.* **2004**, *689*, 1553.

(106) Liu, Z.; Habtemariam, A.; Pizarro, A. M.; Fletcher, S. A.; Kisova, A.; Vrana, O.; Salassa, L.; Bruijnincx, P. C. A.; Clarkson, G. J.; Brabec, V.; Sadler, P. J. *J Med Chem.* **2011**, *54*, 3011.

(107) Schafer, S.; Sheldrick, W. S. *J Organomet Chem.* **2007**, *692*, 1300.

(108) Stinner, C.; Wightman, M. D.; Kelley, S. O.; Hill, M. G.; Barton, J. K. *Inorg Chem.* **2001**, *40*, 5245.

(109) Lo, K. K. W.; Chung, C. K.; Zhu, N. Y. *Chem Eur J.* **2006**, *12*, 1500.

(110) Gencaslan, S.; Sheldrick, W. S. *Eur J Inorg Chem.* **2005**, 3840.

(111) Gras, M.; Therrien, B.; Suss-Fink, G.; Casini, A.; Edafe, F.; Dyson, P. J. *J Organomet Chem.* **2010**, *695*, 1119.

(112) Liu, Z.; Habtemariam, A.; Pizarro, A. M.; Clarkson, G. J.; Sadler, P. J. *Organometallics.* **2011**, *30*, 4702.

(113) Teets, T. S.; Cook, T. R.; McCarthy, B. D.; Nocera, D. G. *Inorg Chem.* **2011**, *50*, 5223.

(114) Rausch, M. D.; Gastinger, R. G.; Gardner, S. A.; Brown, R. K.; Wood, J. S. *J Am Chem Soc.* **1977**, *99*, 7870.

(115) Rasmussen, P. G.; Anderson, J. E.; Bailey, O. H.; Tamres, M.; Bayon, J. C. *J Am Chem Soc.* **1985**, *107*, 279.

(116) Miskowski, V. M.; Smith, T. P.; Loehr, T. M.; Gray, H. B. *J Am Chem Soc.* **1985**, *107*, 7925.

(117) Dunbar, K. R.; Majors, S. O.; Sun, J. S. *Inorg Chim Acta.* **1995**, *229*, 373.

(118) Catalan, K. V.; Hess, J. S.; Maloney, M. M.; Mindiola, D. J.; Ward, D. L.; Dunbar, K. R. *Inorg Chem.* **1999**, *38*, 3904.

(119) Dunbar, K. R.; Pence, L. E. *Abstr Pap Am Chem S.* **1991**, *201*, 35.

(120) Chifotides, H. T.; Catalan, K. V.; Dunbar, K. R. *Inorg Chem.* **2003**, *42*, 8739.

(121) Cotton, F. A.; Lahuerta, P.; Sanau, M.; Schwotzer, W. *Abstr Pap Am Chem S.* **1985**, *190*, 111.

(122) Cotton, F. A.; Poli, R. *Inorg Chim Acta.* **1986**, *122*, 243.

(123) Aguirre, J. D.; Lutterman, D. A.; Angeles-Boza, A. M.; Dunbar, K. R.; Turro, C. *Inorg Chem.* **2007**, *46*, 7494.

VITA

Sarah Margaret Lane received her Bachelor of Sciences degree in biochemistry with a second major in biomedical science from Bridgewater State University in 2007. She entered graduate program in chemistry at Texas A&M University in 2007, where she joined the group directed by Prof. Kim R. Dunbar. Her research interests include bioinorganic chemistry as applied to anticancer research, and inorganic synthesis.

Sarah Lane may be reached at 6 Horton Way, Rehoboth, MA 02769. Her email address is Sarah.M.Lane.84@gmail.com.